M.Sc. Thesis

Investigation of the electrical performance of epoxy/ silicon rubber interface

Design of a standardized 145 kV inner-cone GIS cable termination

Sanjay Ganeshan

Prysmian Group

TUDelft

Investigation of the electrical performance of epoxy/ silicon rubber interface

Design of a standardized 145 kV inner-cone GIS cable termination

by

Sanjay Ganeshan

in partial fulfilment of the requirements for the degree of

Master of Science
in Electrical Engineering

at the Delft University of Technology,
to be defended publicly on Friday July 27, 2018 at 10:00 AM

Student number   :   4614275

Project duration   :   November 8, 2017 – July 27, 2018

Thesis supervisors: Prof. dr. ir. Armando Rodrigo Mor,   Daily Supervisor/ TU Delft
Ir. Panagiotis Tsakonas,   Company Supervisor/ Prysmian Group

Thesis committee :   Prof. dr. Rob Ross,   Full Professor, TU Delft
Prof. dr. ir. Armando Rodrigo Mor,   Assistant Professor, TU Delft
Prof. dr. ir. Milos Cvetkovic,   External Expert, TU Delft

An electronic version of this thesis is available at https://repository.tudelft.nl.

TUDelft

நன்றி மறப்பது நன்றன்று நன்றல்லது
அன்றே மறப்பது நன்று.

Translation
Never forget the (good) deeds that someone did to you,
But, forget the (bad) deeds immediately

*The above verse is a couplet from the Thirukkural, a classic **Tamil language text** consisting of 1,330 couplets, dealing with the everyday virtues of an individual. Considered one of the greatest works ever written on ethics and morality, chiefly secular ethics, it is known for its universality and non-denominational nature. It was authored by Valluvar, also known in full as Thiruvalluvar. The text has been dated variously from 300 BCE to 7th century CE.*

Acknowledgements

Table of contents

List of figures

List of tables

Glossary

XLPE	Cross Linked Poly-Ethylene
SiR	Silicon Rubber
EPDM	Ethylene Propylene Diene Monomer rubber
EPR	Ethylene Propylene Rubber
PD	Partial Discharge
LI	Lightning Impulse
BD	breakdown
BIL	Basic Impulse Level

Abstract

The CIGRE B1 – B3.49 JWG defined a standardised 145 kV inner-cone GIS cable termination design. This standardisation allows the creation of new common interface insulators. This would eliminate the planning hurdles due to the fact that the cable system is not usually defined at the time of switchgear manufacture. The new design also requires a detailed study to find the relation between interfacial pressure and electrical performance of the epoxy/ silicon rubber interface.

The first step is to design and build a test setup to study the epoxy/ silicon rubber interface. Next, AC breakdown and lightning impulse tests are carried out. Additional AC breakdown testing with oil at the interface, defects on epoxy and heated samples are also carried out. The relation between interfacial pressure and electric field strength of the interface is found and documented. The effects of lubricant, defects and heat is used to further characterise the interface. Simultaneously, the silicon rubber is modelled using hyperelastic material modelling techniques.

The results from the tests and FEM models are used to propose two new designs of the 145 kV inner-cone GIS cable termination. The high repeatability of breakdown values and distinct features of this test setup have prompted the sharing of the experimental setup and results through an IEEE publication.

1. Introduction

In this chapter, the first section introduces the topic of the M.Sc. thesis, followed by the motivation. The third and fourth sections explain the current developments/ trends regarding GIS cable terminations and interface study respectively. The fifth section elaborates on the scope of this thesis. The subsequent sections elaborate on the problem statement, research goals and the layout of this thesis report.

1.1 Introduction

The topic of this M.Sc. thesis is "**Design of a standardized inner-cone 145 kV GIS cable termination – Analysis of the epoxy/ silicon rubber interface**".

The main aim of this thesis is to find and document the relation between electrical performance of epoxy/ silicon rubber interface with respect to interfacial pressure. This knowledge is then used as a reference to design, a **145 kV inner-cone GIS cable termination** in accordance with *CIGRE JWG B1-B3.49* recommendations.

1.2 Motivation

Considering the large number of substations and practical planning difficulties because the cable system is usually not defined at the time of switchgear manufacturing. This gave rise to a *CIGRE JWG B1-B3.49* comprising of experts from *CIGRE B1* (cables) and *CIGRE B3* (switchgear). The duty of this JWG was to explore the possibility of a standardized common interface insulator for the dry type, plug-in termination such that it could be supplied independently from the remaining termination components. In other words, the GIS manufacturer will have the possibility to complete the GIS manufacturing independent from the cable and termination supplier.

Following the *CIGRE* JWG study, for a certain range of application a standardized interface is recommended. This means that cable manufactures will need to design new **dry-type** and **plug-in cable termination** that fits the standardized interface. At the other end, it is important that the new dry-type and plug-in cable termination maintains the characteristics the cable manufacturers consider necessary for their specific design.

The interface between silicon rubber and epoxy has a lot of significance in the design of cable accessories. This is because the interface forms the boundary of the 'limit of supply/ responsibilty' of the cable termination manufacturer and the switchgear manufacturer (refer *Fig. 1.1*). With the emerging trend of standardized common interface insulators for dry type terminations, this gains further importance. For this reason, the effect of non-electrical parameters like interfacial pressure, on the electric strength of the epoxy/ rubber interface must be examined before defining the final design of the termination. An experimental approach is necessary to find out this relationship.

After defining the final geometry of the termination, further checks/ tests need to be performed, before and after production of the first prototypes. The results of these tests will validate the design of the termination before releasing it for further short and long term qualification

No.	Description	Manufacturer	
		Switchgear	Cable termination
1	Main circuit end terminal	X	
2	Connection interface	X	
3	Connection interface		X
4	Insulator		X
5	Cable connection enclosure	X	
6	Enclosure flange or intermediate plate	X	
7	Seal	X	
8	Screws, washers, nuts	X	
9	Insulator collar or adaptor		X
10	Intermediate gasket		X (if needed)
11	Flange		X (if needed)
12	Electrical stress control (elastomeric)		X
13	Cable gland		X
14	Gas	X	
15	Non-linear resistors		X (if needed)

Fig. 1.1: Standard dry-type terminations as defined in IEC 62271-209 [23]

1.3 State of the art- GIS terminations

Cable systems have been used since early 1900s, and primitive accessories for joining cables was only manufactured on-site by skilled jointers who would wrap pre-impregnated paper tapes along with a compound filling. It was only in early 1970s that cast resin was used to make joints [6]. With continuous research on new materials and the demand for increased power transmission, cable technology rapidly evolved.

Cable accessories are the vital links between the cables, and this is depicted in *Fig. 1.2*. Dry-type GIS terminations are available up to 550 kV voltage range. There are two possible constructions according to IEC 62271-209, **Type A: Inner cone design** and **Type B: Outer cone design**. The two techniques are represented in *Fig 1.3*.

A large portion of the GIS terminations are typically of the IEC 62271-209 type B (outer-cone design). This was because until recently, IEC did not clearly define the area of responsibility between the switchgear and cable manufacturer [21]. Also, the locking mechanism of the large cross-section cables was not reliable. In order to eliminate this bottleneck, *CIGRE* set up the JWG B1-B3.49 to give a new 'Standard Design of a common dry-type plug-in interface for GIS and power cables up to 145 kV'. This work has been the driving force for this thesis work.
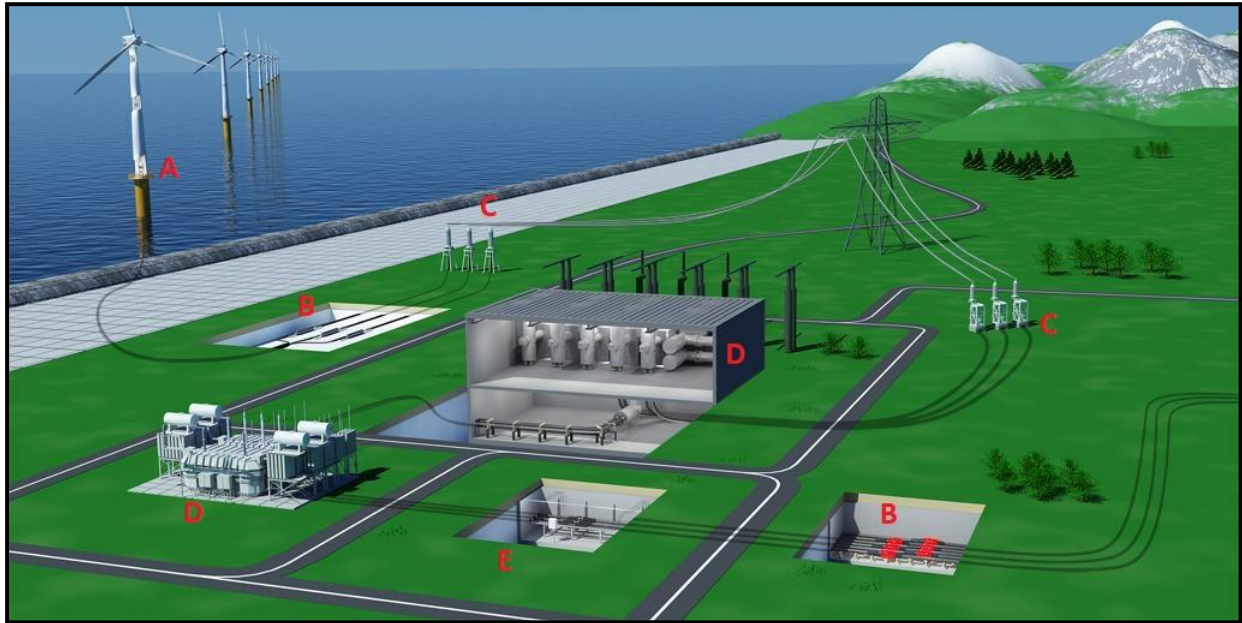
Fig. 1.2: Illustrative diagram of different types of HV cable accessories [38]
(A- Y joint for wind energy application; B- cable joints; C- outdoor terminations;
D- Cable termination for GIS and oil-filled transformers; E- link boxes)

Some manufacturers do have an inner-cone version of GIS terminations [35]; however, they do not adhere to the CIGRE JWG recommendations. Thus, it can be said that all accessory manufacturers are currently designing/ evaluating the JWG recommendations**, and no product** (confirming to the JWG) **is readily available as of the date of this thesis**.
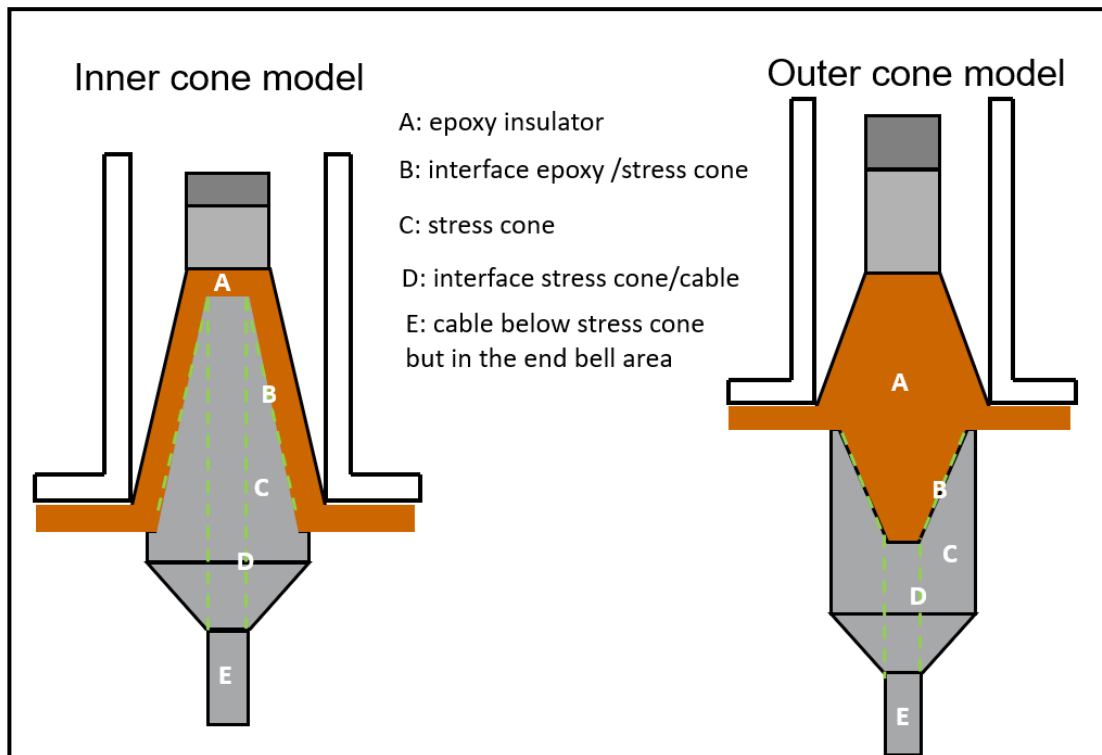
Fig. 1.3: Representation of Type A (inner-cone) and Type B (outer-cone) technologies for GIS terminations

1.4 State of the art – Epoxy/ silicon rubber interface study

The interface of any two materials is always considered as the weakest point in high voltage design [9, 28, 52]. This is due to the fact that the tangential component of the electric field may have high values here and thus get highly stressed. Also factors like interfacial pressure, temperature and material properties play an important role in the electrical performance of the interface.

Interface studies have been carried out for different materials and with/ without other variable parameters like temperature, oil, grease, pressure, etc., A few studies have been carried out regarding epoxy/ silicon rubber interface. A detailed overview of different studies/ research in literature is provided in *Chapter 2*.

However, it is worth mentioning that no standard/ guidelines exist for the standardised procedure to determine the interfacial electrical performance of two materials. This allows researchers to devise their own methods based on experience and literature. One such test setup is also proposed here, and will be explained in detail in *Chapter 4*

1.5 Scope of the thesis

This thesis is aimed to find a relation between interfacial pressure and electrical performance of the epoxy - silicon rubber interface. Experiments are performed to establish this relation.

Develop a test setup:
The test setup was intentionally designed to obtain the worst-case values of the breakdown voltage. Thus, it gives a **conservative estimation** of the breakdown performance of the interface. Many experimental setups were envisioned to study different aspects but due to practical difficulties in sourcing the samples and constraints in time, multiple test setups were not investigated.

Create a material model of the silicon rubber:
To have a very accurate (mechanical) model of the silicon rubber, the material modelling properties of the rubber are investigated. This model would be useful to simulate the behaviour of rubber for different mechanical forces that it experiences during its installation/ operation.

Suggest the final design(s):
The knowledge from the above investigations is combined to propose possible design(s) of the 145 kV inner-cone termination. The design may be extended to other voltage classes, however, that is outside the scope of this thesis. Practical (logistics, installation procedure) and economic (cost, complexity of parts) factors are also considered while designing the terminations.

1.6 Problem statement

The final objective of this M.Sc. thesis is to design a new 145kV inner-cone GIS termination in accordance to *CIGRE JWG B1-B3.49* recommendations. The new (design) technology means that the epoxy/ silicon rubber interface will require a detailed investigation to learn about the relation between the electrical breakdown voltage and interfacial pressure.

During this thesis, it was found that the finite element method of mechanically simulating the silicon rubber needed a new technique – Hyperelastic Material Modelling. This problem is addressed in *Chapter 3* of this thesis work.

1.7 Research goals

To reach the standard of a Master of Science thesis, it is necessary that the research work must answer/ achieve certain research goals. This M.Sc. thesis aims to achieve the following research goals:

1. To **design a test setup** to obtain the relation between electric field strength with respect to interfacial pressure

2. To experimentally obtain the **relation between interfacial pressure and electric performance** of epoxy/ silicon rubber interface.

3. To **propose the design for an inner-cone GIS cable termination** and elucidate its electrical and mechanical features.

The answers to these research goals are explained in detail in the various chapters of this report. A summary of the research findings (answers to research goals) is presented in *Chapter 7.*

1.8 Thesis layout

This document is divided into different chapters, to show clear distinction between different sections/ parts of the thesis work. A representation of the contributions and inter-relation of different chapters is shown in *Fig. 1.4*.

Chapter 2: *Literature review* gives a detailed overview of the literature study that was performed during the course of this thesis. Various test setups and results are elaborated in this chapter. The findings from the literature are used during the design of the test setup *(Chapter 4)* and understanding of solid/ solid interfaces.

Chapter 3: Hyperelastic material modelling of rubber gives insight into the need for such a modelling technique. It then explains the different types of hyperelastic material models. The specific modelling technique chosen for this project is also elaborated.

Chapter 4: Design of test setup for interfacial study explains about how the final design for the test setup was made at with inputs from *Chapter 2*. It explains the distinct features and limitations of the test setup.

Chapter 5: Experimental study of epoxy/ silicon rubber interface refers to the experimentation part of the thesis. Results and inferences are deduced. These results will be used as a reference in *Chapter 6*.

Chapter 6: Design of GIS termination is a product of the results from *Chapter 3 and 5*. Two designs are proposed and discussed in detail.

Chapter 7: Conclusions and future scope is the closing chapter of this thesis. The answers to the research questions and future recommendations for research are provided.

Introduction	• Motivation, State-of-the-art • Scope, Research goals
Literature study	• Solid/ solid interface study • Epoxy/ silicon rubber interface study
Hyperelastic material modelling of silicon rubber	• Drawbacks of linear modelling techniques,- Hyperelastic material model of currently used silicon rubber
Design of test setup for interface testing	• Comparitive study of possible test setups • Proposed test setup - advantages and limitations
Experimental study of epoxy/ silicon rubber interface	• Procedure of testing • Test results and inferences
Design of inner-cone GIS termination	• CIGRE JWG recommendations • Proposed designs 'A' and 'B'
Conclusions and future scope	• Conclusions • Answers to research goals

Fig. 1.4: Outline of thesis

2. Literature study

This chapter provides a summary of various literature regarding solid/ solid interfaces and more particularly about epoxy/ silicon rubber interface. The chapter is divided into different sections and sub-sections based on the topic of research and its results.

2.1 *Solid | solid interface study*

Several failure investigations [9, 40] from the past reiterate the fact that the interface is the weakest point of HV cable and cable systems. The interest of many organisations worldwide to learn about interfaces stemmed from the 1993 blackout in The Netherlands [40]. This has propelled great amount of research to be done to investigate the performance of interfaces to establish a relation between various electrical and non-electrical parameters.

Solid/ solid interface study was done by various experts from different institutes around the globe. A summary of the work by each institute is given below.

2.1.1 *CIGRE WG 15-10*

The focus of this WG was to propose a list [48] of requirements for testing of material interfaces. The recommendations of this WG are used a s a basis to develop several test setups [5, 29, 40, 51] which are explained in the following sub-sections. The requirements enlisted by the *CIGRE 15-10 WG* (1996) are:

- Testing cells should have a **simple configuration** that is **easy to reproduce**.

- Testing cells should have **no metal electrode** surfacing at the interface.

- Testing cells should allow various **defects** to be introduced.

- Testing cells should enable one to study **mechanical pressure** effects.

- Testing cells should enable one to study **surface roughness** effects.

- Testing cells should enable one to study the **effect of silicone oil** or other liquid insulants.

2.1.2 *Study at Hydro-Quebec Institute of Research (IREQ)- Canada*

The works of *Daniel Fournier* and *Laurent Lamarre* serve as a the earliest and yet one of the most relevant literature in interface electrical performance related study.

The works use a slightly-modified Baur breakdown cell as depicted in *Fig.2.1*. They investigate the performance of **EPDM | EPDM** interface [13] and **EPDM | XLPE** interface [12]. The samples in both cases were cut from commercially available pieces.

Two pieces of the material under test are pressed against each other so as to induce breakdown longitudinally along their interface. Two thin tungsten needle electrodes are implanted at the interface, the distance between the electrodes is also varied with respect to electric field. Weights are put on top of the sample to vary the pressure at the interface. The effect of addition of silicon grease at the interface was also studied.

W= Interface width (from 3 to 10 mm)
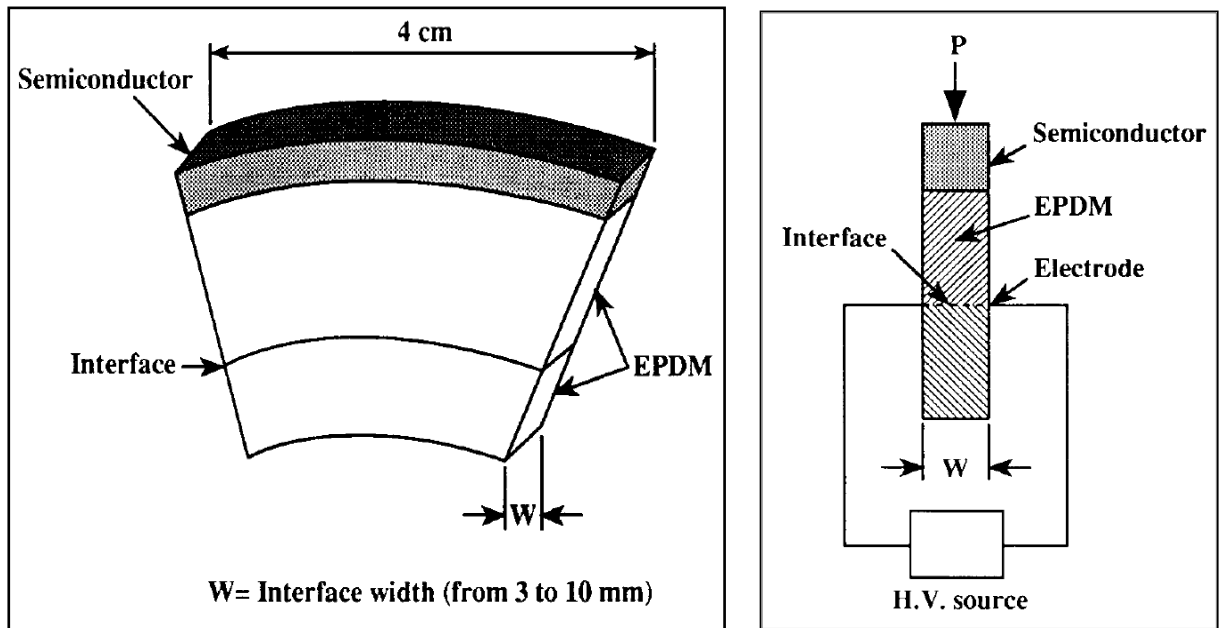
(a)   (b)

Fig. 2.1: Sample description(a) and experimental setup (b) of [12, 13]
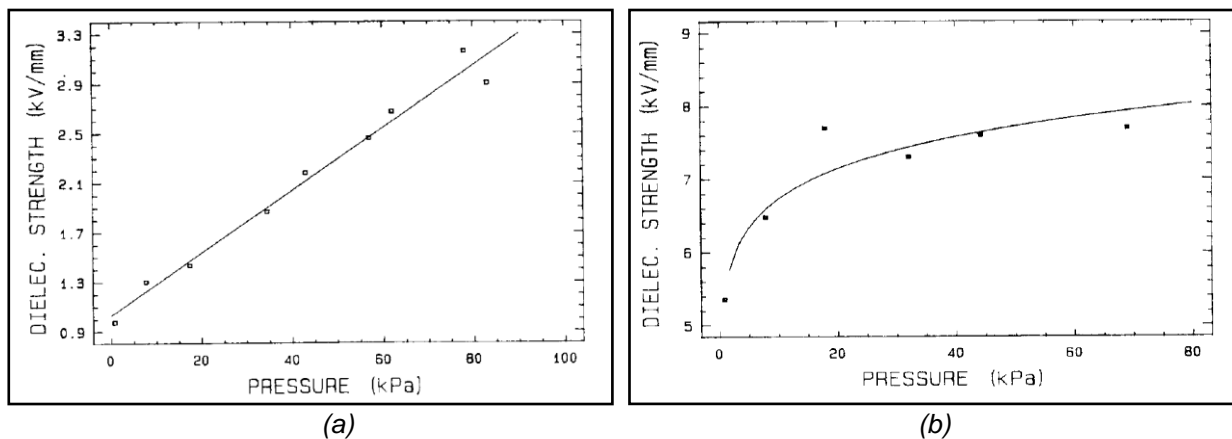
(a)   (b)

Fig. 2.2: Dielectric strength of EPDM/ EPDM interface without (a) and with (b) silicon grease at the interface [12, 13]

The work arrives at the following important conclusions:

- The dielectric strength of bulk EPDM (18.2 kV/mm) is about **6 times higher** than the interfacial performance (~ 3 kV/mm @ 80 kPa).

- Presence of silicon grease at the interface can **improve** its dielectric performance at low pressure and limits the dielectric performance at higher pressures (above 50kPa).

- Interfaces with silicon grease outperform those without grease by a factor of **2 to 3**.

2.1.3 Study at Norwegian University of Science and Technology

The works of *Seyed Majid Hasheminezhad, Erling Ildstad, Arne Nysveen, Erme Kanter* and *Dimitrios Panagiotopoulos* provide a lot of insight into the study of solid/ solid interface study and into the investigations for the relation of electrical breakdown strength with interface pressure, surface roughness and temperature.

The main material interfaces studied in their works are **XLPE | XLPE** [14, 16, 46, 47] **XLPE | SiR** [14, 16], **SiR | SiR** [14, 16]. The motivation for their work was with regard subsea interconnectors. Thus, a lot of focus was given to compare the interface electric performance during a dry and wet condition.
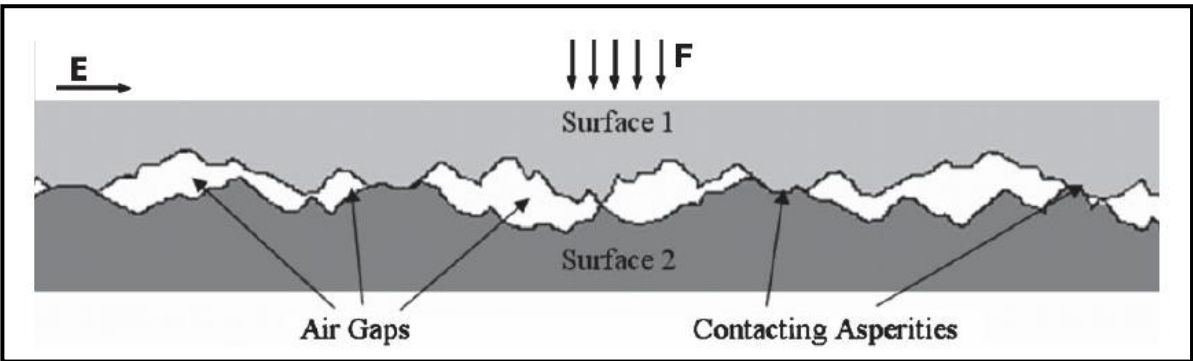
Fig. 2.3: An exaggerated illustration of solid/ solid interface [47]

The work [47] aims to develop a theoretical model for the voids in the interface. A schematic illustration of the voids and contact surfaces at the interface is shown in *Fig. 2.3*. The electrical model for the dry interface is of interest for this thesis. The proposed model is as follows:
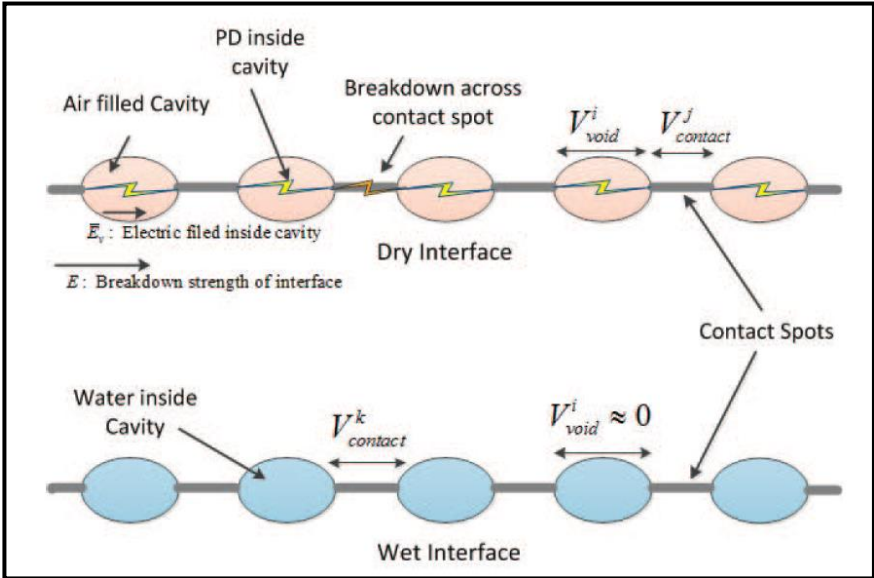
Fig. 2.4: The electrical model of solid/ solid interface as proposed by [47]

It was assumed that the breakdown voltage of the dry parts (V_{dry}) is composed of two parameters (V_{void}) – voltage drops across the voids and $(V_{contact})$ – voltage drops across the contact spots.

$$V_{dry} = \sum_{i} V_{void}^{i} + \sum_{j} V_{contact}^{j}$$

(1)

The work [46] also focuses at giving a microscopic explanation to the breakdown phenomenon. This is done by finding a theoretical relation between the surface roughness and the electrical performance at the interface. They used a test setup as shown in *Fig. 2.5*. Thus, sample surfaces are intentionally grinded using different grits (180 for rough to 1000 for smooth) of sanding paper. However, this work was not carried out at different pressure levels.
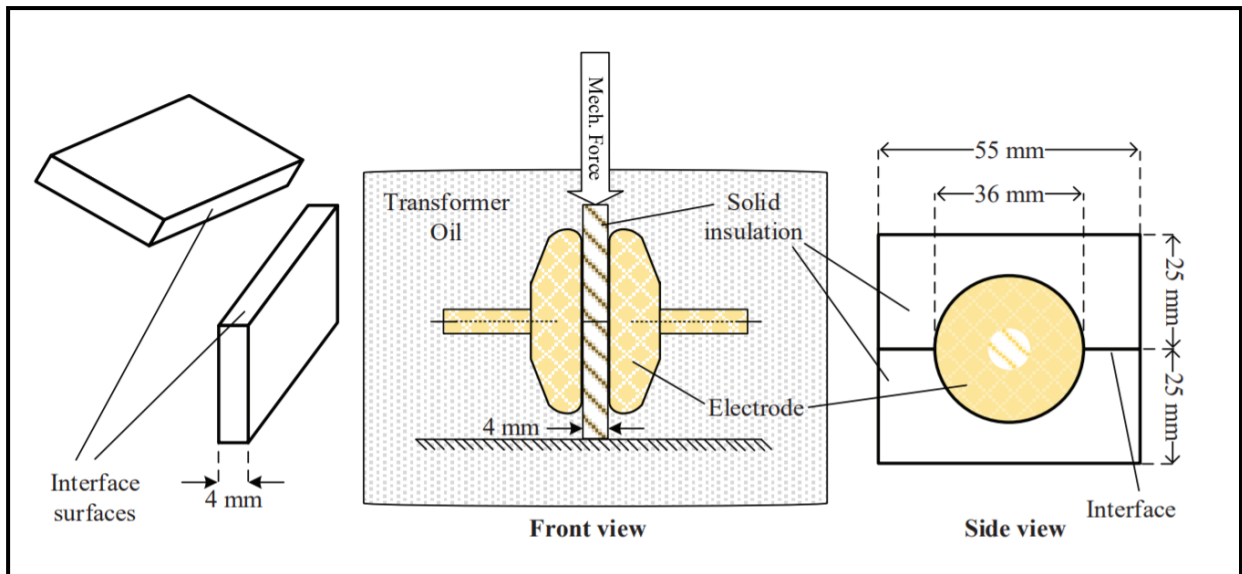
Fig. 2.5: Test setup used in [14, 16, 46, 47]
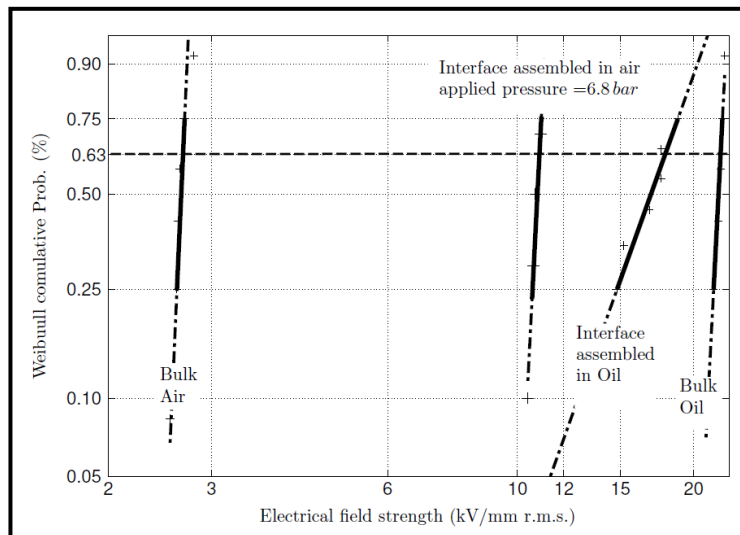
Fig. 2.6: Weibull probability plots of electric field strength by [46]

The works [14, 16] were for **XLPE | XLPE**, **XLPE | SiR** and **SiR | SiR** interfaces. The experimental setup was same as *Fig. 2.5*. The samples were tested while the entire setup was immersed in transformer oil. The samples were cut from existing cable accessories and/ or casted in the lab. To create a smooth surface, the samples were grinded using sand paper.
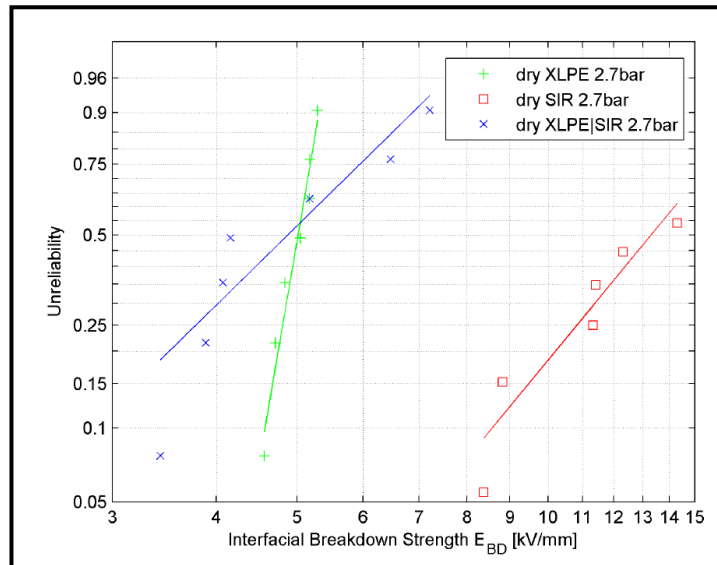
Fig. 2.7: Weibull plots of XLPE/ XLPE, SiR/ SiR and XPLE/ SiR interfaces at 2.7bar pressure [14, 16]

It is important to note that the possibility of oil seeping into the interface and affecting the measurements is very high. Also, the samples were made by hand, which can introduce rough surfaces at the interfaces.

Important conclusions from the works [14, 16, 17, 18, 46, 47] are:

- The presence of water substantially **reduces** the breakdown strength of the interface.

- The interface breakdown stress **increases** with applying more mechanical pressure and is **reduced** by increasing the roughness.

- Highest breakdown strength of was observed in the **smoothest** interfaces.

- Tangential electric fields greater than **2 kV/mm** can initiate creeping discharges at the interface.

- The **modulus of elasticity** (E) of the material also plays a role in the breakdown strength of the interface.

- Oil can easily penetrate in the interface, and thereby increase the breakdown performance.

- Due to buckling of the silicon rubber, pressures beyond 2.7 bar are not possible.

- The modulus of elasticity plays an important role in the breakdown of the interface

2.1.4 Study at Tianjin University, China

The work [5] of *B.X. Du* and *L. Gu*, proposes a test setup that aims to create a relation between interfacial pressure and tracking failure in **XLPE|SiR**. A pair of needle-plate electrodes were used. Thin slices (about 1mm thickness) of SiR and XLPE were cut from existing products. A high-speed camera was used to quantify the light (from discharges) and record the carbonisation (tracking). Image processing techniques were used to aid the investigations.
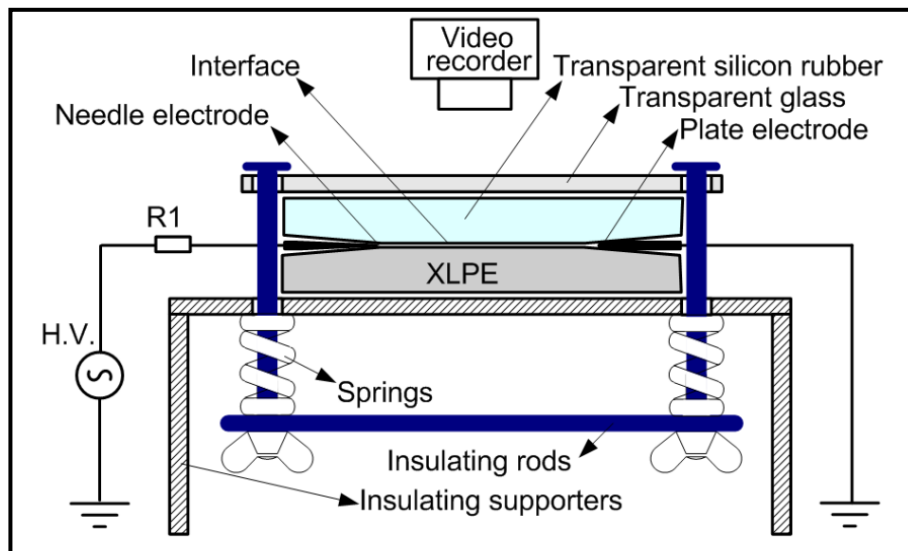
Fig. 2.8: Experimental setup of [5]
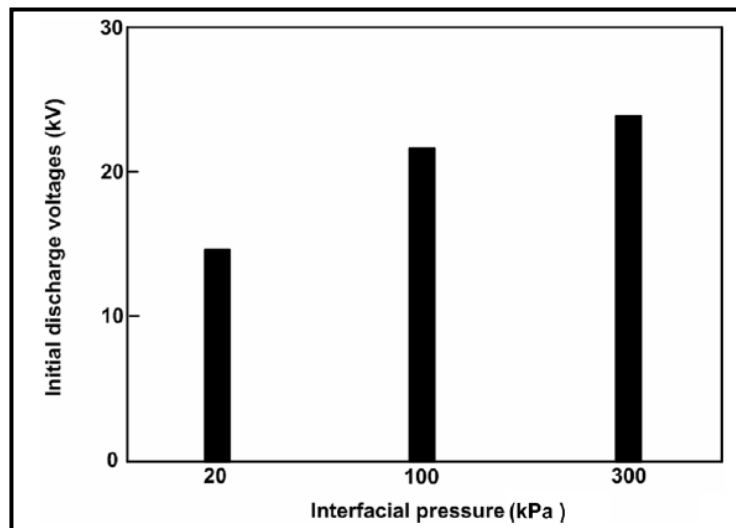
Fig. 2.9: Relation between initial discharge voltage and interfacial pressure [5]

The important conclusions of this work include:

- Initial discharge voltage has **higher** values with increasing interfacial pressure.

- Tracking failure takes a **longer** time to occur with increasing interfacial pressure.

- **Optical techniques** can reveal interfacial tracking failures and carbonization paths.

15

2.1.5 Study at KEMA, Netherlands

The work of *Robert Ross* [40] is a discussion about the 1993 blackout in the Netherlands which was attributed to a cascade of breakdowns in a series of 150 kV terminations. During the investigations, it was found that the **XLPE | SiR** interface was the reason for the series of failures.

The work illustrates how it was concluded that interfacial problems caused the cascade of breakdowns. Important findings of this investigation were as follows:

- Treeing patterns were observed on both XLPE and SiR. The imprints were **negatives of each other**.

- Electrical treeing occurred over a period of **days/ months**.

- Treeing started at the interface **without** any direct connection to any of the electrodes.

- Large increase in discharge activity was observed during temperature change. Difference in thermal expansion coefficients, can cause the cable (XLPE) and termination (SiR) parts to shift/ move along each other.

- In addition to the recommendations of *CIGRE WG 15-10* [48], the test cell must also allow the study of shear effects (motion and rubbing).

- Recommendation: Further investigations to understand the cause of interface problems, introduction of dedicated PD monitoring methods.

The author proposes the test setups as shown in *Fig. 2.10* for interface testing of materials. It is to be noted that these setups can find the tangential electric field value that starts the treeing in interfaces. However, these material samples require embedded electrodes.
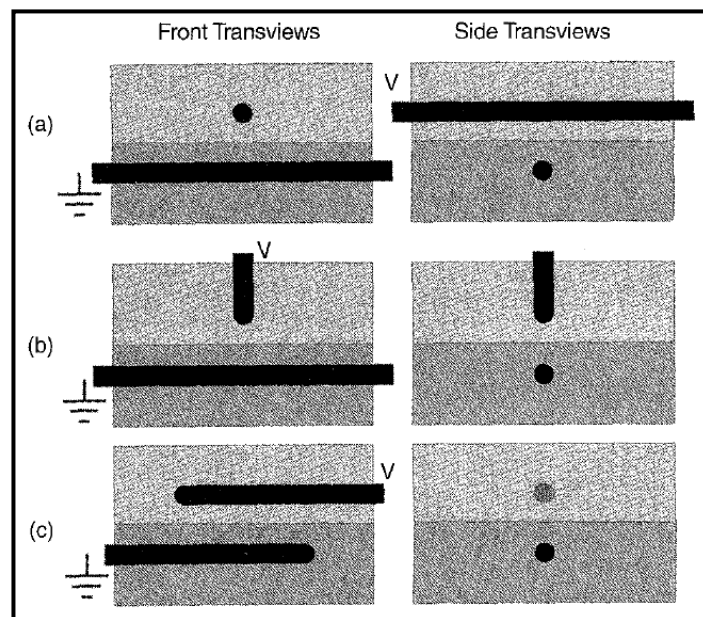
Fig. 2.10: Electrode configurations - interface testing cell for multi-stress ageing [40]

2.2 *Epoxy/ SiR interface study*

The interest of this thesis is to study the **Epoxy | SiR** interface, as this would be required to verify the design of the new inner-cone GIS termination. Some studies have been carried out by different institutes, which is elaborated in this section.

2.2.1 *Study at Chalmers University of Technology, Sweden*

The work of *Johan Andersson*, *Stanislaw Gubanski* and *Henrik Hillborg* [28] aims to design a setup to test the impact of adhesion defects in the **Epoxy | SiR** interface. The effect of primer in the interface was also studied.

The test setup included a specifically designed electrode setup. The samples were artificially aged by exposing them to partial discharges in humid conditions. This degradation was analysed using infrared spectroscopy and optical microscopy. The samples were vertically clamped between two grounded brass plates. 75µm radius tungsten wires were used as HV electrode. The ground was 30 mm away from the HV electrode wire. The aluminium spheres were used to control the electric field strengths at the edges of the samples.
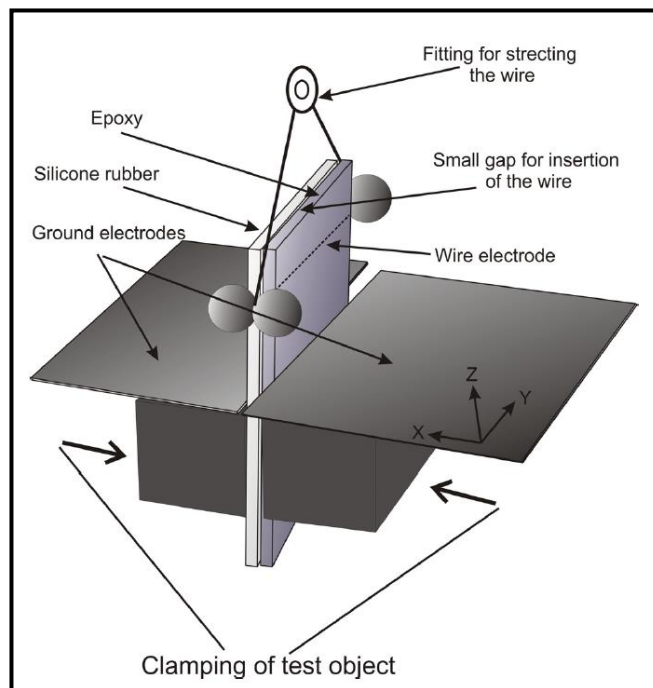
Fig. 2.11: Experimental setup to analyse interfacial tracking in aged interfaces [28]

Some inferences from this work include:

- The test setup produced a tangential component of electric field that was about **10^3 times higher** than the normal electric field.

- The **volume resistivity** of both epoxy and SiR decreased due to boiling (higher temperatures).

- The effect of humidity caused larger **water absorption** in SiR than in epoxy.

- Due to PD, there were **cracks** observed on the surface of the aged samples.

- The degradation of epoxy is due to **hydrolysis** reactions

Although the research did not lead to any specific conclusions, it is specified here to give a feeling of the different test setups and research works in this area.

2.2.2 Study at ABB Corporate Research, Sweden

The works of *Cecilia Forssen*, *Anna Christerson* and *Daniel Borg* proposes a novel test setup for testing the effect of mechanical pressure and surface smoothness on the interfacial electrical performance of the **Epoxy | SiR** interface. The work [7] gives the results of AC breakdown testing while [8] provides an insight into the performance of the same test setup to lightning impulse (LI) breakdown testing.
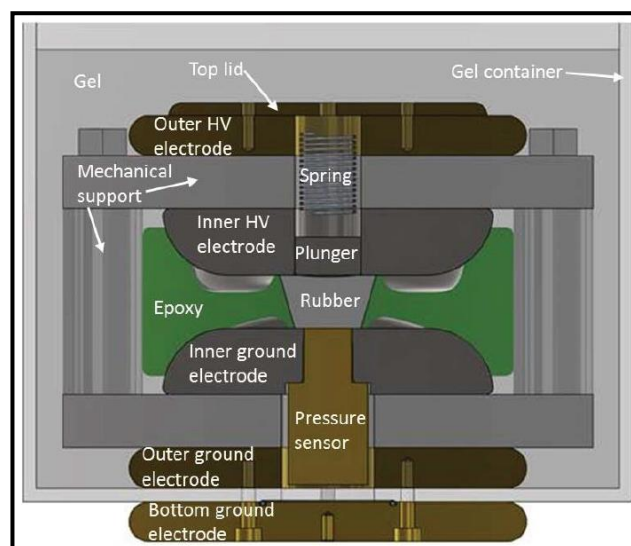
Fig. 2.12: Test setup of [7, 8]

The test setup consists of a conical rubber plug that is fitted into an epoxy disc. This disc is then pressed between two electrodes. The test cell is compressed, and the pressure is controlled through a plunger and spring assembly. There is a pressure sensor in the bottom electrode. The whole test setup was cast in insulating gel to avoid flashover. The difference in breakdown performance for rough and smooth interfaces was studied.

Some noticeable drawbacks of this test setup are as follows:

- the electric field at the epoxy/ SiR interface is **non-uniform**.

- the test setup and samples are **complicated** to reproduce

- the electrically active part of this test setup is only **10mm** long.

- The test setup is cast in insulating gel / transformer oil, thus, there **could** be influence of the gel on the results of the testing

The authors performed experiments for two pressure values (low and high) and two interface types (rough and smooth). The conclusions of [7] was:

- electric strength of the interface **improved** with increase in interfacial pressure and smoothness of the surfaces

- **smaller scatter** was observed for rough surface than the smooth surface.

- AC breakdown tests had satisfactory results for **36 out of 39** tests.

<div align="center">(a)   (b)</div>
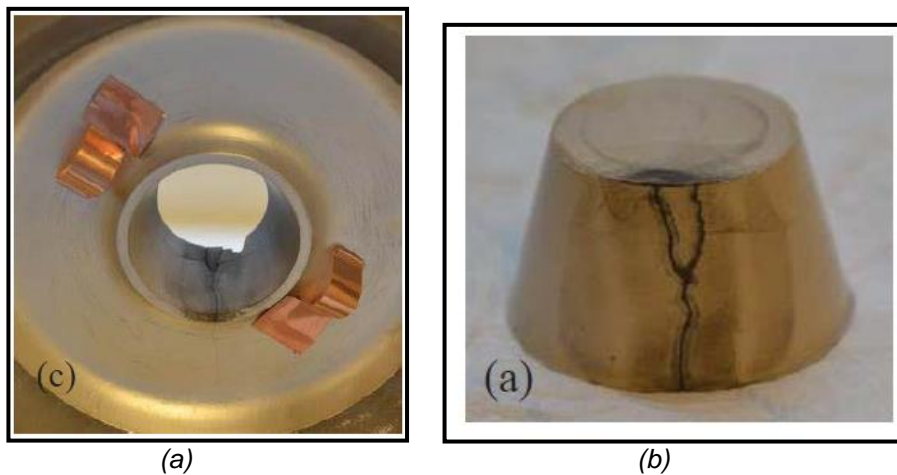
Fig. 2.13: Breakdown tracks in (a) epoxy and (b) SiR for AC breakdown tests [7]

For the lightning impulse testing [8], the same test setup is used. 100kV was applied and the peak voltage was successively increased by 10kV. 24 out of the 30 samples and breakdown at the interface. The difference in breakdown performance for rough and smooth interfaces was studied. As expected, better LI performance was obtained for smoother surfaces.

2.2.3 Study at CRIEPI, Japan

The work of *Toshikoro Takahashi*, *Tatsuki Okamoto*, *Yoshimichi Ohki* and *Kohei Shibata* is in the direction of development of all-solid insulation. The work [52] illustrates the interfacial breakdown performance of two types of model samples (electric field parallel and perpendicular to the interface). PD characteristics of the interface and effect of air at the interface were also studied.

The test setup shown in *Fig. 2.14 (a)* is used to find the PD inception voltage at the interface. Translucent epoxy and SiR were specially moulded to create this test setup. Transformer oil is used to put together the two materials. HV is applied to the right two electrodes while the two electrodes in the left side are grounded.

Fig. 2.14: Test setups of [52] (a) to measure PD inception stresses and (b) to study the interface model

The relation between the breakdown voltage and the thickness of the air layer is examined using the model in *Fig. 2.14 (b)*. The height of the spacers is varied to adjust the thickness of the air layer. A back electrode is used to make the electric field perpendicular.

The conclusions of this research work are:

- Setup shown in *Fig. 2.14 (a)* is sufficient to measure PD inception voltage at the interface. The design stress was proposed to be **10 kV$_{RMS}$/mm**

- Setup shown in *Fig. 2.14 (b)* gives a good approximation of the delamination that is caused due to aging. For parallel electric fields, the breakdown voltage increases with decrease in the thickness of the air layer. For perpendicular electric fields, different inferences are made for positive and negative applied voltages.

The conclusions/ inferences from the literature study are presented in the form of 'guidelines for the test setup'. This is presented in Chapter 4.

3. Hyperelastic material modelling of silicon rubber

This chapter provides a detailed explanation about the need for such a material modelling technique. It provides a detailed study of different modelling techniques (including linear elastic modelling). It then explains about the different types of hyperelastic models and the model that is chosen for the type of silicon rubber used in the GIS cable termination.

3.1 Stress – strain curves

Every engineering material is subject to external forces. When a solid object is deformed, an internal reactive force tends to resist the deformation. This force is called **stress**. The measure of deformation is called **strain**.

Every material is represented by a graphic figure known as the 'stress-strain curve'. These curves give a good understanding of the type of material and its behaviour to various types of mechanical forces [15].
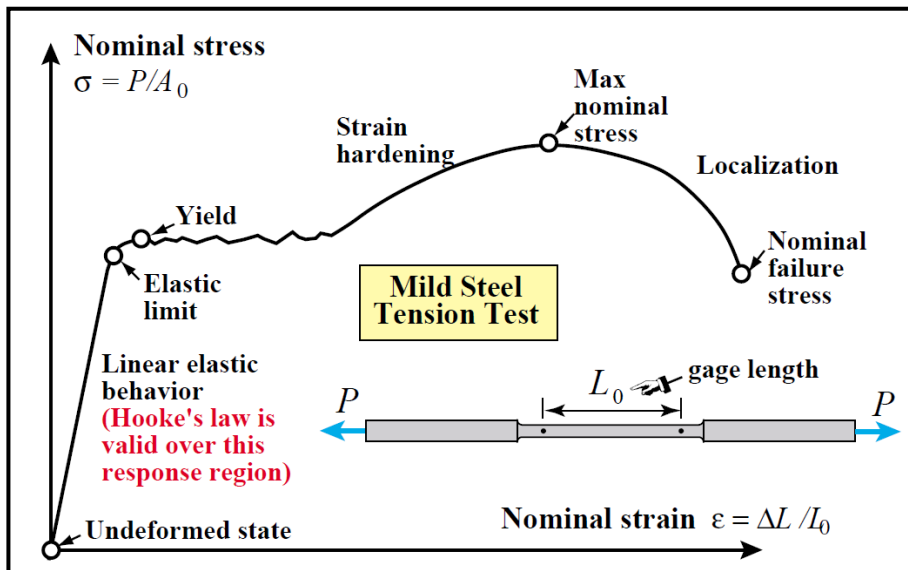
Fig. 3.1: Stress – strain curve of mild steel [54]

The stress-strain plots of materials are used as an important tool to classify their use for different applications. The structural loadability of materials is found from this curve. The curve also gives an understanding of properties like stiff/ elastic, hard/ soft, strong/ weak, brittle/ tough.

This thesis focusses on silicon rubber, as it would be the primary material of the inner-cone termination. So, the mechanical tests on rubber will be explained here. Several tests are performed to plot the stress strain curves. Each test helps to understand properties and (possible) applications of the material.
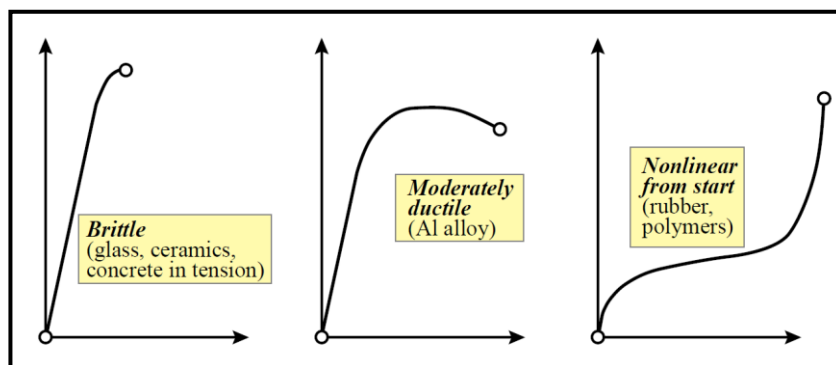
Fig. 3.2: Types of stress-strain curves of different material types [54]

3.2 *Need for hyperelastic material modelling*

Rubber is a unique material by being very soft, exhibits very large strains, has a very nonlinear stress-strain relation, has a low elastic modulus and is highly elastic [2, 30]. This allows rubber are used for a variety of purposes from vehicle tyres, seals, hoses and so on.
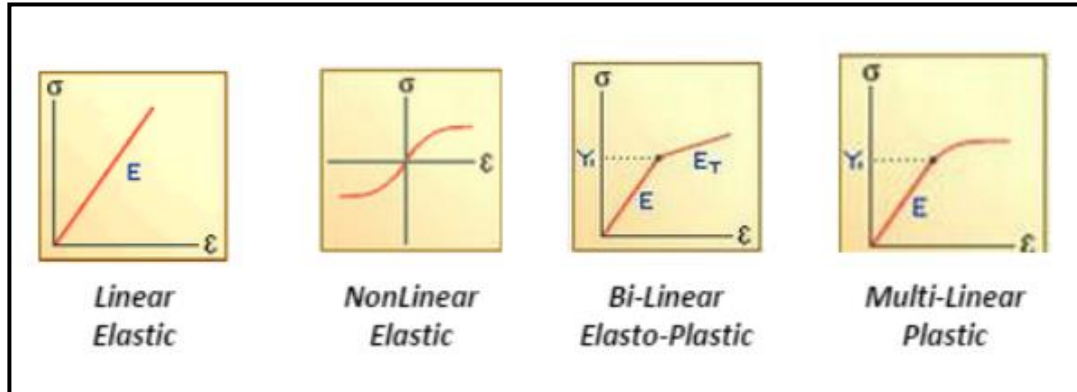
Fig. 3.3: Types of stress strain curve of different material classifications [33, 54]

Linear elastic material follows the Hooke's law which is given by the following relation where, '**σ**' is the **stress**, '**ε**' is the **strain** and '**E**' is the constant known as the **Young's modulus** or **modulus of elasticity** of the material.

$$\sigma = E. \, \varepsilon \tag{2}$$

Elastomers like rubber are modelled as hyperelastic materials instead of linear elastic. This is because the stress is determined by the current state of deformation and not the path or history of deformation. This is shown in *Fig. 3.4*.
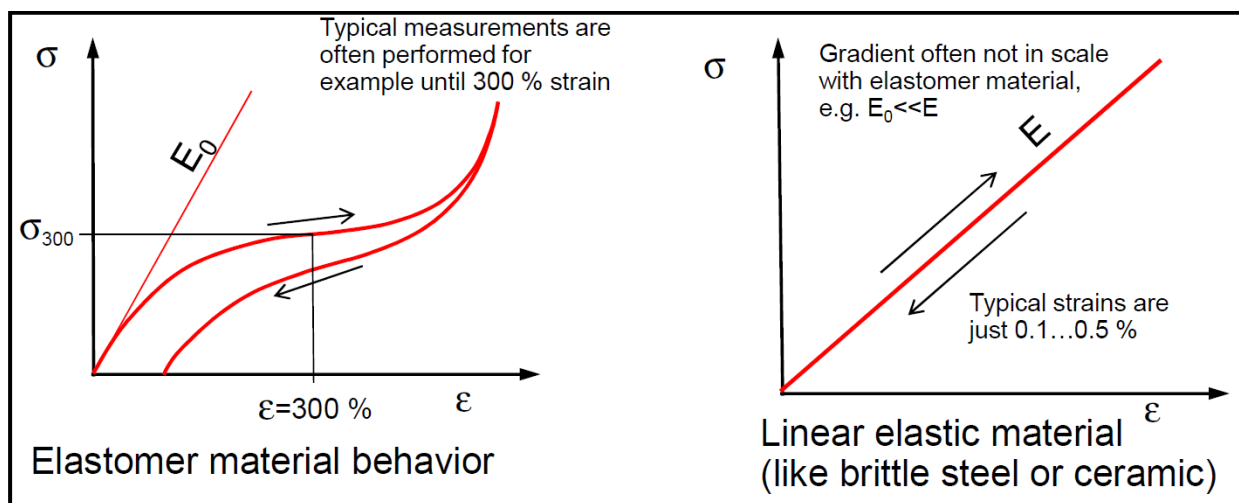
Fig. 3.4: Stress-strain curves of elastomers and linear elastic materials. [39]

Some important differences between linear elastic and elastomers are as follows:

Linear elastic material	Hyperelastic material
Stress varies linearly with respect to strain	Stress can only be determined by current state of deformation
Typical strains are **less than 100 %**	Typical strains are until **700 %**
Extrapolation of existing stress-strain data is possible	Extrapolation is not possible
Loading and unloading curves are (almost) identical	Loading and unloading curves differ
Example: *Steel, ceramic, wood, etc.,*	Examples: *Silicon rubber, biological tissues, heart stents*, etc.,

Table. 3.1: Comparison of linear elastic and hyperelastic materials

To demonstrate the need for hyperelastic material modelling, a COMSOL [10] simulation was performed. A 2D axisymmetric simulation was done using a cylindrical block of rubber of diameter 28.6mm and height 12.5mm. The SiR block is compressed by 5mm on one side ((a) of *Fig. 3.5)* and the other side ((b) of *Fig. 3.5*) is fixed.

(a)   *(b)*
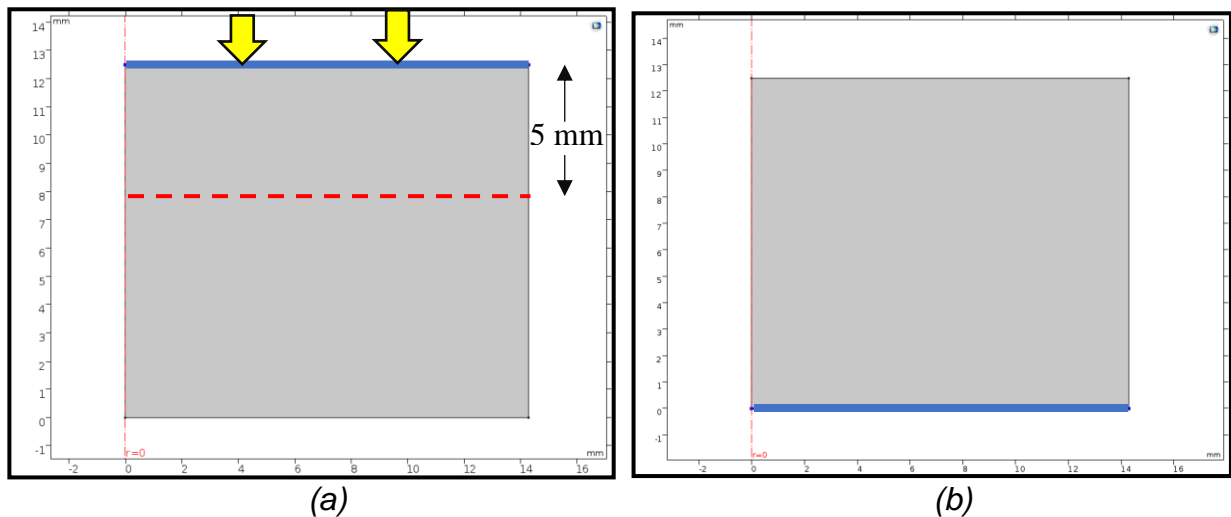
Fig. 3.5: Boundary conditions [in blue] (a) displacement of -5mm and (b) fixed constraint of SiR used in 2D axisymmetric FEM simulation

The same boundary conditions are applied to a linear elastic model and some important types of hyperelastic material models (explained in *section 3.3*). The results are as follows:
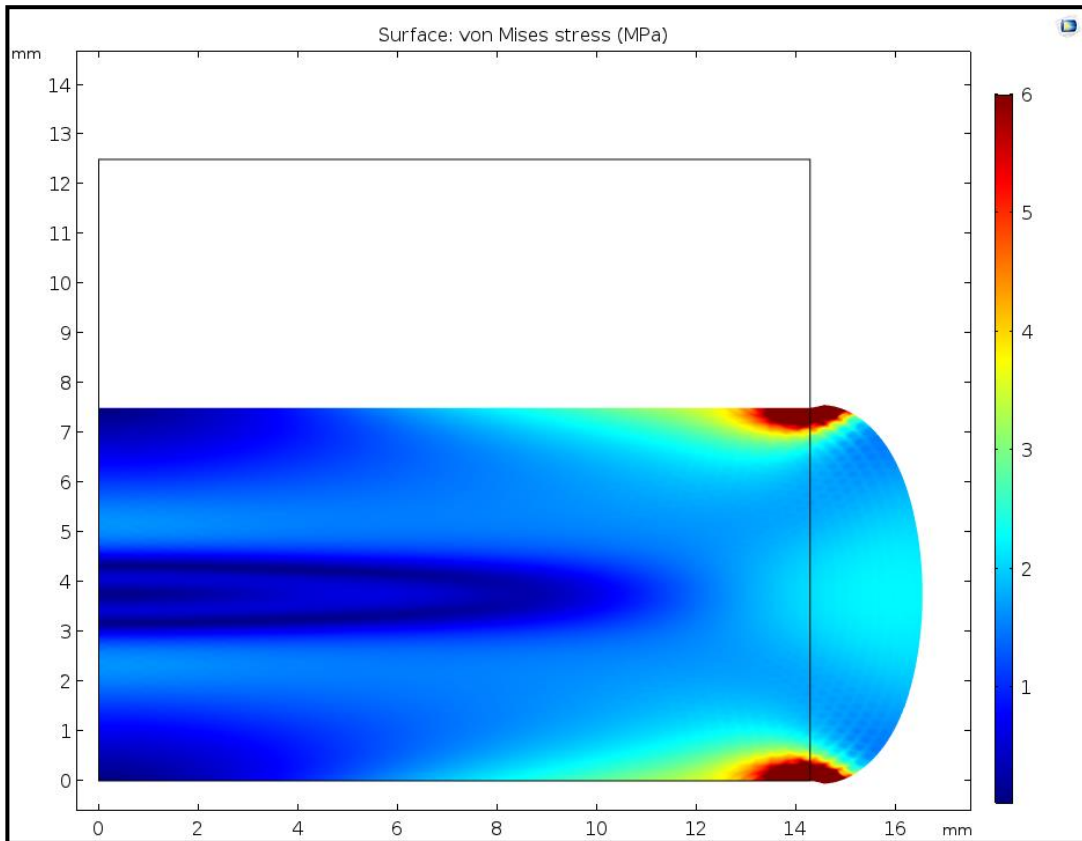
Fig. 3.6 (a): Plot of von Mises stress (in MPa) for Linear Elastic model
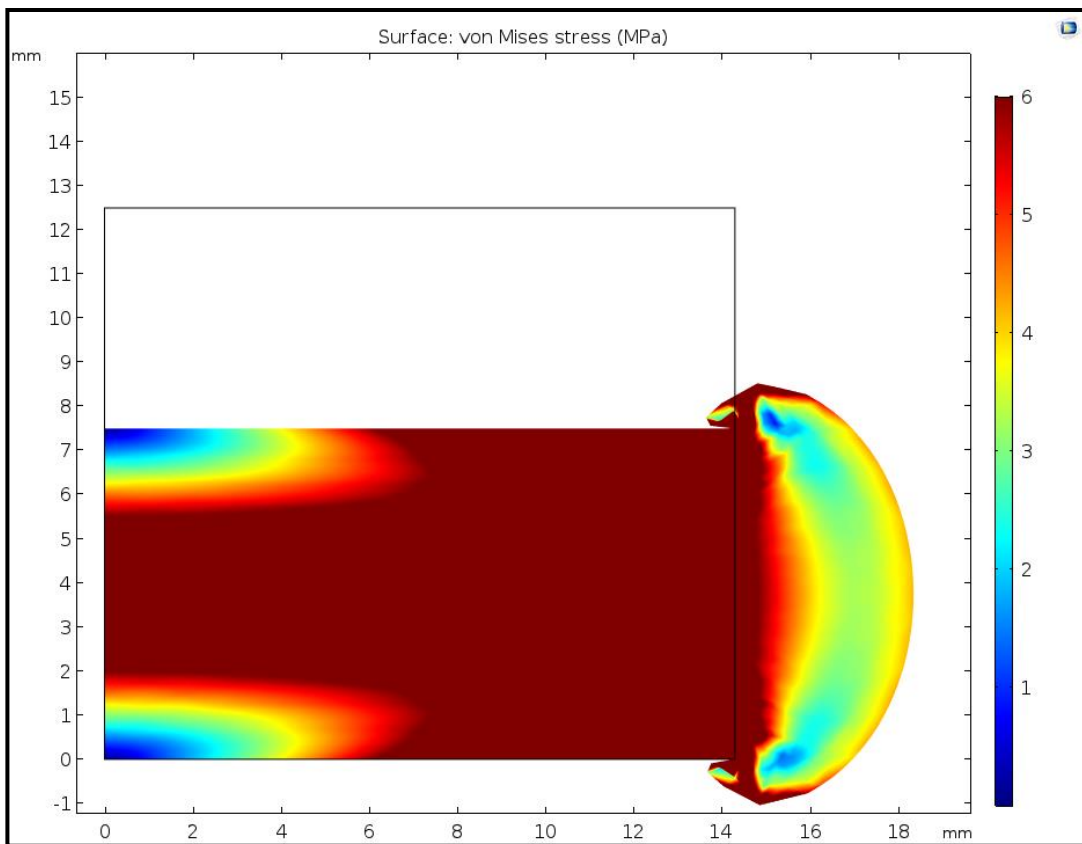
Fig. 3.6 (b): Plot of von Mises stress (in MPa) for Mooney-Rivlin 2 parameter model
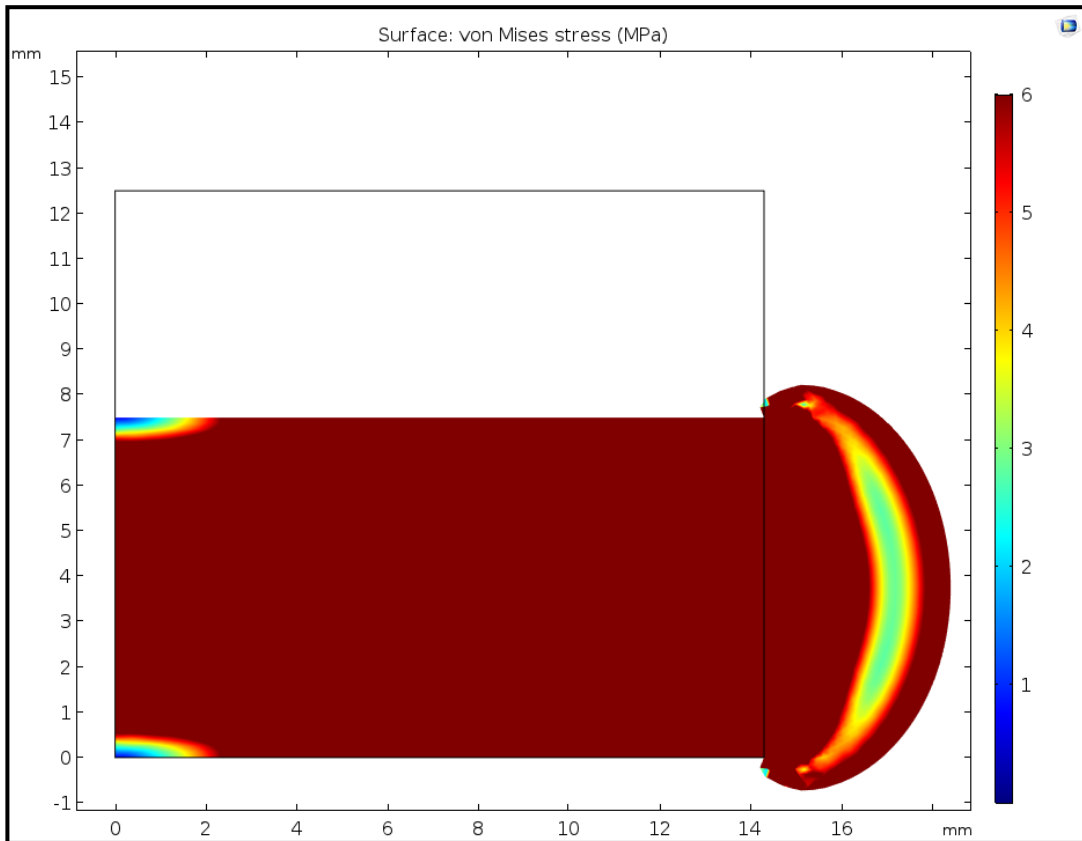
Fig. 3.6 (c): Plot of von Mises stress (in MPa) for Mooney-Rivlin 5 parameter model
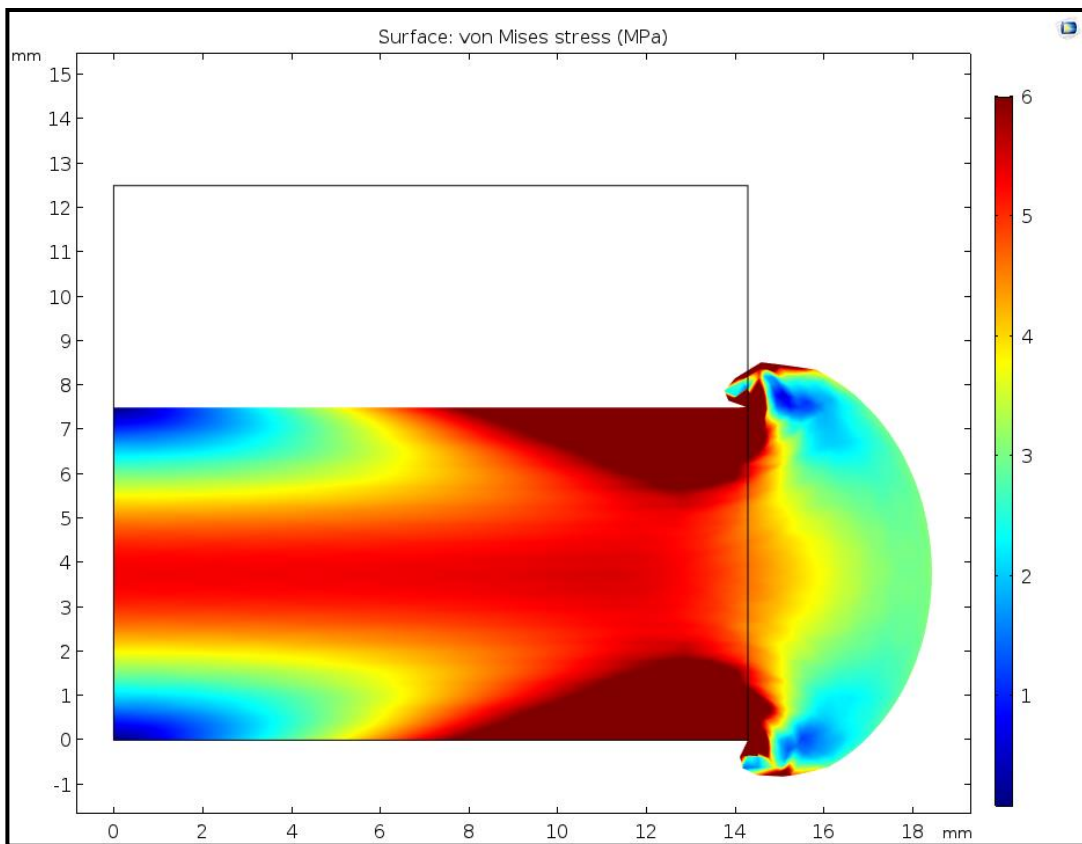
Fig. 3.6 (d): Plot of von Mises stress (in MPa) for Arruda Boyce model
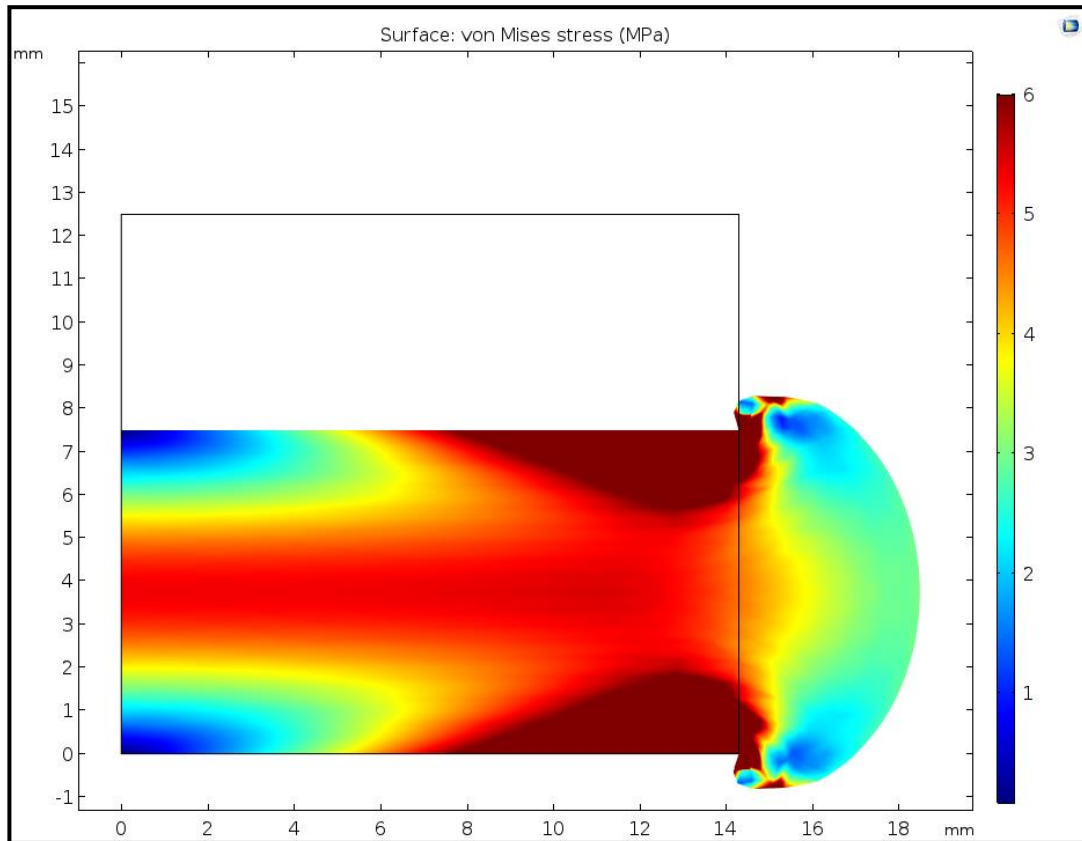
Fig. 3.6 (e): Plot of von Mises stress (in MPa) for Neo-Hookean model

The various plots of the von Mises stress show, how the cylindrical block of silicon rubber would behave when modelled using linear elastic method (*Fig. 3.6 (a)*) and using different hyperelastic modelling techniques (*Fig. 3.6 (b)- Fig. 3.6 (e)*). It must be noted that almost all the hyperelastic models exhibit a similar behaviour in terms of the deformation of rubber. It is also important to note the difference in internal stresses between each type of modelling.

Another important feature that must be noted is during the bulging of rubber in *Fig. 3.6 (c),* the high magnitude of forces/ stresses in the exterior (outer-most part) of the material to control the shape of the rubber is visible – notice the high stress region at the edge of the bulged SiR. This feature is also present in a lesser extent in the other hyperelastic simulations. This is clearly absent in linear elastic model (*Fig. 3.6 (a)*) simulation.

3.3 *Types of hyperelastic material modelling*

To understand the different types of hyperelastic models, it is necessary to understand some properties of hyperelastic materials.

Strain (ε) is defined as the ratio of the change in length of material ($l_1 - l_0$) to the original length (l_0).

$$\varepsilon = \frac{l1-l0}{l0} = \frac{\Delta l}{lo} \tag{3}$$

27

Stretch ratio (λ) is defined as the ratio of the current length to the original length of the material.

$$\lambda = \frac{l1}{l0} = \frac{l1 - l0 + l0}{l0} = \varepsilon + 1 \tag{4}$$

Similarly, the principal strains in the three axes are represented as λ1, λ2 and λ3. The three directions (axis) also have stretch invariants known as I1, I2 and I3. For hyperelastic materials, another important property is the *strain energy density function* (W). It is a function that relates the strain energy density to the deformation gradient. The general form of strain energy density function equations is:

$$W = \sum_{i+j=1}^{N} C_{ij}(I_1 - 3)^i (I_2 - 3)^j + \sum_{k=1}^{N} \frac{1}{D_k} (J - 1)^{2k} \tag{5}$$

Where C_{ij} and D_k are material constants that are determined by curve fitting/ tests on the material. *Eqn. 5* shows that the strain energy density is a polynomial function and depending on its order, one or more curves (inflection points) may appear.

Different types of hyperelastic models are created and modelled depending on the strain rate of the material (SiR). Each of the types have distinct strain energy density function. Some of the most commonly used types of modelling are as follows:

- Mooney Rivlin (2 parameter, 3 parameter, 5 parameter and 9 parameter model)

- Arruda Boyce model

- Neo Hookean model

- Ogden model (1st, 2nd and 3rd order models)

- Yeoh model (1st, 2nd and 3rd order models)

- Gent model

- Blatz – Ko

- Response Function model

- Polynomial model (1st, 2nd and 3rd order models)

Each of the above-mentioned material models are used for different types of elastomers and for different applications (elevated temperature, different strain rates, etc.,). Detailed explanation of the different model types is avoided in view of the objective of this thesis report.

3.4 *Mechanical tests of SiR*

To quantify the silicon rubber used as an electrical insulator for the proposed GIS cable termination, the first step is to perform some mechanical tests, in order to accurately obtain the stress – strain relationships. These tests were carried out in accordance with various NEN/ ISO standards.
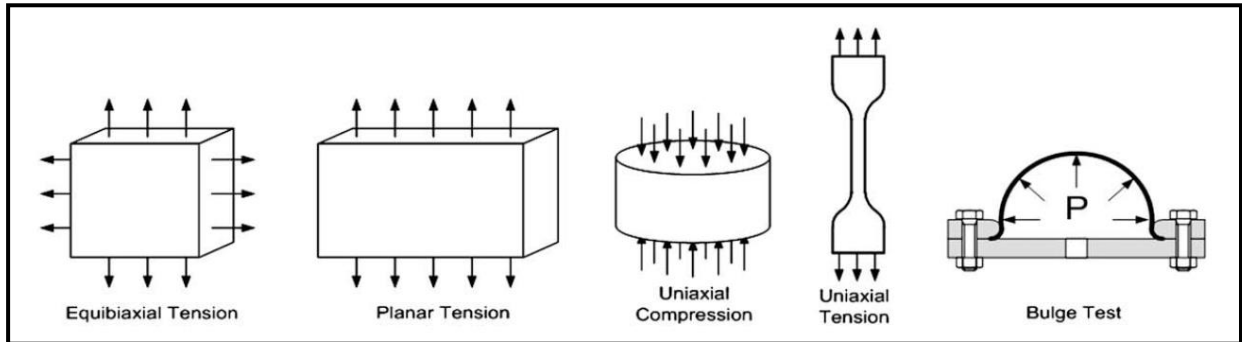
Fig. 3.7: Types of mechanical tests performed on rubber [31]

Two frequently used tests for rubber are tensile (uniaxial, planar or biaxial) and compression (uniaxial). NEN ISO – 37 [42] is used for the tensile strength measurements while NEN ISO – 815/ NEN ISO - 7743 [43, 50] is used for the compression tests [31]. Uniaxial tensile strength measurements were made at room temperature and at elevated temperature of 80 °C. The higher temperature was chosen as 80 °C because the maximum operating temperature of the cable conductor is 90 °C.
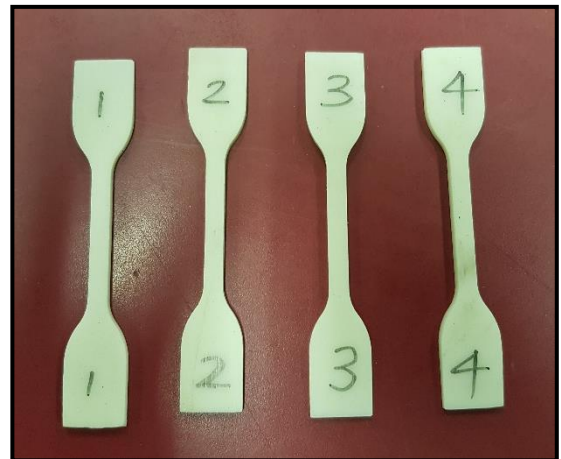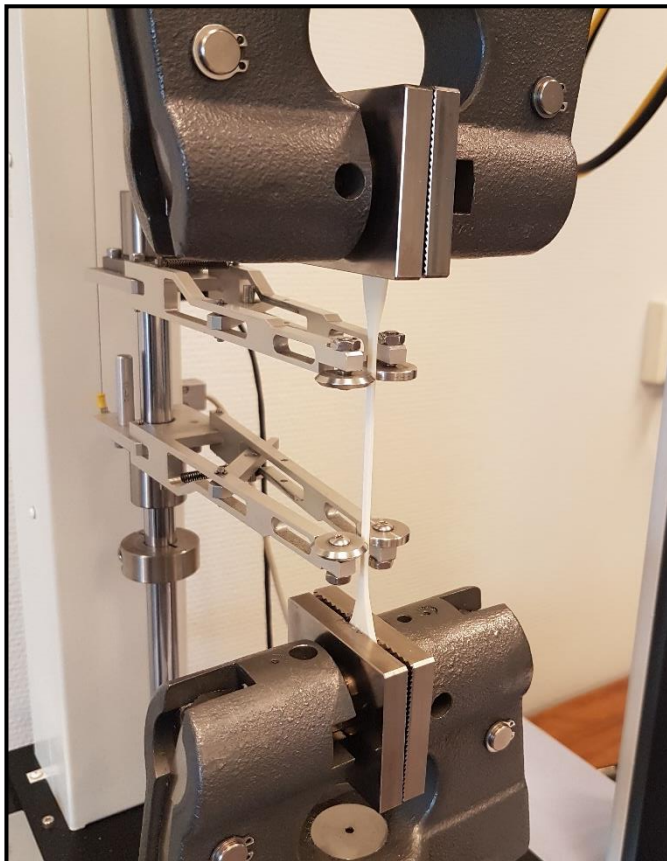
Fig. 3.8: (b): Dumbbell shape samples

Fig. 3.8 (a): Test setup for tensile strength measurements

The tests at two different temperatures showed varied results for the performance of silicon rubber. These curves were plotted as shown in *Fig, 3.9.*
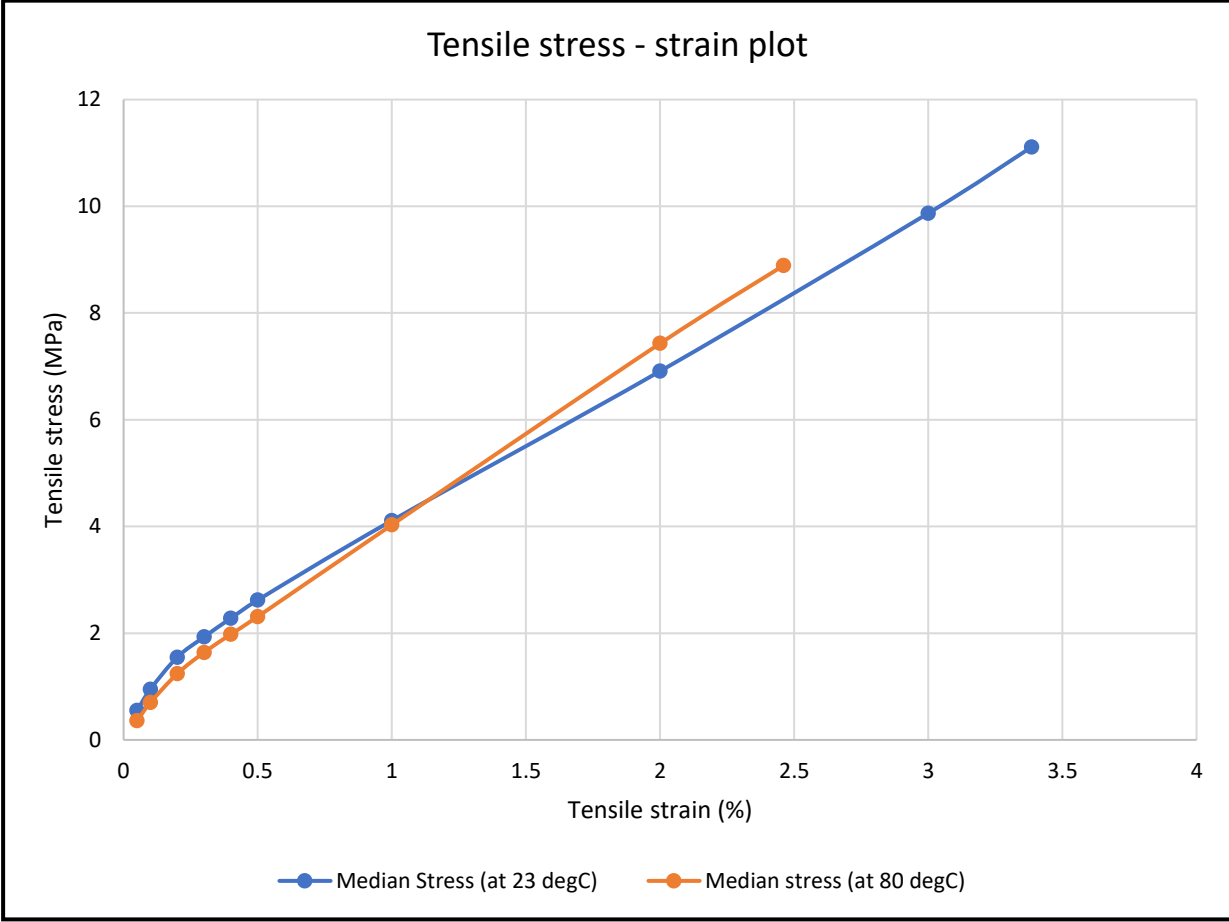
Fig. 3.9: Median tensile stress-strain plots of SiR at 23℃ and 80℃
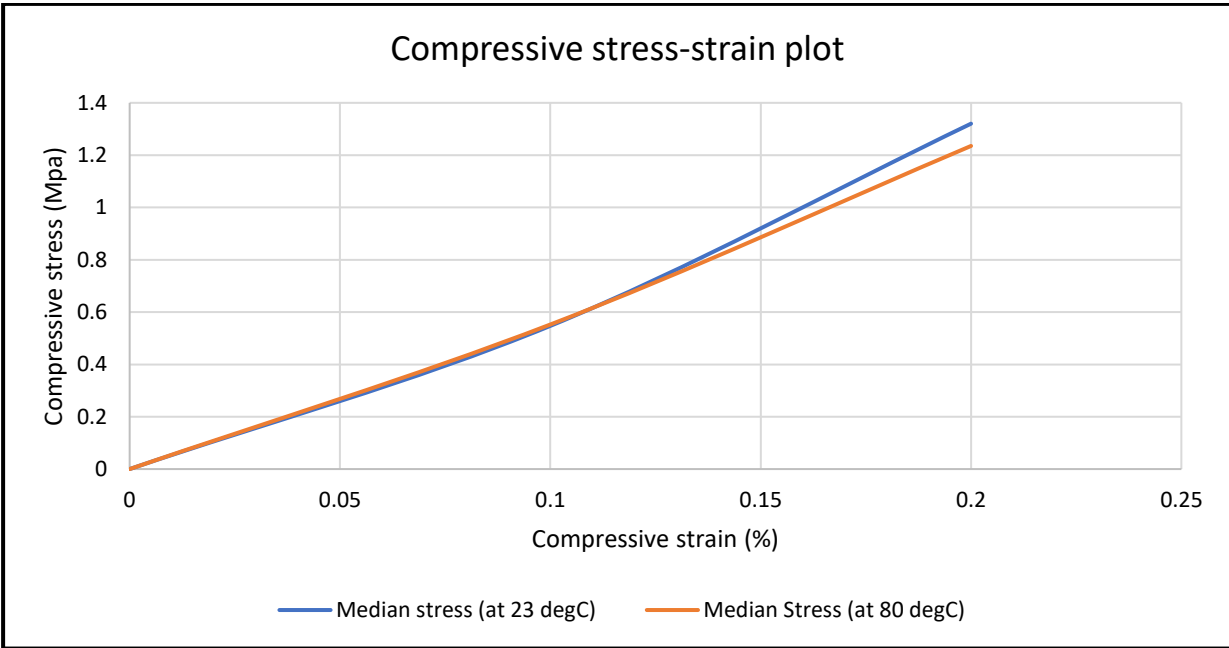
Fig. 3.10: Median compressive stress-strain plots of SiR at 23℃ and 80℃

30

As per NEN ISO – 37 [42], the samples must be cut according to a predefined shape and size. Then, the samples must be tested at a constant nominal velocity of 500 mm/ min. Five samples were tested, and the median of the individual values were taken as the final values of the material. Any test sample that breaks outside the narrow portion of the dumbbell is discarded and a repeat measurement was done. It must be noted that the last point of each of the curves is the point at which the sample broke.

Compressive tests were also performed on the silicon rubber at the two temperatures in accordance to NEN ISO – 7743. Limited readings were taken due to practical limitations in the test setup. The results of the tests are shown in *Fig. 3.10.*

A combined plot of the silicon rubber is given in *Fig. 3.11* just to give an idea of the complete stress strain relation.
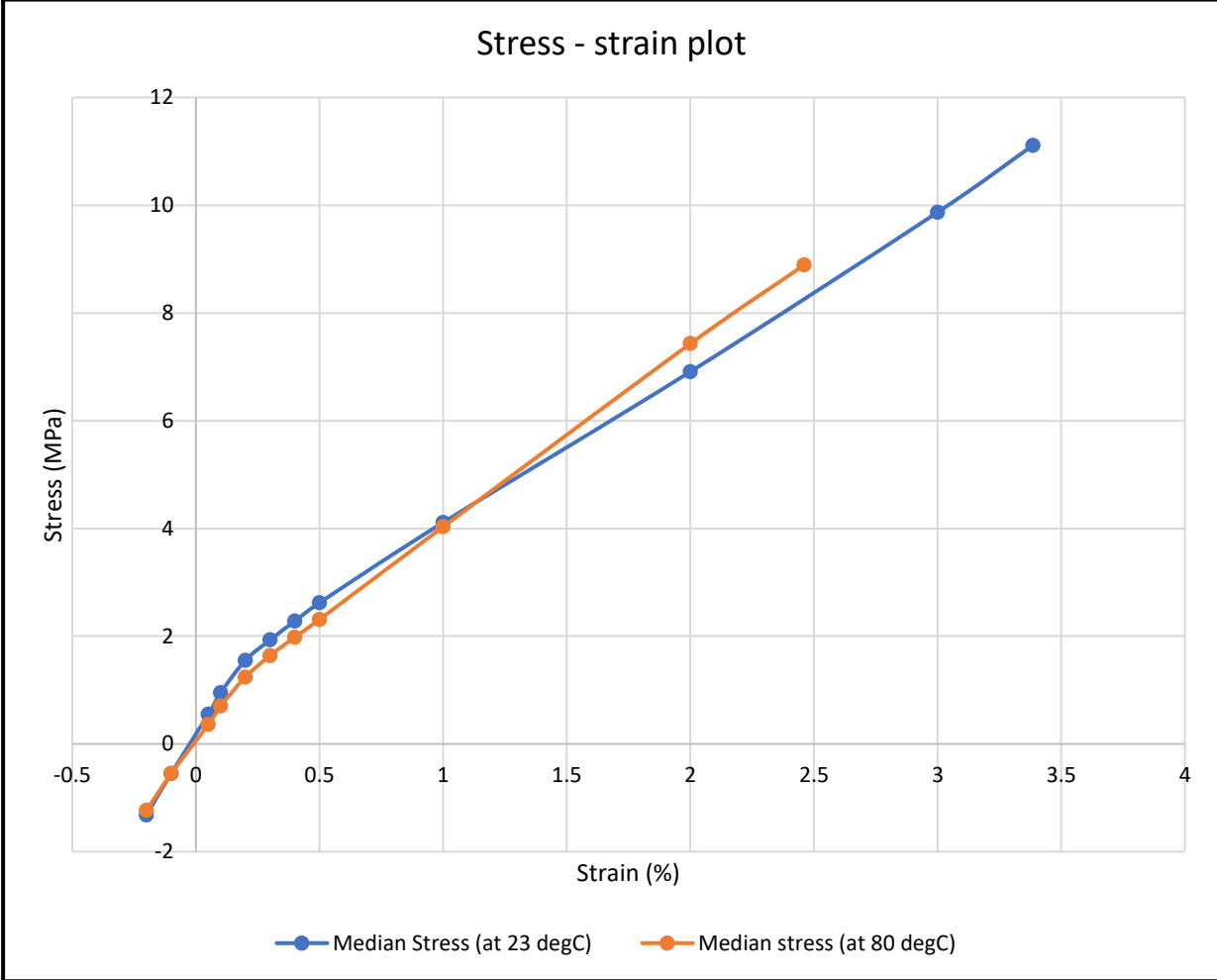
Fig. 3.11: Median stress-strain plots of SiR at 23℃ and 80℃
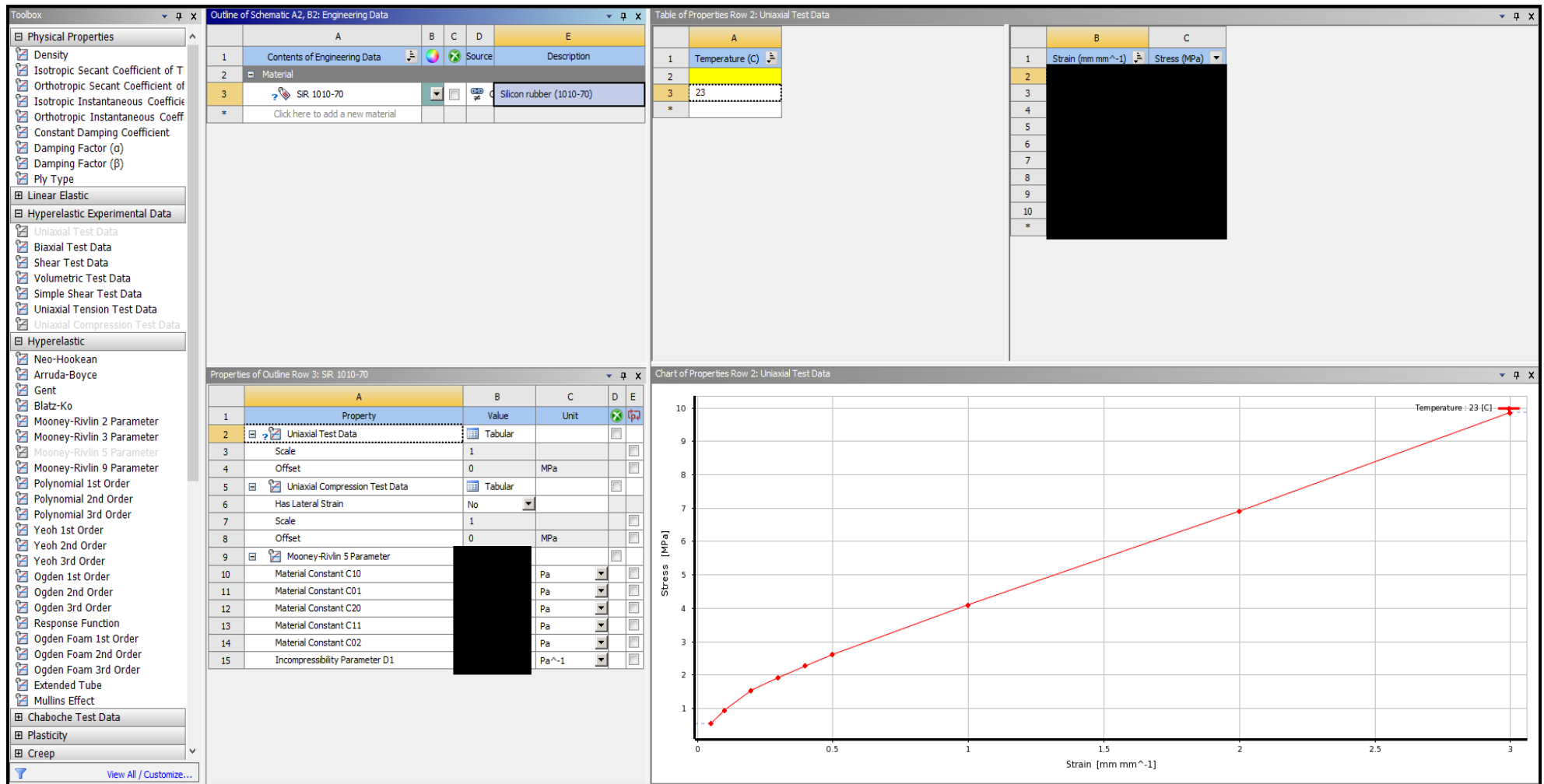
Fig. 3.12: Screenshot of ANSYS workbench for hyperelastic material data curve-fitting

3.5 *Determining the type of material model*

The stress-strain plots from *Fig. 3.9* is used as an input to the ANSYS workbench [3]. The data is plotted and each method of hyperelastic material modelling is chosen and curve-fitting is performed [11, 22, 32, 41, 51]. The software gives a curve-fit plot of the test data along with the characteristic material constants (*Eqn. 5*). A screenshot of the ANSYS Workbench window is shown in *Fig. 3.12*.

Each type of material model is checked with the available test data. The results of the curve fitting process provide the material constants of the best fitted model (refer *Eqn. 5*). The results from ANSYS workbench are as follows:

Results: Mooney Rivlin 5 parameter model (at 23°C)

Material constant C10

Material constant C01

Material constant C20

Material constant C11

Material constant C02

Results: Mooney Rivlin 5 parameter model (at 80°C)

Material constant C10

Material constant C01

Material constant C20

Material constant C11

Material constant C02

For 23°C, it is found that the curve fitting algorithm of ANSYS recognizes **Mooney Rivlin 5 parameter model** as the best curve fit. Thus, this model is chosen as the Hyperelastic material model for the silicon rubber at 23°C.

For 80°C, it is found that the curve fitting algorithm of ANSYS recognizes **Mooney Rivlin 5 parameter model** as the best curve fit. Thus, this model is chosen as the Hyperelastic material model for the silicon rubber at 80°C.

3.6 Conclusions

Mooney Rivlin 5 parameter model is chosen as the Hyperelastic material model of the silicon rubber that is being used for this thesis (for experimental testing and for the GIS cable termination).

The results of the curve fitting provide the material constants which are the parameters of the strain energy density equation *(Eqn. 5)*. These parameters will become the input for the FEM software. However, it must be noted that the properties of rubber vary with temperature.

4. Design of test setup for interfacial study

This chapter provides a detailed explanation about the process of designing the test setup that is used for interfacial testing. It then explains about the samples and each component of the test setup. The chapter ends with a summary of the newly designed test setup.

4.1 Learning outcomes from literature study

A large variety of test setups are proposed by different authors in their respective works for interfacial study. These setups were analysed in detail along with the *CIGRE 15-10* [29] recommendations. The drawbacks of each test setup were analysed in detail and some important requirements for the test setup (for this thesis) were drafted. They are as ranked in descending order of their importance, as follows:

1. Setup must withstand about **40 - 45 kV** AC voltage without flashover. *This numerical value was estimated from literature study of similar interfaces.*

2. Setup must withstand **Lightning Impulse (LI)** voltages up to 2-3 times the AC breakdown value.

3. Setup must be able to mechanically withstand about **3 - 4 bar** of interfacial pressure.

4. Setup must not be immersed in **oil/ gel.**

5. Setup must have **no metal electrode** at the interface [29].

6. Setup must have a **simple** configuration.

7. Setup must be **modular** i.e. easy to replace and upscale/ downscale if necessary.

8. Setup must not allow any **misalignment** of samples.

9. Samples should be **easily producible**.

10. Setup should be **mechanically robust**.

11. Setup should allow various surface **defects** to be introduced.

12. Setup should allow the study **mechanical pressure** effects.

13. Setup should enable one to study the **effect of silicone oil** or other liquid insulants.

These requirements were used as a basis to design the test setup. Different configurations were analysed in detail. The test setup used in this thesis is explained in the next sections and the reasons behind each feature/ parameter is also explained in detail.

4.2 *Test setup – draft designs*

A few draft designs were simulated using COMSOL Multiphysics, to understand the electric field distribution and estimate the voltage levels needed. Some of the models are mentioned here.

4.2.1 *Draft setup #1: SiR- Epoxy*

This setup involved thin layers of silicon rubber and epoxy being placed on top of each other as shown in *Fig. 4.1*. Two circular electrodes are used for the HV and ground terminals respectively. The electrodes are present on opposite sides. Non-metallic blocks are used as weights to apply interfacial pressure. The FEM simulation of this setup was done at 1 kV of applied voltage.
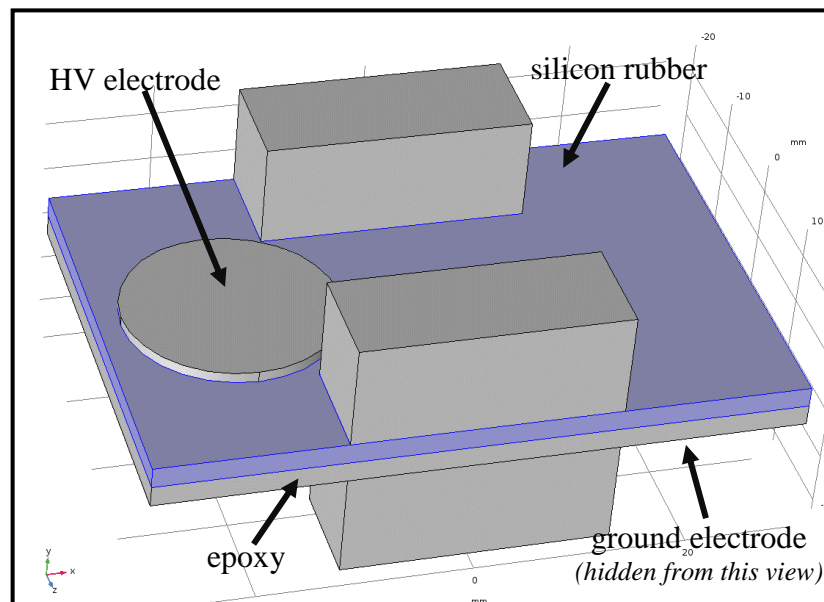
Fig. 4.1: Draft setup #1 - components

This setup has the following advantages:

- It had a tangential and normal component of electric field which is **similar** to the actual interface in a GIS termination.

- The application of weights (interfacial pressure) is **relatively simple** as different weights could be used to simulate different interfacial pressures.
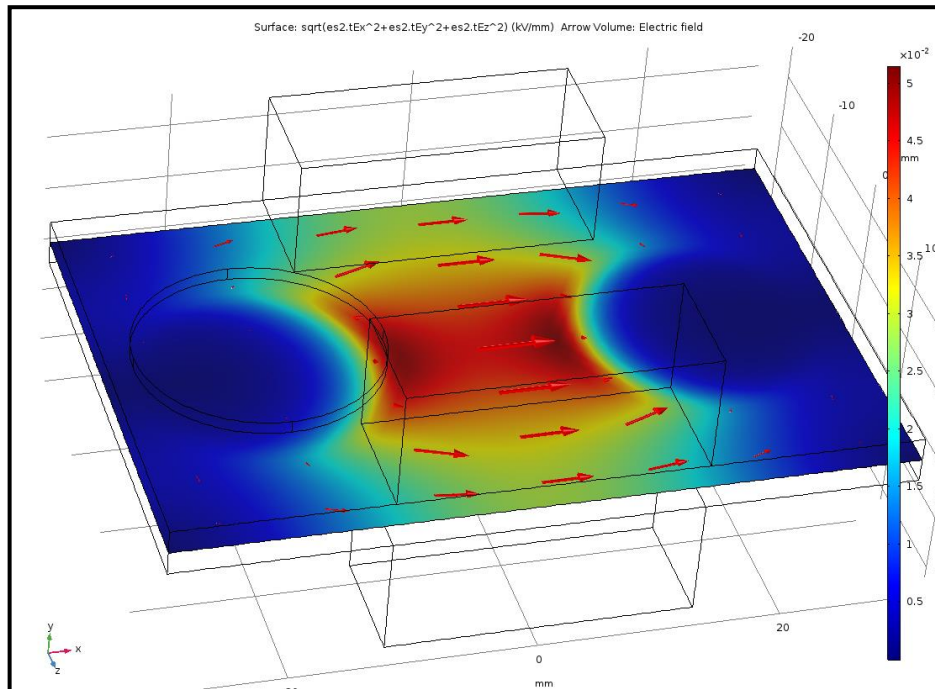
Fig. 4.2: Draft setup #1 – Tangential electric field at the interface

This setup has the following disadvantages:

- The tangential component of electric field is very small (**0.05 kV/mm for 1 kV of applied voltage**). This would mean that very large voltages should be applied to observe interfacial breakdown.

- The **contact area** of the epoxy and silicon rubber is large – thus the manufacturing of multiple samples for such a test setup would be cumbersome.

- The **contact area** of the epoxy and silicon rubber is large – thus large weights would be necessary to create interfacial pressure of a few bar.

4.2.2 Draft setup #2: SiR – Epoxy – SiR

This setup involved three layers of materials – two epoxy and one silicon rubber. Two circular electrodes are used for the HV and ground respectively. Non-metallic blocks can be used as weights to simulate interfacial pressure. This setup allows for two contact surfaces and thus more active area for investigation.
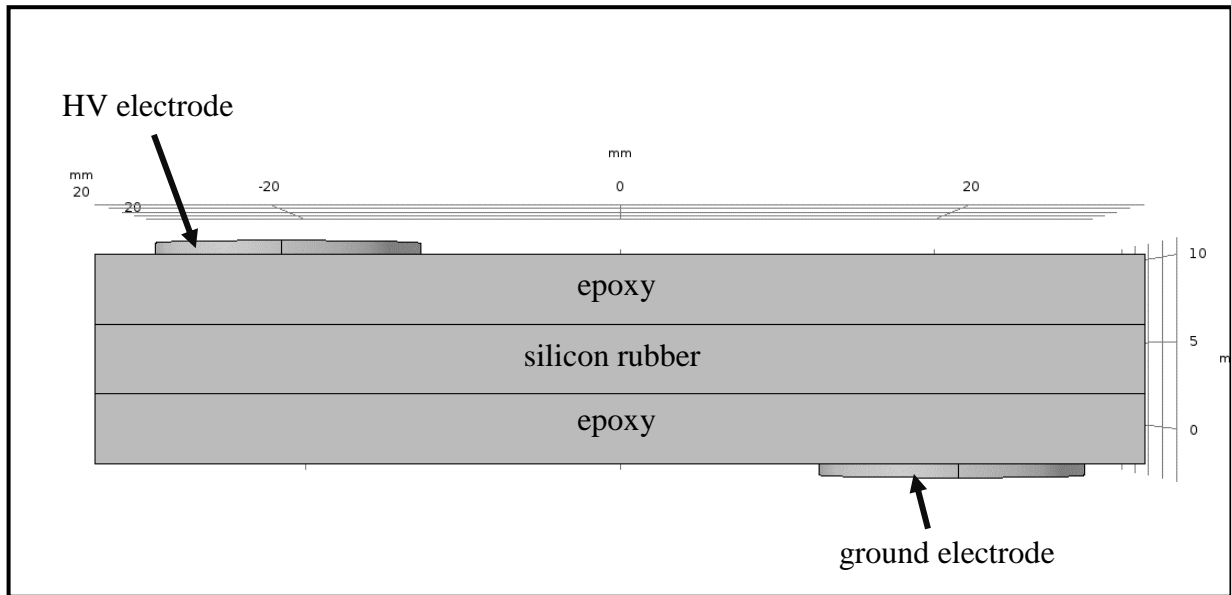
Fig. 4.3: Draft setup #2 - components

This setup has the following advantages:

- It has a tangential and normal component of electric field which is **similar** to the actual interface in a GIS termination.

- The application of weights (interfacial pressure) is **relatively simple** as different weights could be used to simulate different interfacial pressures.

- Two active surfaces meant that more investigation could be carried out into the performance of the interface.
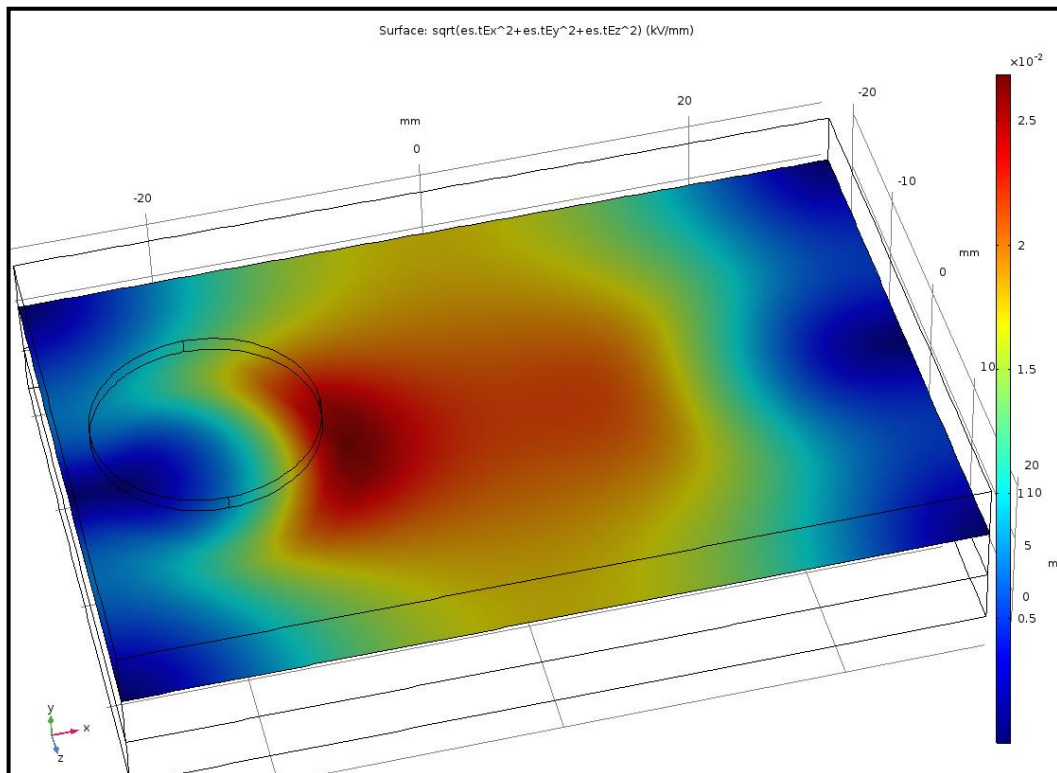
Fig. 4.4 (a): upper interface

39
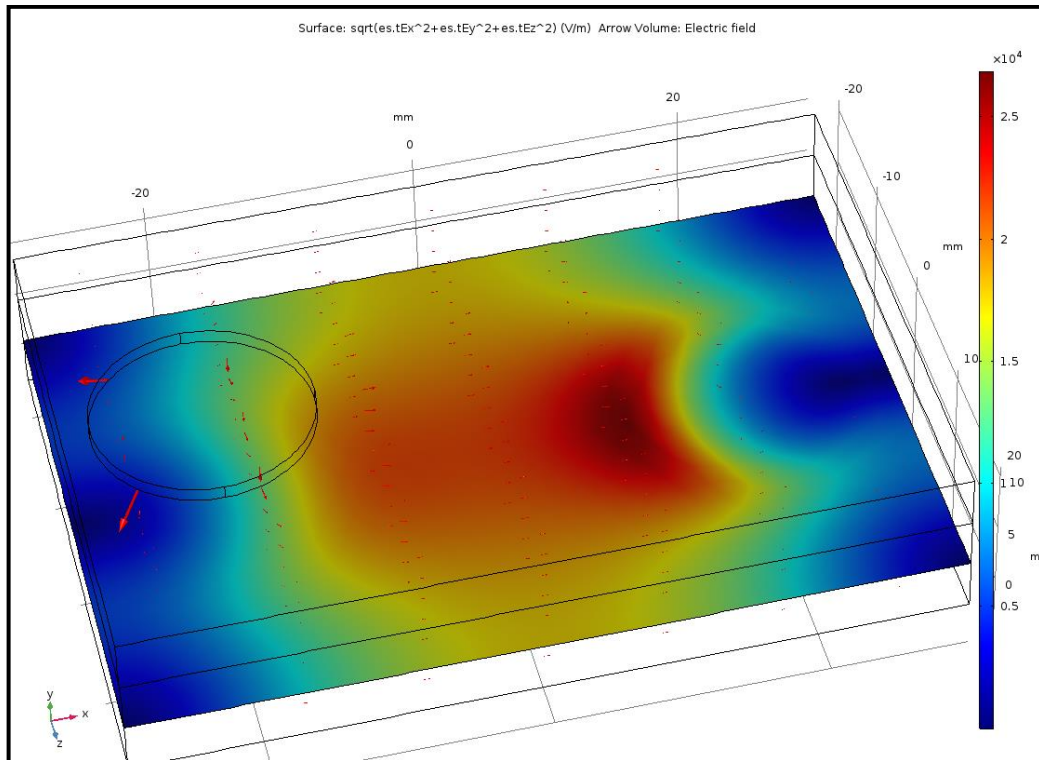
(b) lower interface

Fig. 4.4: Draft setup #2 – Tangential electric field at the interface

This setup has the following disadvantages:

- The tangential component of electric field is very small (**0.025 kV/mm for 1 kV of applied voltage**). This would mean that extremely large voltages should be applied to observe interfacial breakdown.

- The **contact area** of the epoxy and silicon rubber is large – thus the manufacturing of multiple samples for such a test setup would be cumbersome.

- The **contact area** of the epoxy and silicon rubber is large – thus large weights would be necessary to create interfacial pressure of a few bar.

4.2.3 Draft setup #3: Circular electrode configuration

This setup had a vertical construction. Two thin layers of epoxy and silicon rubber were kept one on top of the other as shown in *Fig. 4.5*. This setup has two circular electrodes at the interface. This setup was designed considering its smaller contact area and thus simpler construction.
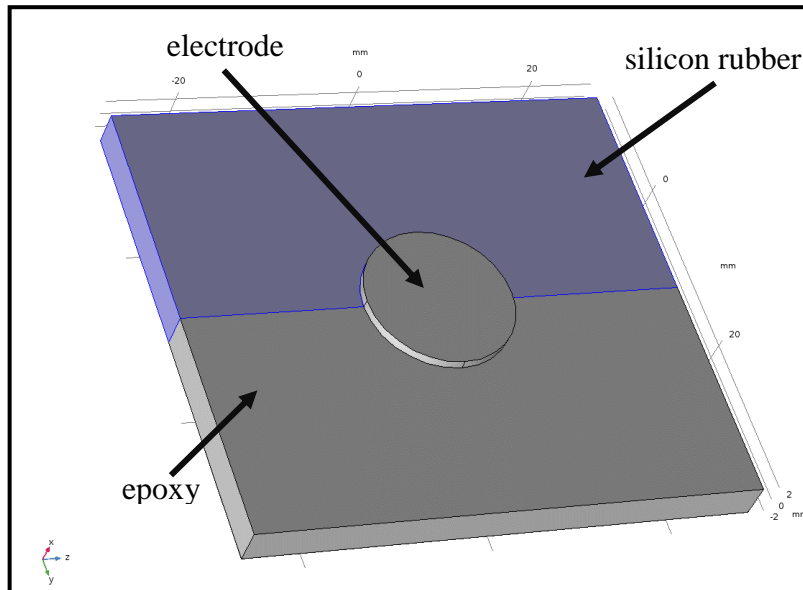
Fig. 4.5: Draft setup #3 – components

This setup has the following advantages:

- The level of voltages required to cause interfacial breakdown is **lower** than setups #1 and #2. For a 5mm thick sample, an electric field of **0.2kV/mm** is achieved for 1 kV of applied voltage.

- The application of weights (interfacial pressure) is **simple** as a smaller contact area would require less weights to simulate large interfacial pressure.

- The contact area is small; thus, the manufacture of the samples is **simpler** compared to setups #1 and #2. It is **easier** and **faster** to manufacture a smaller sample that requires high levels of smoothness.
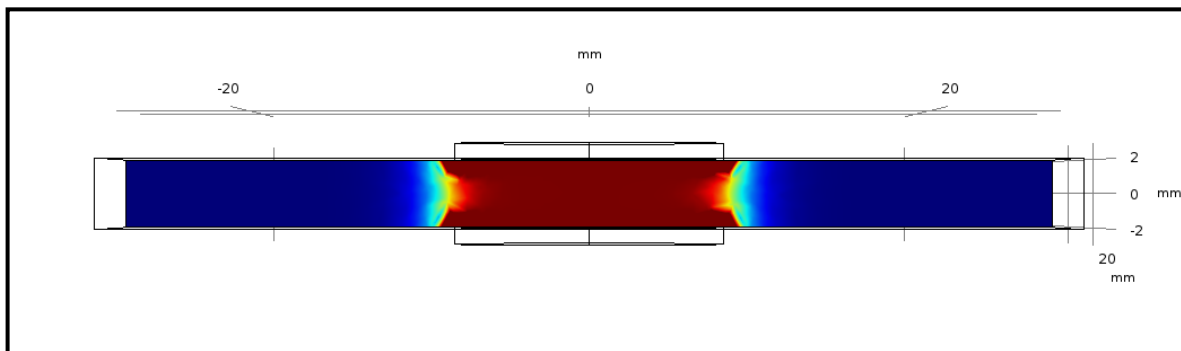
Fig. 4.6: Draft setup #3 – Electric field at the interface [red colour indicates the highest electric field]

This setup has the following disadvantages:

- There is only the **tangential component of electric field** present at the interface. This would give a conservative estimation of the breakdown values.

- The electrically active area is **small**.

4.2.4 Draft setup #4: Oval electrode configuration

The setup is similar to setup #3. The only change is that the electrodes are made oval shaped in-order to increase the electrically active area.
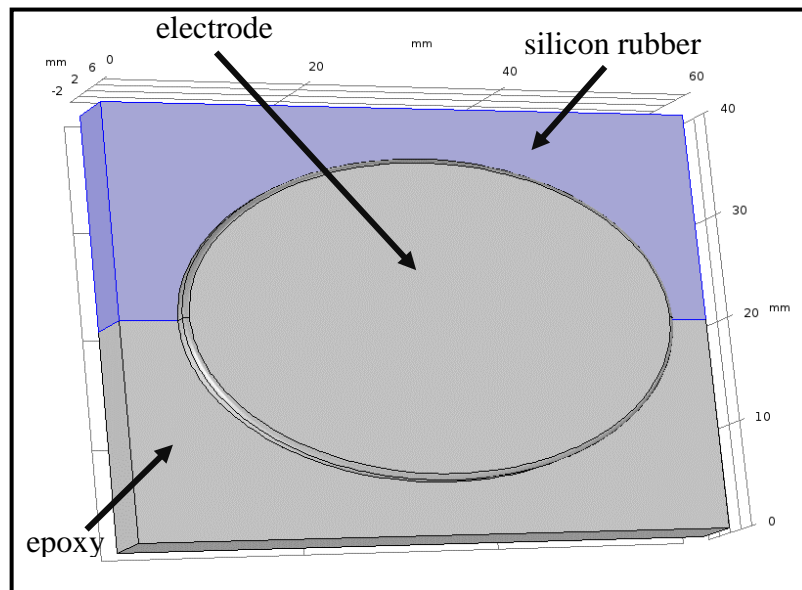
Fig. 4.7: Draft setup #4 – components

Compared to the earlier configuration, this setup has an advantage of a larger electrically active area. Similarly, in comparison with the previous configuration, the drawback due to the larger electrodes is due to a higher probability of a **flashover** through the sides of the samples.
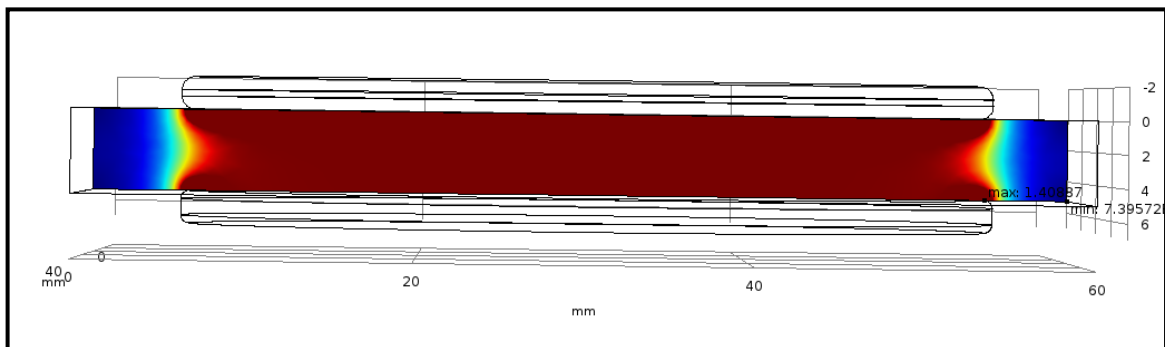
Fig. 4.8: Draft setup #4 – Electric field at the interface [red colour indicates the highest electric field]

An overview of the four different configurations is presented below in *Table 4.1*. The table uses colours to represent advantages *(in green)*, disadvantages *(in red)* and neutral points *(in yellow)* of the test setups. The last column also gives the preference (1 – highest; 4 - lowest) for each type of setup.

	ELECTRICAL	MECHANICAL	OTHER PARAMETERS	PREFERENCE [1 = HIGHEST; 4= LOWEST]
DRAFT SETUP #1: SIR - EPOXY	High values of applied voltage required	Large weights required	Complexity to manufacture large test sample	3
DRAFT SETUP #2: SIR – EPOXY - SIR	High values of applied voltage required	Large weights required	Increased complexity in manufacture of test samples	4
DRAFT SETUP #3: CIRCULAR ELECTRODE CONFIGURATION	Small values of voltages are required	Smaller weights required	-	1
DRAFT SETUP #4: OVAL ELECTRODE CONFIGURATION	Small values of voltages are required	Smaller weights required	Risk of flashover along the sides	2

Table 4.1: Summary of draft test setup designs.

4.3 *Preliminary testing- sizing of samples and test setup*

From *Table 4.1*, it is clear that a vertical assembly of epoxy and silicon rubber samples is the most practical configuration. This not only lowers the required levels of applied voltage but also lowers the amounts of weights required to create the interfacial pressure.

In this line, preliminary testing was carried out to verify if this was practically feasible. The purpose of this test was to get an idea of the relation between the width and height of the sample and the flashover voltage. Also, the effect of the thickness of the sample was to be investigated.

Silicon rubber samples of the same type (as used in power cable accessories) were specifically moulded by the rubber manufacturer to $50 \times 50 \times 5$ mm *(L × W × H)* dimensions. The four 50×5 mm sides were as smooth as casted (just like the surface of commercially used accessories). These samples were pressed against each other as shown in *Fig. 4.9 by* using two wooden blocks. HV was applied from the electrode on the top while the large electrode on the bottom was grounded.
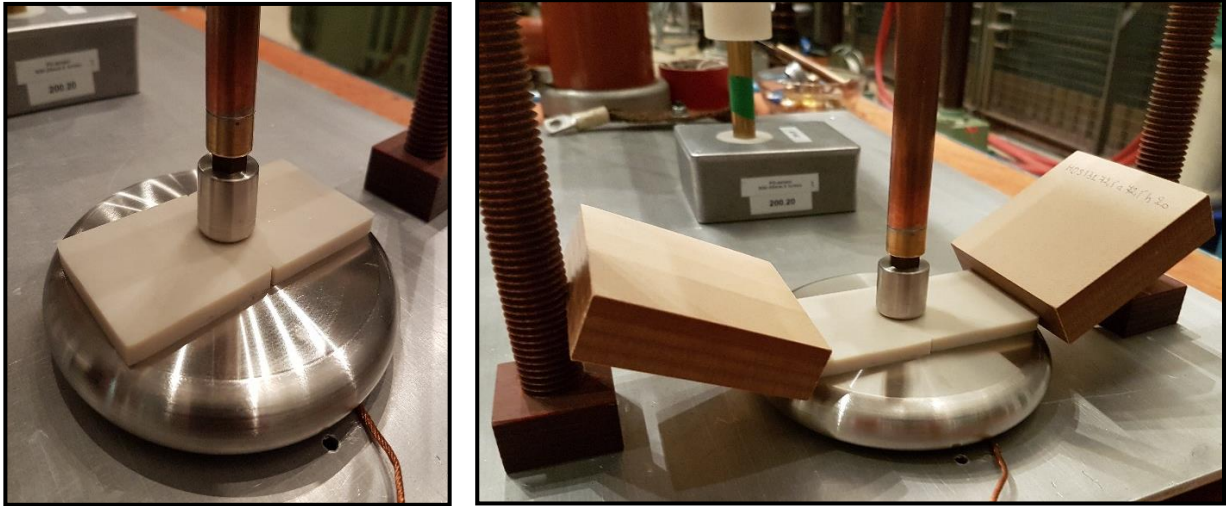
Fig. 4.9: Preliminary testing for sample dimensions – two SiR samples.

AC voltage was applied. Initially the sample interface broke down at low values of applied voltage. The pressure in the interface was increased by pushing the wooden blocks towards each other. The interfacial breakdown voltage increased as the interfacial pressure was increased.

Next, a slit was made in one piece of silicon rubber and this was pressed together to validate our observations. This experiment also gave similar results and there was flashover around the sides at around 28 kV. The setup arrangement is shown in *Fig. 4.10*.
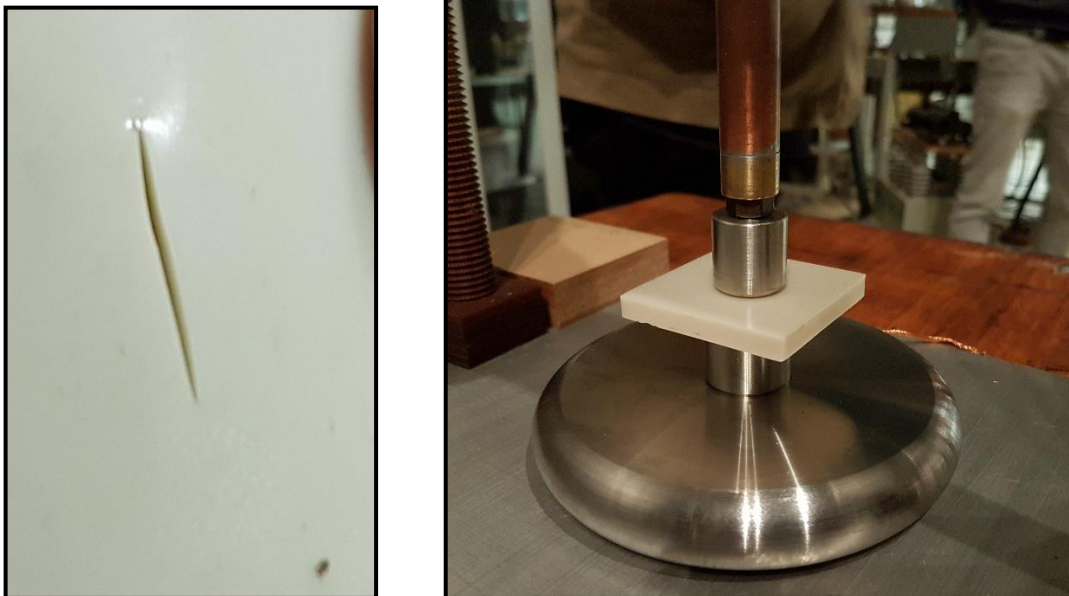
Fig. 4.10: Preliminary testing for sample dimensions – slit in SiR.

The following observations were made:

- It was noticed that the samples had flashover around 28 kV. This value is very low; therefore, it was decided that **wider samples were necessary**.

- The rubber was beginning to bend at higher pressures. Thus, it would be **better to increase the thickness of rubber** for better stability.

4.4 Design of test setup

Based on the requirements that were formulated in *section 4.1* and the observations from the preliminary testing (*section 4.3)* a test setup was designed such that it would incorporate all the inferences/ conclusions. The reasoning and the final design is explained in detail in this section.

4.4.1 Sample material

The samples were sourced directly from the supplier/ manufacturer of the epoxy and silicon rubber respectively. This was done for the following reasons:

- The testing of actual materials would give a **better estimation** of the electric breakdown performance.

- The manufacturer could smoothen/ polish the active surfaces (two 80 × 6 mm sides) to be **as smooth as casted**. The samples would be as smooth as those used in commercial cable accessories. This would eliminate 'surface roughness' problems that is common in laboratory made samples.

- **Time saving** measure. The process of manufacturing samples in the laboratory was found to be cumbersome and time consuming. Also, the risk of contamination of samples is high due to non-industrial conditions.

4.4.2 Sample size

From the preliminary tests *(section 4.3),* it was clear that the samples must be wider than 50 mm. However, it must not be too wide as a wider sample (especially silicon rubber) risks deformation/ buckling. Also, a large contact area would mean that larger weights are required to create the required interfacial pressure.

Thus, the sample dimensions were decided to be $80 \times 60 \times 6$ mm *(L × W × H)*. The active surfaces would be the two 80×6 mm sides of the samples.
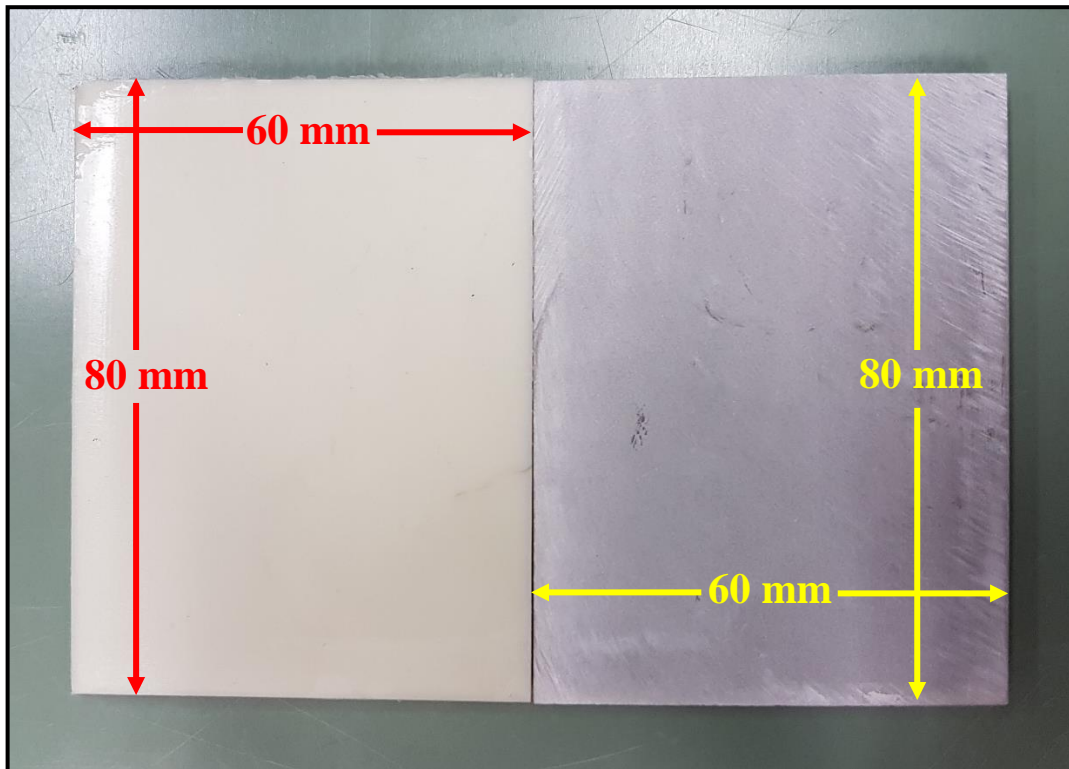
Fig. 4.11: Samples of silicon rubber (left) and epoxy (right).

4.4.3 Test holder

The setup is designed to withstand up to 40 - 45 kV of AC voltage without flashovers. Also, it was strictly desired that the test setup would not be immersed in oil. Therefore, the sides of the test setup were intentionally enlarged so as to avoid flashovers and to provide good mechanical stability. The test setup was made **completely modular** – all parts of the test setup can be replaced/ scaled if necessary.

The material of the test holder was designed of PVC. This is because of the good **mechanical** properties, good **electrical** properties, ease to **modify/ re-machine** (if necessary) and ease of **manufacturing**.

For ease of explanation, each part of the test setup is numbered as shown in *Fig. 4.12*.
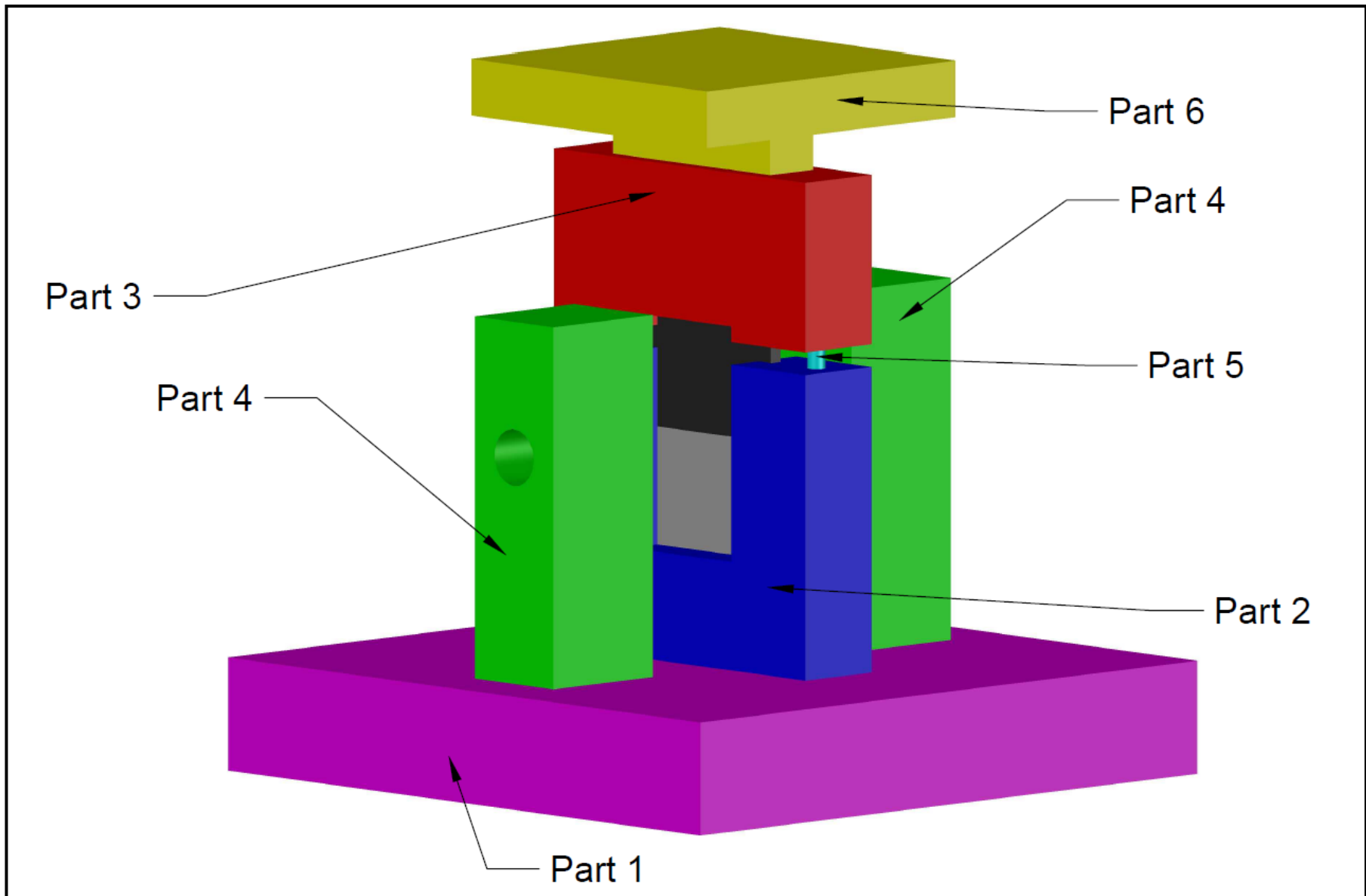
Fig. 4.12: 3D drawing of test setup

Part #1: Base plate

The base plate is made of a mechanically stronger variant of PVC. It is designed to withstand the entire setup and any mechanical weights that would be needed to create the interfacial pressure. It is designed to be 60 mm thick. Slots were made to plug-in the other parts of the setup.
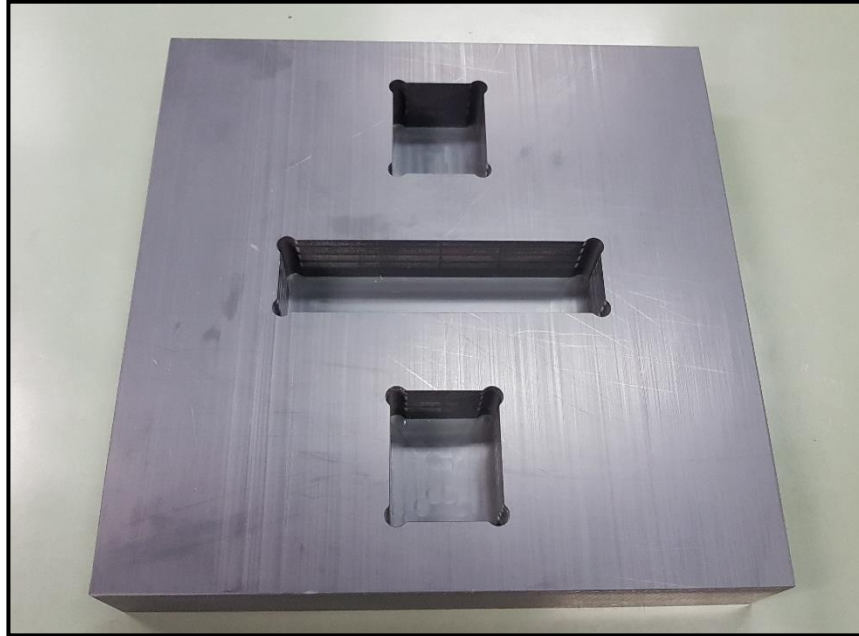
Fig. 4.13: Base plate [part #1]

Part #2: Sample holder (bottom)

The sample holder (bottom) is made to hold the silicon rubber and the epoxy samples vertically. To avoid mis-alignment, the holder has a slit (of 6 mm thickness) which could exactly fit the test samples. This part also has two holes on its either sides to accommodate the guiding rods *(part #5)* which acts as a mechanical support for the upper part of the sample holder *(part #3)*.
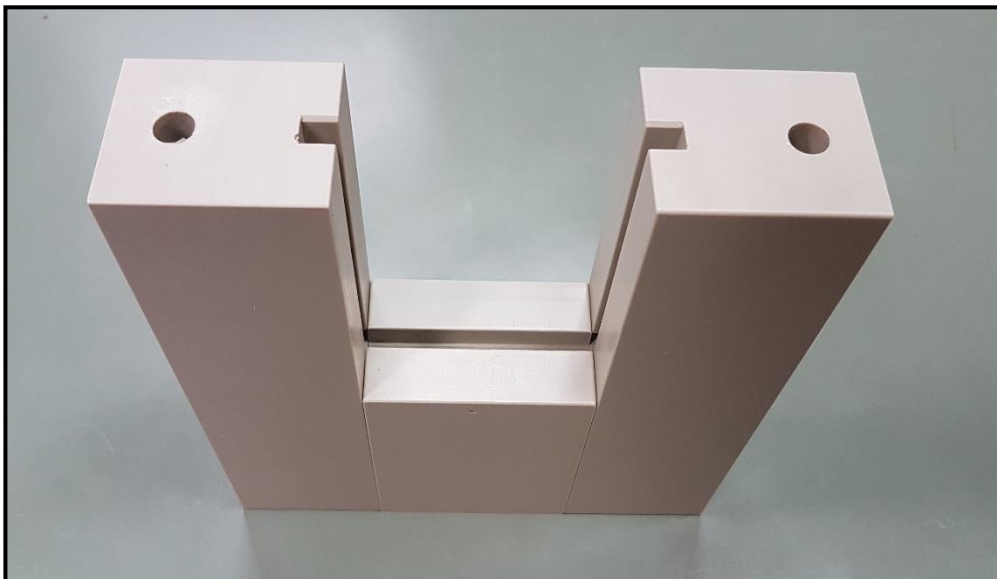
Fig. 4.14: Sample holder (bottom) [part #2]

48

Part #3: Sample holder (top)

The sample holder (top) is made to press the silicon rubber (sample on the top). It also has slits (of 6mm thickness) as shown in *Fig. 4.15 (b)*. This part also has two cylindrical holes on either side to allow the guiding rods *(part – 5)*. The upper part *(Fig. 4.15 (a))* of this sample has a cavity to allow connection to the weight carrying plate *(part #6)*.
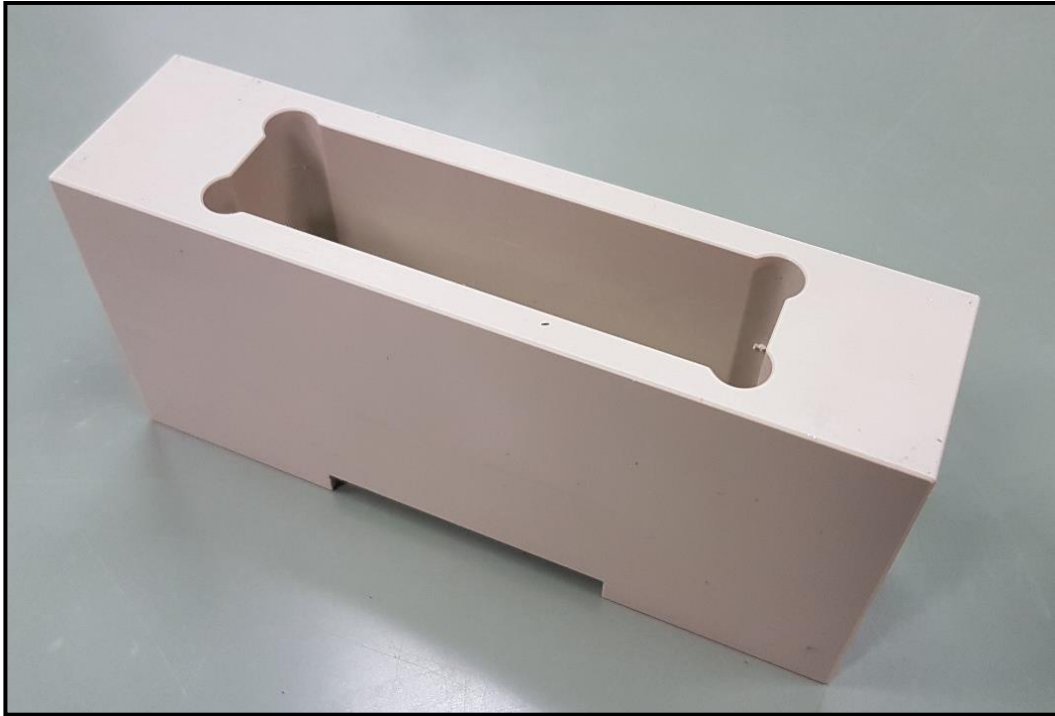
Fig. 4.15 (a): Sample holder (top) [part #3]
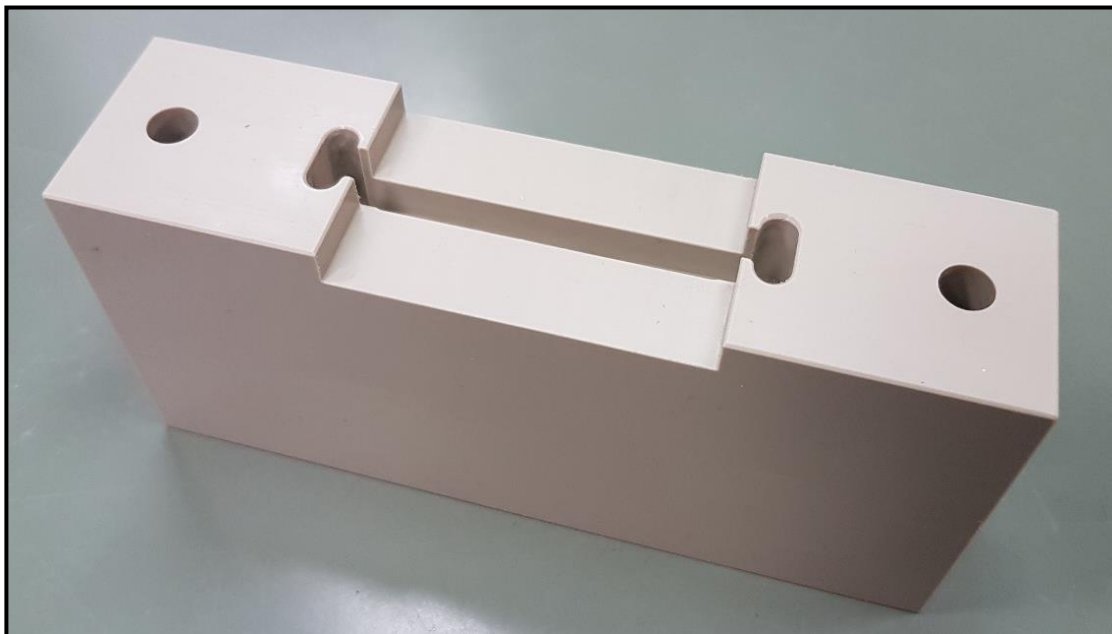
Fig. 4.15 (b): Sample holder (top) [part #3]

49

The two electrode holders are plugged into the base plate on either side of the interface. The holder is a PVC block with a cylindrical cavity of φ 20 mm to slide the electrode assembly inside.

Fig. 4.16: Electrode holder(s) [part #4]

Part #5: Guiding rod

The guiding rods are also made of a mechanically stronger variant of PVC. Its main function is to guide the upper electrode holder *(part #3)* in correct alignment with the lower electrode holder *(part #2).* Its main function is to ensure that the setup does not collapse due to the weights that will be placed on the top of the setup.

Fig. 4.17: Guiding rod(s) [part #5]

Part #6: Weight carrying plate

The weight carrying plate is the surface where the weights would be placed such that the interfacial pressure is created. For mechanical support, a long protrusion is made in its lower half. This protrusion is made to lock into the cavity of the sample holder [top] *(part #3)* as shown in *Fig. 4.18 (b)*.

Fig. 4.18 (a): Weight carrying plate – top view [part #6]
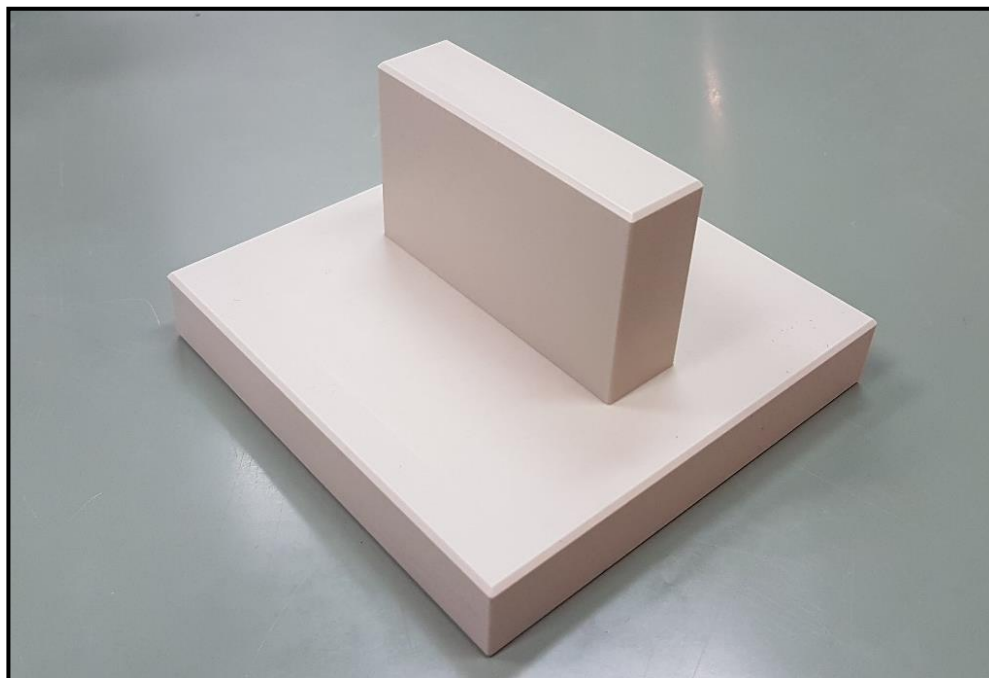
Fig. 4.18 (b): Weight carrying plate – bottom view [part #6]

4.4.4 Electrode design

The electrode assembly consists of two parts – the electrode itself and a long cylindrical brass rod to connect the electrode to the HV and ground wires of the test cell. The electrodes are made of stainless steel. The ϕ 25 mm cylindrical rods are made of brass. They have a male M8 thread on one side and a female banana plug on the other.

Fig. 4.19: Stainless steel electrode (left) and the entire electrode assembly (right)
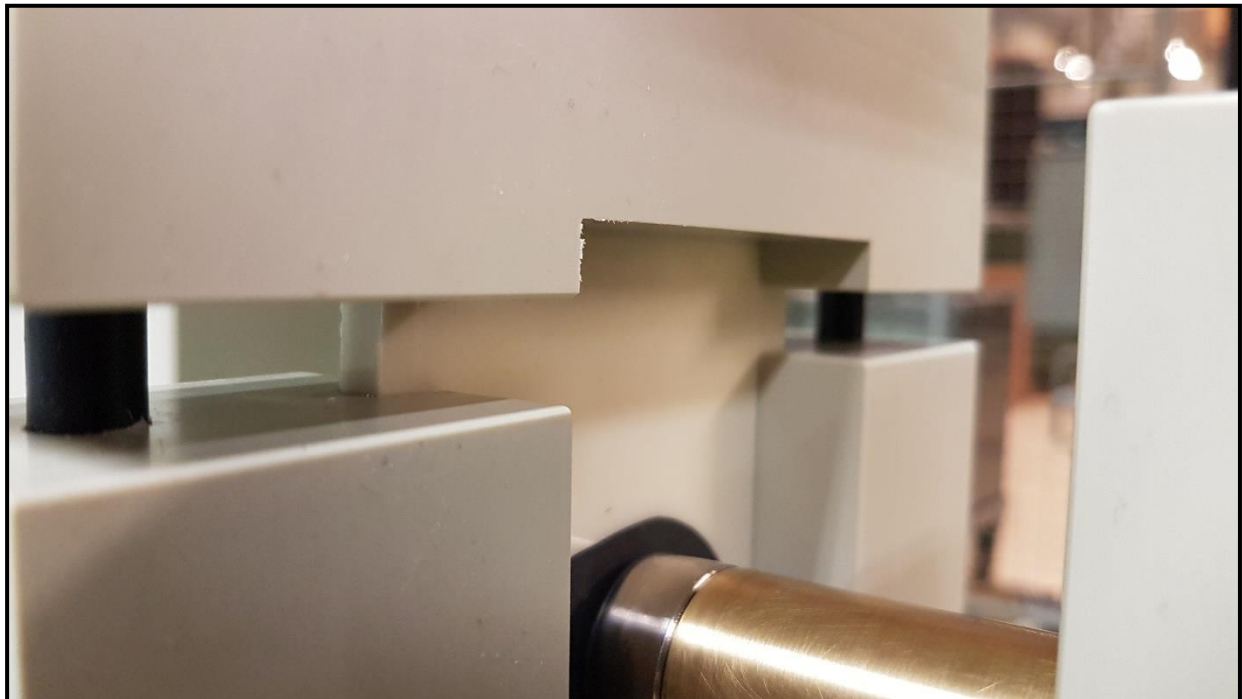
Fig. 4.20: Zoomed image of space between the upper and lower sample holder(s)

4.5 *Relationship between weight and interfacial pressure*

The **interfacial pressure** is calculated using the following relation:

$$Interfacial\ pressure\ (bar) = \left[\frac{Weight\ (kg)}{Area\ (m^2)} \times 9.80665\right]\frac{1}{10^5} \tag{6}$$

The surface area of the active part is the 80×6 mm surfaces. This is 480 mm^2, which is 0.00048 m^2. Thus, on solving for the relation between interfacial pressure and weight, we obtain the following empirical relation:

$$\mathbf{1\ kg\ weight = 0.2043\ bar}$$

Weight (kg)	Interfacial pressure (bar)
1	0.20
2.4	0.50
5	1.02
7.4	1.51
10	2.04

Table 4.2: Relation between applied weights (kg) and interfacial pressure (bar)

4.6 Summary

The test setup proposed, incorporates all the learning outcomes that is discussed in *Section 4.1*. The test setup has the following salient features:

1. The test setup was **simple** and **modular**. It could be scaled up/ down if necessary.

2. In order to prevent metal electrode from touching the interface (as suggested by the CIGRE 15- 10 recommendation), semi-conductive tape is used in between the electrode and the interface.

3. The oversizing of the test setup ensured that immersion of the test setup in oil is not necessary.

4. The 6 mm thick slits in the sample holders ensured that there was **no mis-alignment** of samples

5. The electrode holders ensured that there was **no mis-alignment in applying voltage** to the interface.

6. The guiding rods ensured that the setup would not **topple** (due to heavy weights). If the rubber buckled, then the entire weight would be taken over by the guiding rods.

7. The setup was oversized intentionally to prevent **flashovers** and withstand larger weights.

8. 20 mm of length was allowed for the silicon rubber to compress (refer *Fig. 4.20*).

9. It was possible to study the effect of defects on the material and the effect of silicone oil and other liquid insulants.

10. The electrode size could be increased/ decreased if necessary.
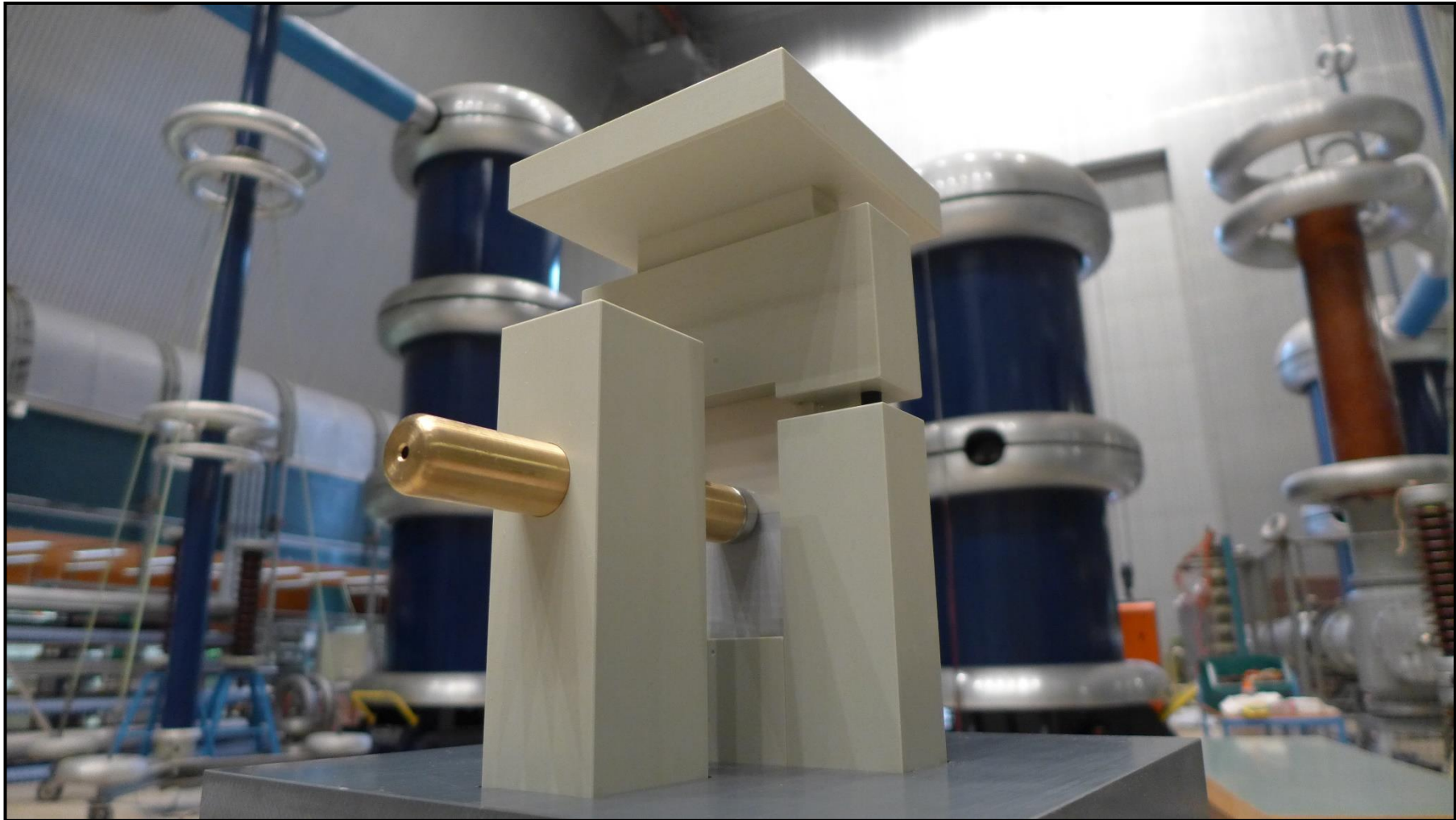
Fig. 4.21: Fully assembled test setup

5. Experimental study of epoxy/ silicon rubber interface

This chapter explains about the various tests (AC breakdown and lightning impulse tests) that were performed on the epoxy/ silicon rubber interface. The test protocol for each test and the corresponding results are provided. Pictures from the investigation and findings are also included.

5.1 Test cell and test preparation

This section elaborates on the test cells used for the different tests. It also explains about the process of sample preparation and about the semi-conductive tape that is used between the electrode and the interface under study.

5.1.1 Test cell – AC breakdown testing

The test cell is equipped with a fast-tripping switch. This is used to prevent the short circuit current (after breakdown) to damage the test setup by creating carbonised paths. High voltage is produced from a single-phase 500 V/ 200 kV, 100 kVA test transformer. It is then connected to a 400 pF, 600 kV capacitive voltage divider. The voltage is then applied via a cable to the test object (where it is applied to the brass rod of the high voltage electrode).
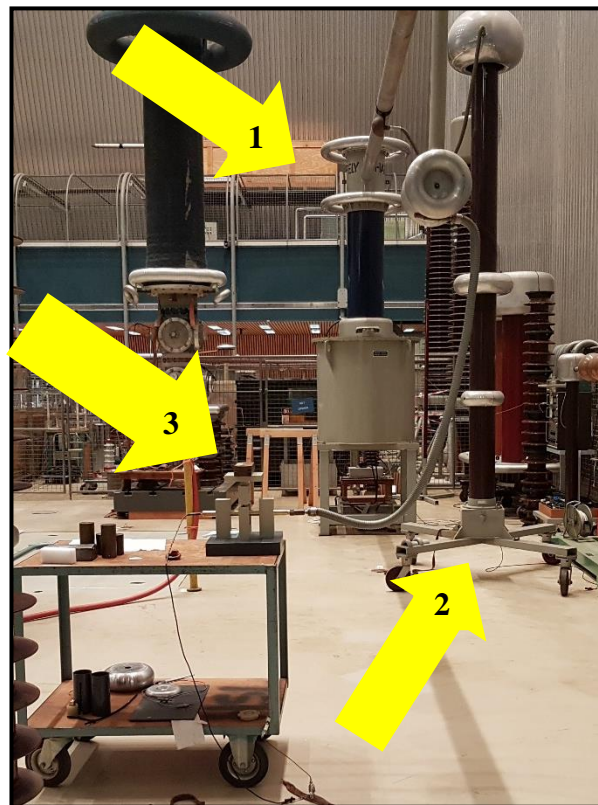
Fig. 5.1: Test setup for AC breakdown testing
[1 – HV transformer; 2 - voltage divider; 3 – test object]

Voltage is applied using a variac. The applied voltage is monitored by a digital voltmeter and an analog voltmeter for redundancy.

5.1.2 Test cell – Lightning Impulse testing

The test voltage was applied using a 4 MV Marx impulse generator. Due to the specific requirements of this test, only two stages of the generator were used to create a maximum of 200 kV. The voltage was applied across a 400 pF, 500 kV capacitive voltage divider and then to

the test setup. The 1.2/ 50 µs LI voltage was controlled and applied through a *Hafely Hipotronics Impulse Analysing* computer system.

Fig. 5.2: Test setup for Lightning Impulse testing

5.1.3 *Sample preparation*

Each individual sample was carefully wrapped in tissue papers to prevent damage. The samples were un- wrapped when ready to be tested and cleaned with **isopropyl alcohol** (*Isopropanol 2-propanol*) because of its property of not reacting with PVC (material of the test holder), silicon rubber and epoxy. Also, isopropyl alcohol could dissolve oils (which will be used at the interface, during testing).

It was noticed that normal microfiber cloth was producing a lot of paper dust during cleaning with isopropyl alcohol. Thus, **tightly woven nylon microfiber** is used as cleaning cloth.

59

5.1.4 Semi-conductive tape

Fig. 5.3: Oval shaped hand-cut semi-conductive tapes

In-order to prevent the metal electrodes from making physical contact with the interface under test [40, 48], it was decided to use semi-conductive tape at the interface. The tape is 30 mm wide and 1.5 mm thick. The tapes were cut by hand into oval shape. This also helped to subside the electric field enhancement at the edges of the metal electrodes. Any sharp edges in the tapes were manually rounded-off to prevent field enhancement.

5.2 AC Breakdown tests

The aim of this thesis is to deduce a relation between the interfacial pressure and the AC breakdown voltage of the interface. This test is explained in detail in this section. It starts with the test procedure and then shows the results.

5.2.1 Test procedure

The **test cell** is cleaned, and all unnecessary equipment is disconnected/ moved. Then, the cell is checked for its safety systems by applying a small voltage and tripping the system. This allows us to check if the power electronics based fast switch is working. Also, the interlocking gates of the test cell are checked in this way.

The **semi-conductive tape** is cut by hand into oval pieces as shown in *Fig. 5.3*. Any sharp corners in the tape are rounded off. The plastic cover on one side of the tape is removed just before the testing.

The **test setup** is assembled by cleaning each of the parts with isopropyl alcohol and drying them. The **electrodes** are also thoroughly cleaned. The parts are then plugged-into the base plate and the entire test setup is assembled. The test setup was placed on a movable cart, to enable the moving of the test setup for cleaning and other practical reasons.

The **epoxy and silicon rubber samples** are first checked for defects/ scratches in the active region (80 × 6 mm sides). If no problems are found, they are cleaned using isopropyl alcohol and allowed to dry.

The samples and the electrodes are assembled together. The oval semi-conductive tape is stuck to the interface and then the electrode is pressed on the tape to allow good adhesion. The specific weights are then kept on the *weight carrying plate*. It is ensured that the weights are kept in the middle to prevent the setup from toppling.

The grounding stick is removed, and test cage is closed. Then, the voltage is applied at a rate of **1kV/second.** This rate of rise is within the short-time test requirements as stipulated by ASTM standards [4]. Applied voltage is monitored on both the voltmeters.

After breakdown, the fast switch trips the circuit. Then, the variac is brought back to zero and the breakdown voltage is recorded. The test cell is opened, and the grounding stick is then put in place to ground the secondary of the HV transformer and the voltage divider.

The weights are removed and the top sample (silicon rubber) is removed to investigate the breakdown area. If the breakdown originates at the triple point (at the edge of the semi-conductive tape), the reading is discarded.

The breakdown paths are photographed. Then, the samples are marked with permanent marker and safely stored in zip lock pouches. The test setup and the electrodes are then cleaned with isopropyl alcohol and the next sample is prepared for investigation.

The entire process is shown as a flowchart in Fig. 5.4.
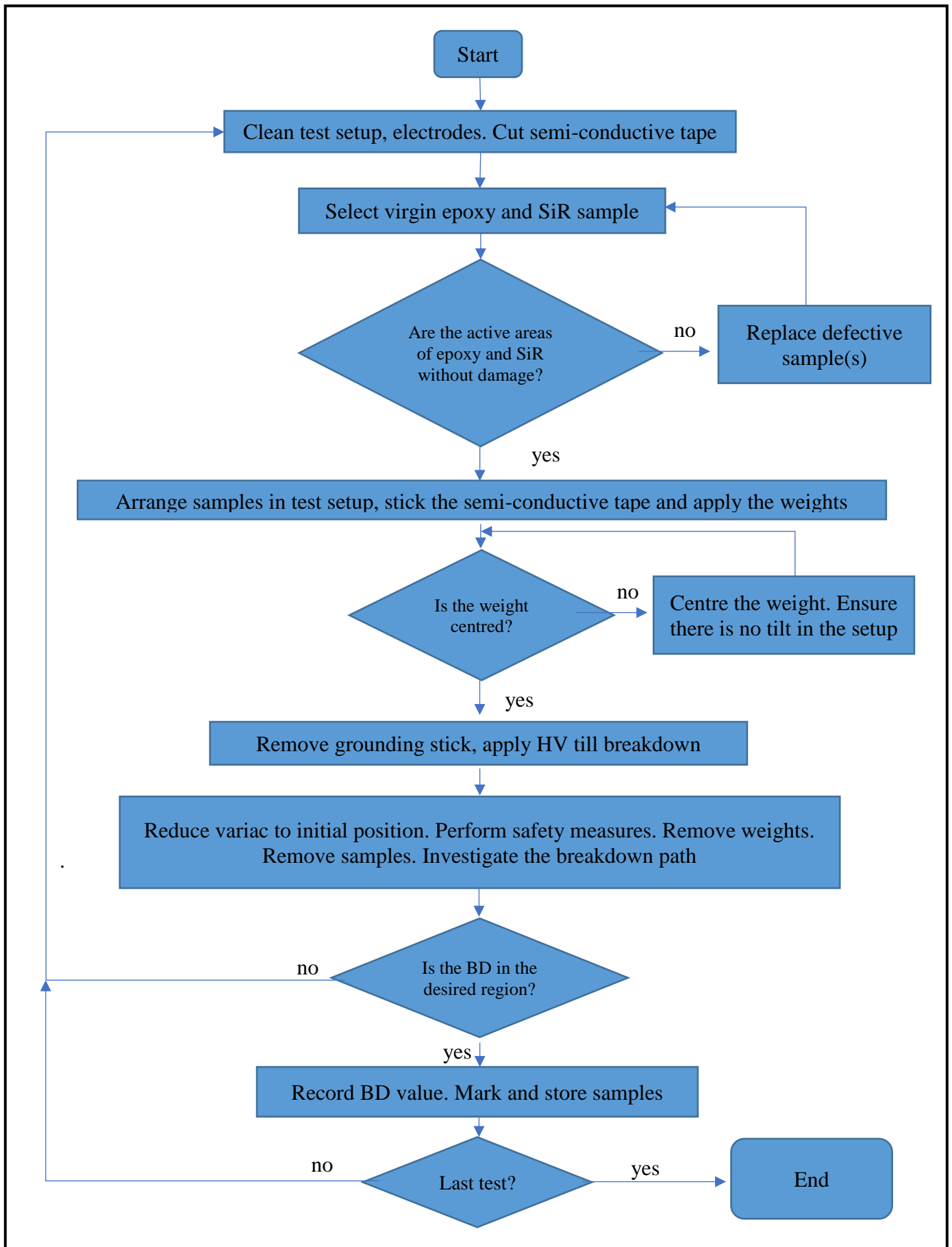
Fig. 5.4: Flowchart- AC breakdown test

5.2.2 Test results

The AC breakdown tests were carried out at 0.2 bar, 0.5 bar, 1 bar,1.5 bar, and 2 bar. Only samples that had breakdown in the region of the electrode were taken into consideration. Other breakdowns (at the edge of the semi-conductive tape) were discarded.

Initially it was planned to perform 10 AC breakdown tests for each value of interfacial pressure [25]. During the experiments it was found that the AC breakdown voltages have **high repeatability** (low error). This was verified for all the pressure values and thus a lesser number of AC breakdown tests were performed. It was planned to use the remaining samples for different kinds of tests which will be elaborated in *Sections 5.3 – 5.6*. A comparison of all the results of the AC breakdown tests is presented at the end of this section.

5.2.2.1 Interfacial pressure 0.2 bar

The interface testing for 0.2 bar interfacial pressure was tested according to the procedure explained in *Section 5.2.1*. Standard weights of 1 kg (refer *Table 4.1*) was used to create the interfacial pressure.
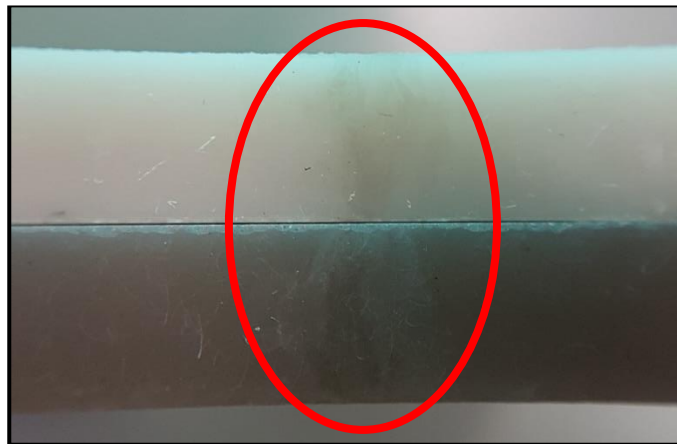
Fig. 5.5: AC breakdown path – 0.2 bar
[lower material- epoxy; upper material- silicon rubber]

Pressure (bar)	AC Breakdown voltage (kV)	Electric field (kV/mm)
0.2	26	4.33
0.2	27.4	4.57
0.2	26	4.33
0.2	27	4.50

Table 5.1: AC breakdown results – 0.2 bar

The observations are as follows:

- The breakdown electric field is around **4.33 kV/mm**

- The breakdown path is **not distinct and clear**.

- There is **no carbonised breakdown track**.

- **Multiple** or **branched tracks** were observed.

The interface testing for 0.5 bar interfacial pressure was tested according to the procedure explained in *Section 5.2.1*. Standard weights of 2.4 kg (refer *Table 4.1*) was used to create the interfacial pressure.
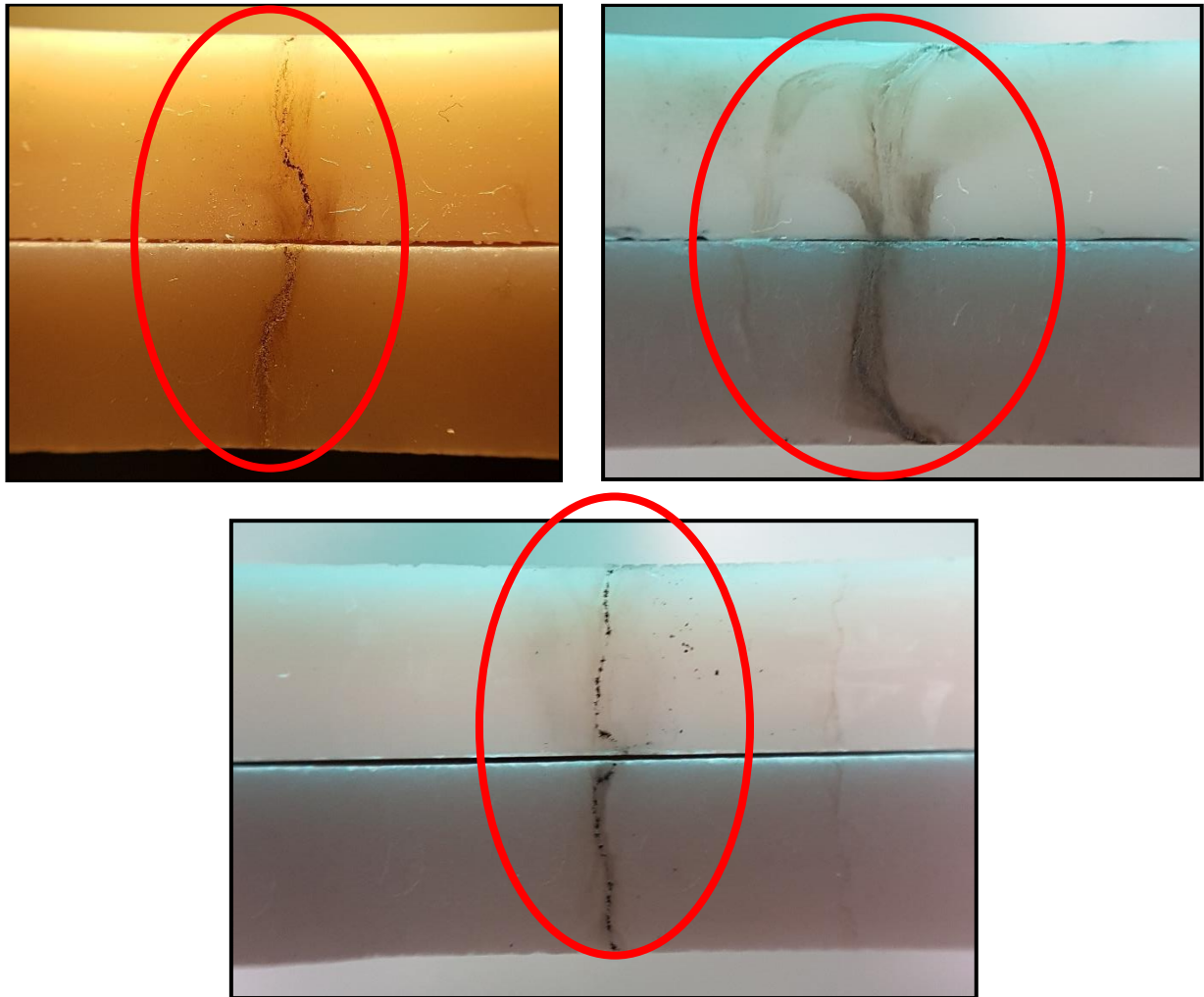
Fig. 5.6: AC breakdown path – 0.5 bar
[lower material- epoxy; upper material- silicon rubber]

Pressure (bar)	AC Breakdown voltage (kV)	Electric field (kV/mm)
0.5	30.7	5.11
0.5	31.7	5.29
0.5	31.7	5.29
0.5	30.7	5.11

Table 5.2: AC breakdown results – 0.5 bar

The observations are as follows:

- The breakdown electric field is around **5.2 kV/mm**.

- The breakdown path is **clear** and **distinct**.

- There are **carbonised breakdown tracks**.

- The breakdown tracks appeared to be **straight** (unlike the tracks seen for 1 bar and above).

- Multiple or branched tracks are **not** observed.

5.2.2.3 Interfacial pressure 1 bar

The interface testing for 1 bar interfacial pressure is tested according to the procedure explained in *Section 5.2.1*. Standard weights of 5 kg (refer *Table 4.1*) was used to create the interfacial pressure.

Fig. 5.7: AC breakdown path – 1 bar
[lower material- epoxy; upper material- silicon rubber]

Pressure (bar)	AC Breakdown voltage (kV)	Electric field (kV/mm)
1	35.9	5.99
1	36.0	6.00
1	36.0	6.00
1	35.9	5.98
1	36.0	6.00
1	35.8	5.97

Table 5.3: AC breakdown results – 1 bar

The observations are as follows:

- The breakdown electric field is **6 kV/mm**.

- The breakdown path is **clear** and **distinct**.

- There are **carbonised breakdown tracks**.

- The tracks appeared to be **curved** (unlike Fig, 5.5 -5.6).

- Multiple or branched tracks are **not** observed.

5.2.2.4 Interfacial pressure 1.5 bar

The interface testing for 1.5 bar interfacial pressure is tested according to the procedure explained in *Section 5.2.1*. Standard weights of 7.4 kg (refer *Table 4.1*) is used to create the interfacial pressure.
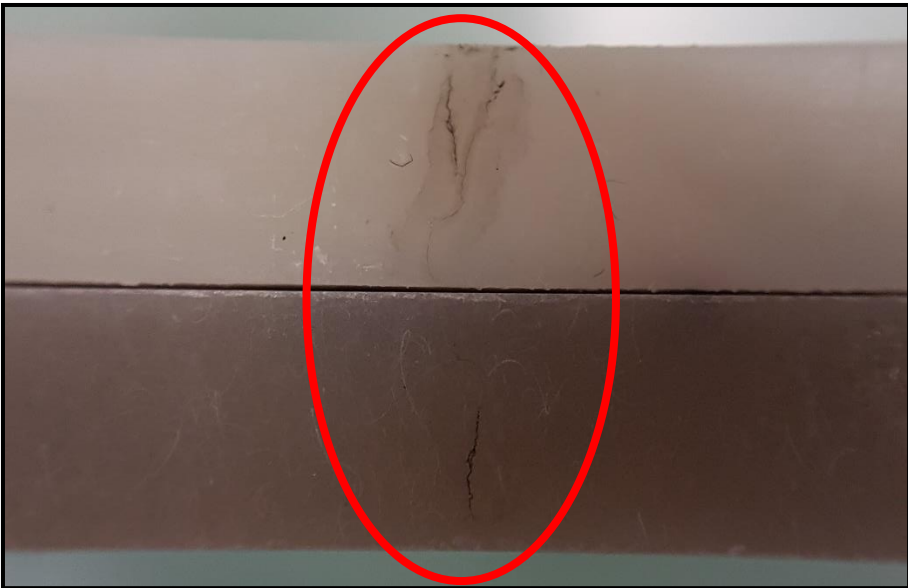
Fig. 5.8: AC breakdown path – 1.5 bar
[lower material- epoxy; upper material- silicon rubber]

Pressure (bar)	AC Breakdown voltage (kV)	Electric field (kV/mm)
1.5	37.0	6.17
1.5	37.0	6.17
1.5	37.4	6.23
1.5	38.0	6.33

Table 5.4: AC breakdown results – 1.5 bar

The observations are as follows:

- The breakdown electric field is **around 6.2 kV/mm**.

- The breakdown path is **clear** and **distinct**.

- There are **carbonised breakdown tracks**.

- The tracks appeared to be **curved** (unlike *Fig, 5.5 -5.6*).

- Multiple or **branched tracks** are observed in all the samples.

5.2.2.5 Interfacial pressure 2 bar

The interface testing for 2 bar interfacial pressure is tested according to the procedure explained in *Section 5.2.1*. Standard weight of 10 kg (refer *Table 4.1*) is used to create the interfacial pressure.
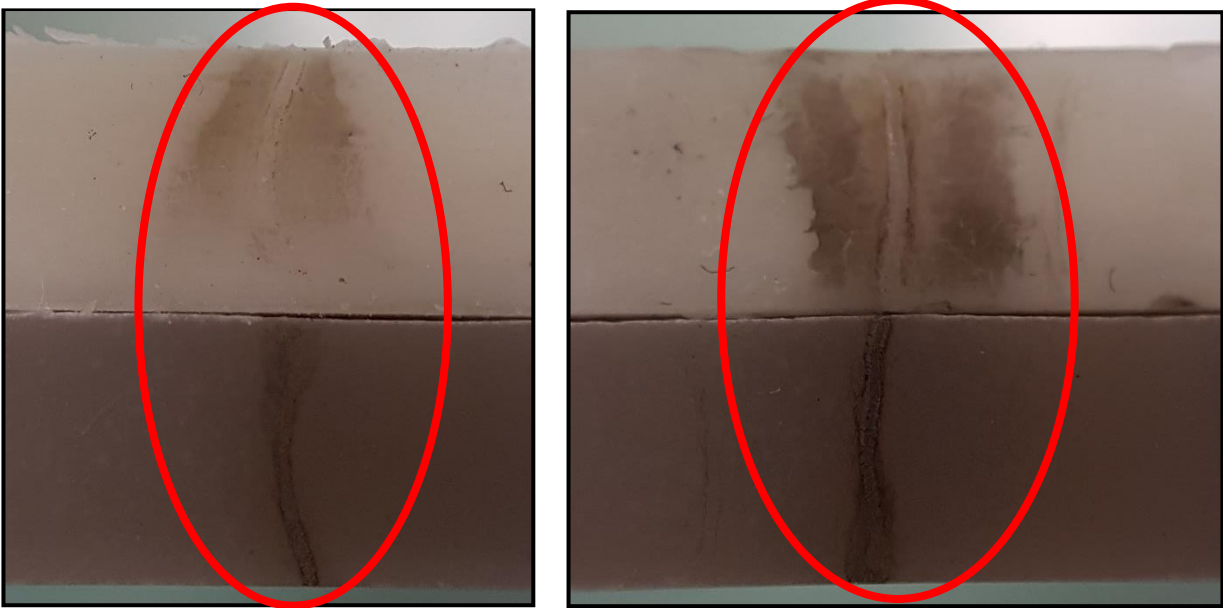
Fig. 5.9: AC breakdown path – 2 bar
[lower material- epoxy; upper material- silicon rubber]

Pressure (bar)	AC Breakdown voltage (kV)	Electric field (kV/mm)
2.0	40.2	6.69
2.0	40.2	6.69
2.0	40.2	6.69
2.0	40.2	6.69

Table 5.5: AC breakdown results – 2 bar

The observations are as follows:

- The breakdown voltage is around **6.7 kV/mm**.

- The breakdown path is **clear** and **distinct**.

- There are heavily **carbonised breakdown tracks**.

- The tracks appeared to be **straight** (like *Fig, 5.5 -5.6*).

- Multiple or branched tracks are not observed in the samples.

5.2.3 Summary

As stated in literature, it is observed that the **breakdown voltage increases with increase in interfacial pressure**. This is illustrated in *Fig. 5.10*.

It must be noted that these AC breakdown values are **conservative**. Thus, in actual setting, higher electric field strengths can be withstood by the interface for each respective interfacial pressure. This is because, in this test setup, the electrodes are very close to the interface. This would produce a very strong/ harsh electrical field. However, in a real termination the high voltage and ground parts are far away from the interface. Thus, the effect of the electric field may be milder compared to the test setup.
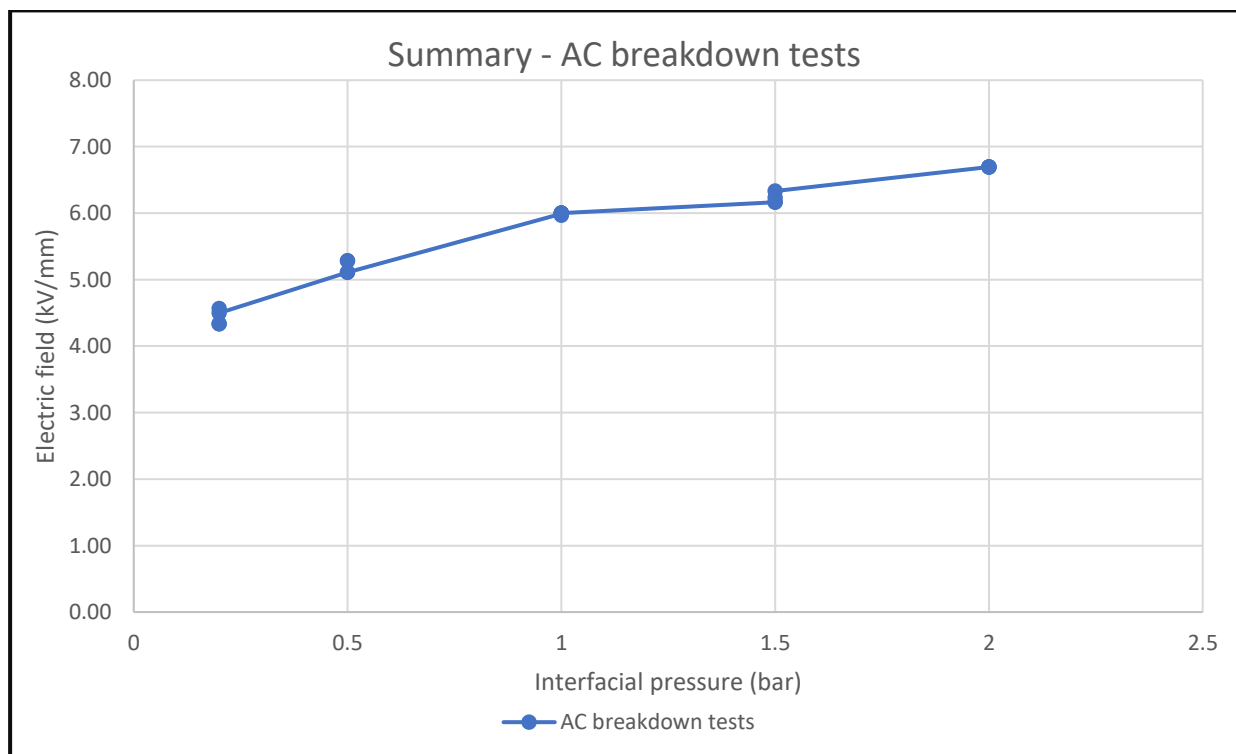
Fig. 5.10: AC breakdown field strength - summary

From a design perspective, it is desired to have a design in a flat (steady/ stable) portion of the curve. Thus, an interfacial pressure **greater than 1 bar** is preferred.

5.3 AC Breakdown tests with oil at the interface

During installation of cable accessories, silicon oil is applied on the rubber to easily slide the rubber into the epoxy insulator. It is found that this silicon oil is absorbed by the silicon rubber over time (few weeks – few months). The effect of this oil is investigated in this section.

The silicon oil used for the following experimental study was sourced from *Prysmian Group*. The oil is currently used during all cable accessory installations. The oil is available in a variety of packaging based on application.

Fig. 5.11: Silicon oil used as a lubricant during installation

5.3.1 Test procedure

The **test cell** is cleaned, and all unnecessary equipment is disconnected/ moved. Then, the cell is checked for its safety systems by applying a small voltage and tripping the system. This allows us to check if the power electronics based fast switch is working. Also, the interlocking gates of the test cell are checked in this way.

The **semi-conductive tape** is cut by hand into oval pieces as shown in *Fig. 5.3*. Any sharp corners in the tape are rounded off. The plastic cover on one side of the tape is removed during final assembly.

The **test setup** is assembled by cleaning each of the parts with isopropyl alcohol and drying them. The **electrodes** are also thoroughly cleaned. The parts are then plugged-into the base plate and the entire test setup is assembled. The test setup was placed on a movable cart, to enable the moving of the test setup for cleaning and other practical reasons.

The **epoxy and silicon rubber samples** are first checked for defects/ scratches in the active region (80 × 6 mm sides). If no problems are found, they are cleaned using isopropyl alcohol and allowed to dry.

The samples and the electrodes are assembled together. A few drops of **silicon oil** from the bottle shown in *Fig. 5.11* is applied at the 80×6 mm surface of epoxy and silicon rubber and evenly spread. The samples are assembled together and the oval **semi-conductive tape** is stuck to the interface. The electrode is pressed on the tape to allow good adhesion. The specific **weights** are then kept on the *weight carrying plate*. It is ensured that the weights are kept in the middle to prevent the setup from toppling.

The grounding stick is removed, and test cage is closed. Then, the voltage is applied at a rate of **1kV/second.** This rate of rise is within the short-time test requirements as stipulated by ASTM standards [4]. Applied voltage is monitored on both the voltmeters.

After breakdown, the fast switch trips the circuit. Then, the variac is brought back to zero and the breakdown voltage is recorded. The test cell is opened, and the grounding stick is then put in place to ground the secondary of the HV transformer and the voltage divider.

The weights are removed and the top sample (silicon rubber) is removed to **investigate** the breakdown area. If the breakdown originates at the triple point (at the edge of the semi-conductive tape), the reading is discarded.

The breakdown paths are photographed. Then, the samples are marked with permanent marker and safely stored in zip lock pouches. The test setup and the electrodes are then cleaned with isopropyl alcohol and the next virgin sample is taken for investigation.

The abovementioned process was followed initially for the first few tests. It was observed that there were **flashovers from the inner-side** (through the 6mm slits in which the samples are placed) setup. Thus, insulating silicon grease was applied by hand at all the corners of the test setup. This prevented flashovers from the inner sides of the test setup. This is shown in *Fig. 5.12*.

A detailed flowchart of the test procedure is shown in *Fig. 5.13*.
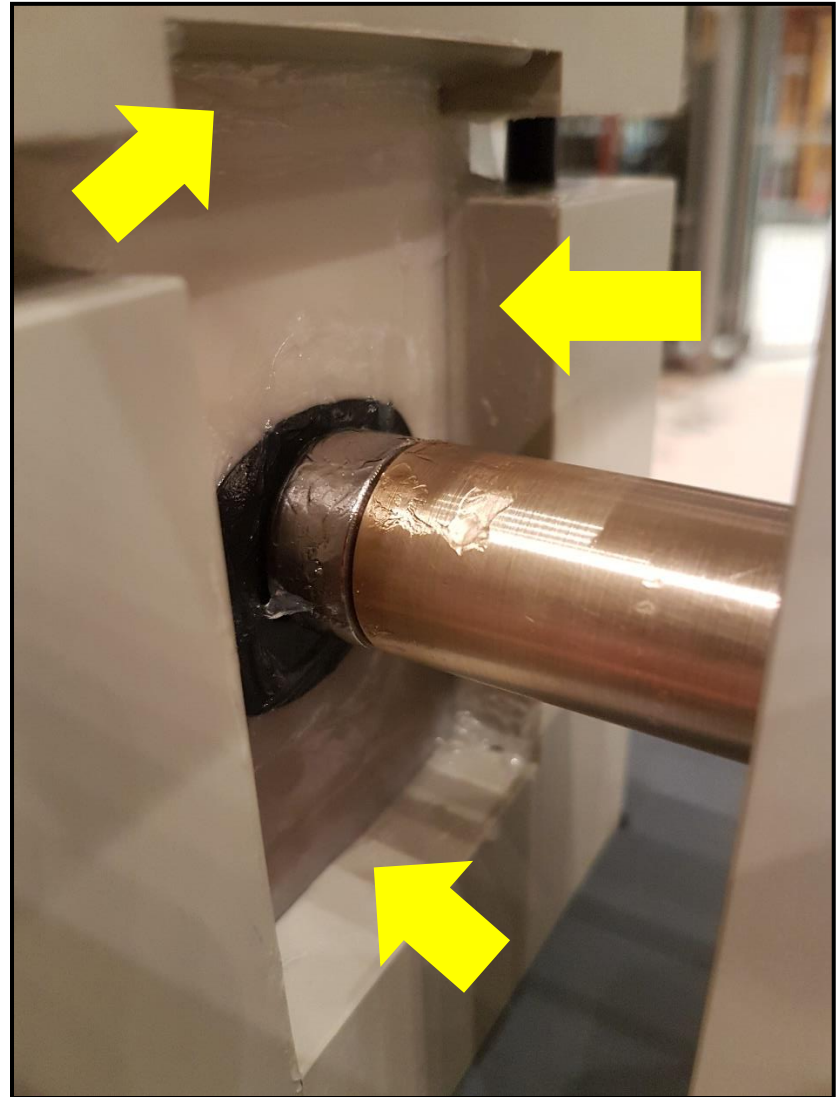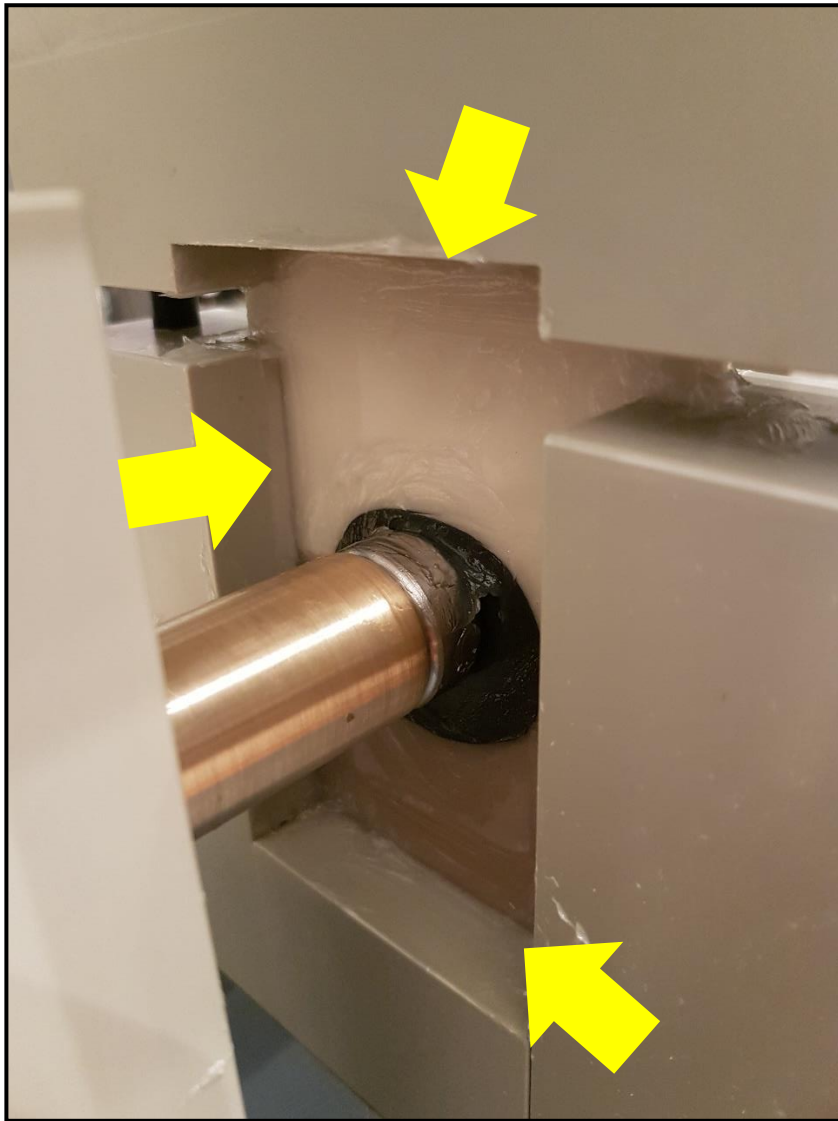
Fig. 5.12: Silicon grease used to prevent inner-side flashovers
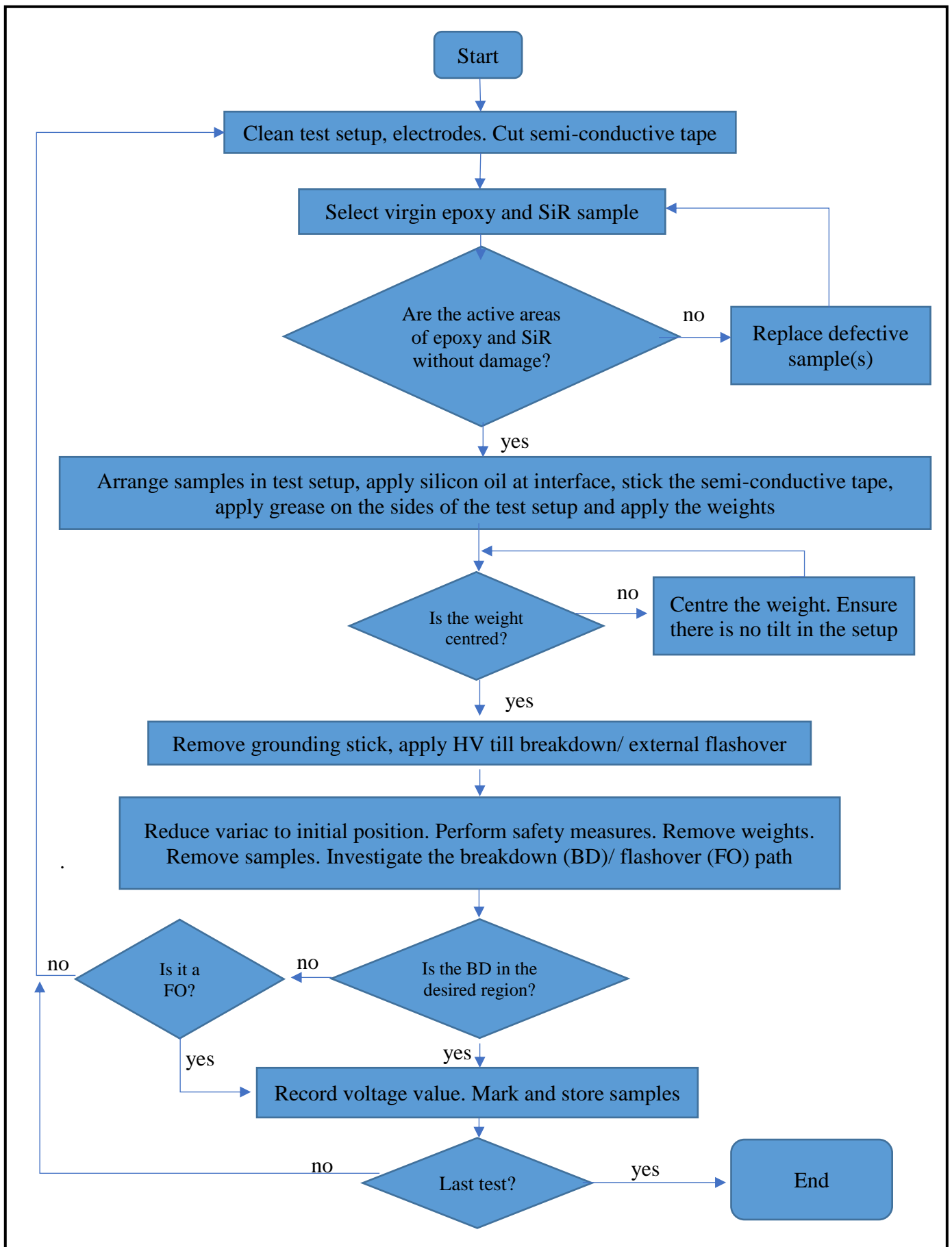
Fig. 5.13: Flowchart- AC breakdown test with oil at the interface

5.3.2 Test results

As explained in the earlier sub-section, silicon grease was applied at all the inner-sides/ corners to prevent flashovers. This type of tests was performed at 2 different pressure values 0.5 bar and 1 bar.

5.3.2.1 Interfacial pressure 0.5 bar

The interface testing for 0.5 bar interfacial pressure was tested according to the procedure explained in *Section 5.3.1*. Standard weights of 2.4 kg (refer *Table 4.1*) was used to create the interfacial pressure.

Pressure (bar)	AC Breakdown voltage (kV)	Electric field (kV/mm)
0.5	> 50*	> 8.33
0.5	> 48*	> 8.00

Table 5.6: AC breakdown with oil at the interface – 0.5 bar
[* indicates that there was no breakdown at the interface.
There was a flashover from the outside of the test setup]

Initially, there were flashovers at around 30 kV from the inner sides of the test setup (through the 6 mm slits in the test holder). Silicon grease was applied (as shown in *Fig. 5.*12) to prevent these flashovers. At around 50 kV, there were flashovers from the outside of the tests setup. There was **no breakdown at the interface**.

5.3.2.2 Interfacial pressure 1 bar

The interface testing for 1 bar interfacial pressure was tested according to the procedure explained in *Section 5.3.1*. Standard weights of 1 kg (refer *Table 4.1*) was used to create the interfacial pressure.

Pressure (bar)	AC Breakdown voltage (kV)	Electric field (kV/mm)
1	> 50*	> 8.33
1	> 48.7*	> 8.12
1	> 47*	> 7.83
1	> 50*	> 8.33
1	> 49*	> 8.17
1	> 48*	> 8.00
1	> 47*	> 7.83

Table 5.7: AC breakdown with oil at the interface – 1 bar
[* indicates that there was no breakdown at the interface.
There was a flashover from the outside of the tests setup]

Silicon grease was applied (as shown in *Fig. 5.*12) to prevent these flashovers. At around 50 kV, there were flashovers from the outside of the tests setup. There was **no breakdown at the interface**.

5.3.3 Summary

Initially the tests were performed at 1 bar, however due to flashovers from the outside of the test setup (around the test setup), it was decided to lower the interfacial pressure to 0.5 bar. Even then, there were flashovers from the outside of the test setup. Thus, it is concluded that because of oil at the interface, the interface can withstand **at least 50 kV** (8.33 kV/mm).

Due to exterior flashovers, further tests of this type were not conducted. The AC voltage of 50 kV was thus deduced to be the **AC voltage limit of the test setup**. There was **no breakdown of the interface** up to 8.33 kV/mm.
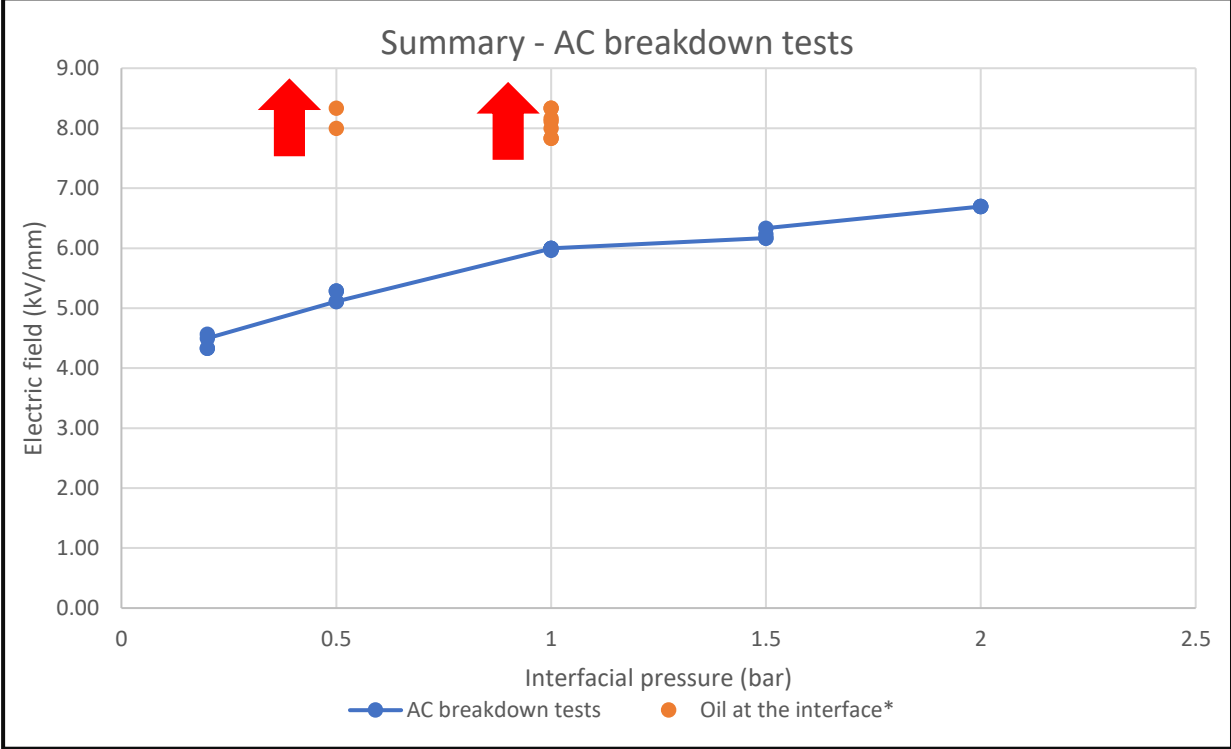
Fig. 5.14: AC breakdown field strength with oil at interface – summary

The reason behind the better electric breakdown performance with oil at the interface is attributed to the fact that oil covers/ fills-up the voids in the interface of the two materials [13]. Thus, it does not allow the initiation of a breakdown channel.

74

5.4 AC breakdown tests with scratch on epoxy

During the installation of accessories, it is sometimes observed that there can be some scratches on the epoxy surface. Although it is rare, it is attributed to improper installation/ mounting techniques. Also, sometimes installation tools may scratch the surface of the epoxy. This section aims to find the effect of such scratches on the electrical performance of the epoxy/ silicon rubber interface. Single scratches are made by using a knife. The scratches are made parallel and perpendicular to the applied electric field.

5.4.1 Test procedure

The **test cell** is cleaned, and all unnecessary equipment is disconnected/ moved. Then, the cell is checked for its safety systems by applying a small voltage and tripping the system. This allows us to check if the power electronics based fast switch is working. Also, the interlocking gates of the test cell are checked in this way.

The **semi-conductive tape** is cut by hand into oval pieces as shown in *Fig. 5.3*. Any sharp corners in the tape are rounded off. The plastic cover on one side of the tape is removed during final assembly.

The **test setup** is assembled by cleaning each of the parts with isopropyl alcohol and drying them. The **electrodes** are also thoroughly cleaned. The parts are then plugged-into the base plate and the entire test setup is assembled. The test setup was placed on a movable cart, to enable the moving of the test setup for cleaning and other practical reasons.

The **epoxy and silicon rubber samples** are first checked for manufacturing defects/ scratches in the active region (80 × 6 mm sides). A **scratch** is made using a knife. The samples are then cleaned using isopropyl alcohol and allowed to dry.

The oval **semi-conductive tape** is stuck to the interface and then the electrode is pressed on the tape to allow good adhesion. The specific **weights** are then kept on the *weight carrying plate*. It is ensured that the weights are kept in the middle to prevent the setup from toppling.

The grounding stick is removed, and test cage is closed. Then, the voltage is applied at a rate of **1kV/second.** This rate of rise is within the short-time test requirements as stipulated by ASTM standards [4]. Applied voltage is monitored on both the voltmeters.

After breakdown, the fast switch trips the circuit. Then, the variac is brought back to zero and the breakdown voltage is recorded. The test cell is opened, and the grounding stick is then put in place to ground the secondary of the HV transformer and the voltage divider.

The weights are removed and the top sample (silicon rubber) is removed to **investigate** the breakdown area. If the breakdown originates at the triple point (at the edge of the semi-conductive tape), the reading is discarded.

The breakdown paths are photographed. Then, the samples are marked with permanent marker and safely stored in zip lock pouches. The test setup and the electrodes are then cleaned with isopropyl alcohol and the next virgin sample is taken for investigation.

A detailed flowchart of the test procedure is shown in *Fig. 5.15.*

Fig. 5.15: Flowchart- AC breakdown test with scratch on epoxy

5.4.2 Test results

The AC breakdown tests with scratch (horizontal and vertical) on the epoxy surface were carried out at 1 bar and 2 bar interfacial pressures. Only samples that had breakdown in the region of the electrode were taken into consideration. Other breakdowns (at the edge of the semi-conductive tape) were discarded.

5.4.2.1 Interfacial pressure 1 bar

The interface testing for 1 bar interfacial pressure was tested according to the procedure explained in *Section 5.4.1.* Standard weights of 5 kg (refer *Table 4.1*) was used to create the interfacial pressure.

(a) Perpendicular to applied field

(b) Parallel to applied field

(c) Perpendicular to applied field

(d) Perpendicular to applied field
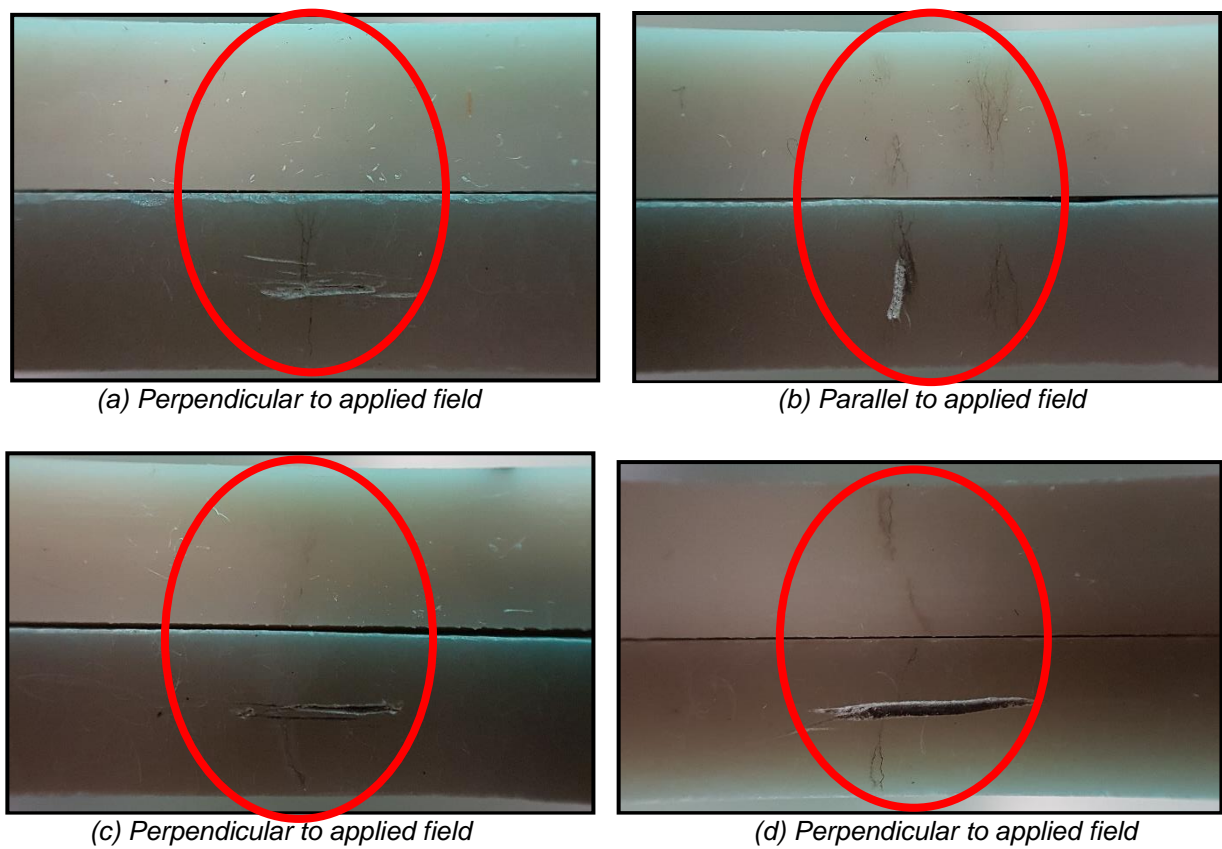
Fig. 5.16: AC breakdown path with scratch on epoxy – 1 bar
[lower material- epoxy; upper material- silicon rubber]

Pressure (bar)	AC Breakdown voltage (kV)	Electric field (kV/mm)	Position of defect w.r.t. electric field
1	31	5.17	Perpendicular
1	32	5.33	Perpendicular
1	32	5.33	Perpendicular
1	28	4.67	Parallel
1	32	5.33	Perpendicular

Table 5.8: AC breakdown with scratch on epoxy at 1 bar - results

The observations are as follows:

- The breakdown electric field is around **5.2 kV/mm** compared to 6 kV/mm that was obtained from *Section 5.2.2.3*.

- The rubber samples have a **mark of the scratch** on the epoxy (like a negative of the scratch)

- The breakdown path is **distinct and clear**.

- Multiple or branched tracks are observed.

- Lower electric breakdown voltage is observed when the defect is parallel to the applied electric field

5.4.2.1 Interfacial pressure 2 bar

The interface testing for 2 bar interfacial pressure was tested according to the procedure explained in *Section 5.4.1*. Standard weights of 10 kg (refer *Table 4.1*) was used to create the interfacial pressure.

(a) Parallel to applied field

(b) Perpendicular to applied field

(c) Perpendicular to applied field
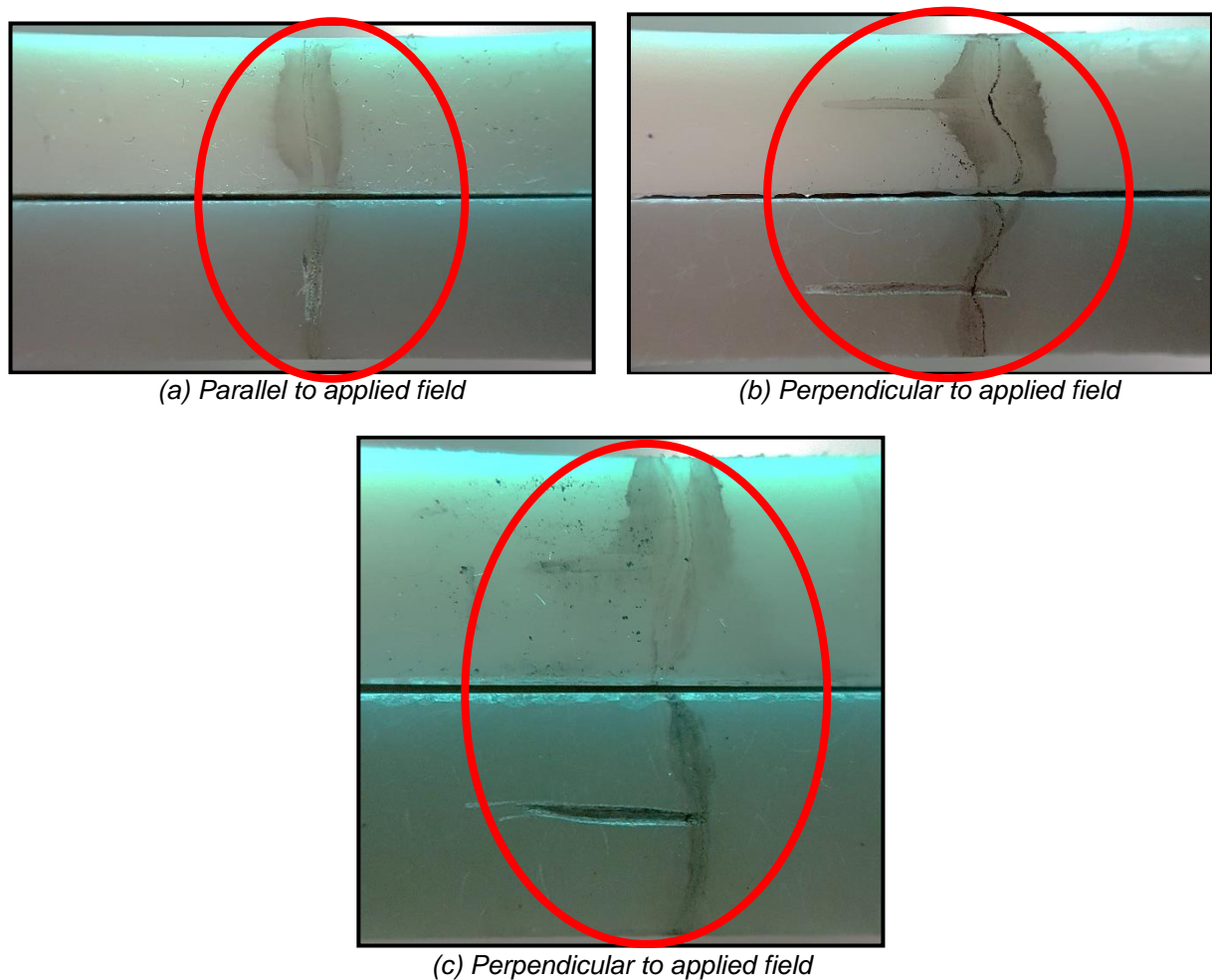
Fig. 5.17: AC breakdown path with scratch on epoxy – 2 bar
[lower material- epoxy; upper material- silicon rubber]

Pressure (bar)	AC Breakdown voltage (kV)	Electric field (kV/mm)	Position of defect w.r.t. electric field
2	34	5.67	Perpendicular
2	34	5.67	Perpendicular
2	32	5.33	Parallel
2	36	6.00	Perpendicular

Table 5.9: AC breakdown with scratch on epoxy at 2 bar - results

The observations are as follows:

- The breakdown electric field is around **5.3 - 6 kV/mm** compared to 6.7 kV/mm that was obtained from *Section 5.2.2.5*.

- The rubber samples have a **mark of the scratch** on the epoxy (like a negative of the scratch)

- The breakdown path is **distinct and clear**.

- Multiple or branched tracks are **not** observed.

- Lower electric breakdown voltage is observed when the defect is parallel to the applied electric field

5.4.3 Summary

Fig. 5.18 explains the effect of the scratch on epoxy surface in comparison to the normal AC breakdown tests that is explained in *Section 5.2*. As expected, the electrical performance of the interface reduces for the same interfacial pressure.
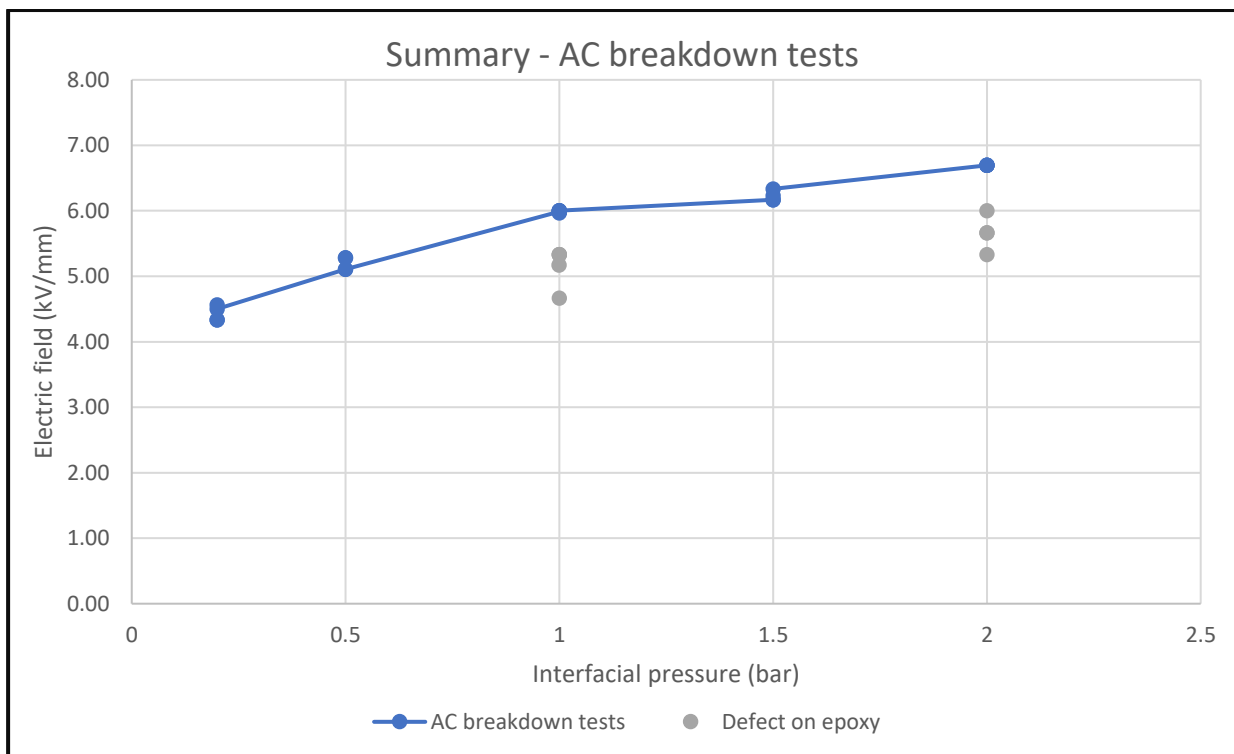
Fig. 5.18: AC breakdown field strength with scratch on epoxy – summary

79

The scatter/ spread in readings in attributed to the dimensions of the scratch and types of scratch (vertical or horizontal). Thus, it can be said that a **scratch on the epoxy can reduce the electrical performance of the interface by 11.7 %. This is equivalent to a 0.5 bar decrease in interfacial pressure**.

It is also to be noted that lower electric breakdown voltage is observed when the defect is parallel to the applied electric field

5.5 *AC breakdown tests with heated samples*

The maximum permissible operating temperature of power cables is 90°C. Thus, it is obvious that the cable accessories will also get heated to about 85 - 90°C during normal operation. Silicon rubber is known to become soft at high temperatures. This could influence the electrical performance of the interface. This section is aimed at investigating this condition further.

5.5.1 *Test procedure*

The **test cell** is cleaned, and all unnecessary equipment is disconnected/ moved. Then, the cell is checked for its safety systems by applying a small voltage and tripping the system. This allows us to check if the power electronics based fast switch is working. Also, the interlocking gates of the test cell are checked in this way.

The **semi-conductive tape** is cut by hand into oval pieces as shown in *Fig. 5.3*. Any sharp corners in the tape are rounded off. The plastic cover on one side of the tape is removed during final assembly.

The **test setup** is assembled by cleaning each of the parts with isopropyl alcohol and drying them. The **electrodes** are also thoroughly cleaned. The parts are then plugged-into the base plate and the entire test setup is assembled. The test setup was placed on a movable cart, to enable the moving of the test setup for cleaning and other practical reasons.

The **epoxy and silicon rubber samples** are first checked for defects/ scratches in the active region (80 × 6 mm sides). The samples are then cleaned using isopropyl alcohol and allowed to dry. Both the samples are then placed in an oven at 90°C. After **24 hours** of heating, the samples are immediately assembled in the test setup.
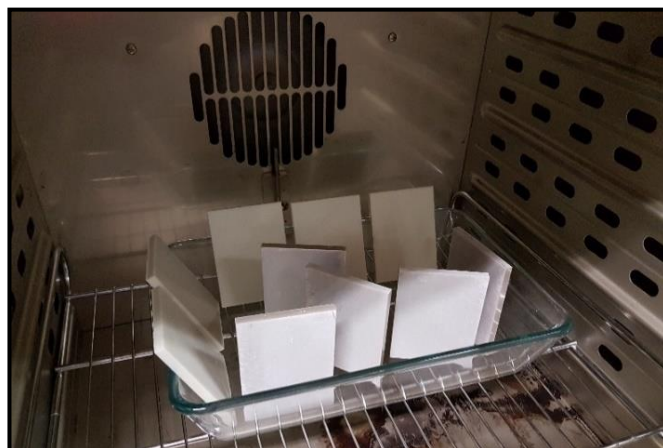
Fig. 5.19: Heating of epoxy and silicon rubber samples

The oval **semi-conductive tape** is stuck to the interface and then the electrode is pressed on the tape to allow good adhesion. The specific **weights** are then kept on the *weight carrying plate*. It is ensured that the weights are kept in the middle to prevent the setup from toppling.

The grounding stick is removed, and test cage is closed. Then, the voltage is applied at a rate of **1kV/second.** This rate of rise is within the short-time test requirements as stipulated by ASTM standards [4]. Applied voltage is monitored on both the voltmeters.

After breakdown, the fast switch trips the circuit. Then, the variac is brought back to zero and the breakdown voltage is recorded. The test cell is opened, and the grounding stick is then put in place to ground the secondary of the HV transformer and the voltage divider.

The weights are removed and the top sample (silicon rubber) is removed to **investigate** the breakdown area. If the breakdown originates at the triple point (at the edge of the semi-conductive tape), the reading is discarded.

The breakdown paths are photographed. Then, the samples are marked with permanent marker and safely stored in zip lock pouches. The test setup and the electrodes are then cleaned with isopropyl alcohol and the next virgin sample is taken for investigation.

A detailed flowchart of the test procedure is shown in *Fig. 5.20.*

Fig. 5.20: Flowchart- AC breakdown test with heated samples

5.5.2 Test results

The AC breakdown tests for heated samples were carried out at 0.5 bar, 1 bar and 2 bar. Only samples that had breakdown in the region of the electrode were taken into consideration. Other breakdowns (at the edge of the semi-conductive tape) were discarded.

5.5.2.1 Interfacial pressure 0.5 bar

The interface testing for 0.5 bar interfacial pressure was tested according to the procedure explained in *Section 5.5.1*. Standard weights of 2.4 kg (refer *Table 4.1*) was used to create the interfacial pressure.

Fig. 5.21: AC breakdown path of heated samples - 0.5 bar
[lower material- epoxy; upper material- silicon rubber]

Pressure (bar)	AC Breakdown voltage (kV)	Electric field (kV/mm)
0.5	29.82	4.97
0.5	30.65	5.11

Table 5.10: AC breakdown with heated samples at 0.5 bar – results

The observations are as follows:

- The breakdown electric field was around **4.9 kV/mm** this is same as the values obtained from *Section 5.2*.

- The breakdown path was **clear** and **distinct**.

- There were **carbonised breakdown tracks**.

- The breakdown tracks appeared to be **straight** (unlike the tracks seen for 1 bar and above). This shows that the interfacial pressure did not play a large role in preventing the interface from breaking down.

- **Multiple** or **branched tracks** were observed.

83

The interface testing for 1 bar interfacial pressure was tested according to the procedure explained in *Section 5.5.1*. Standard weights of 5 kg (refer *Table 4.1*) was used to create the interfacial pressure.
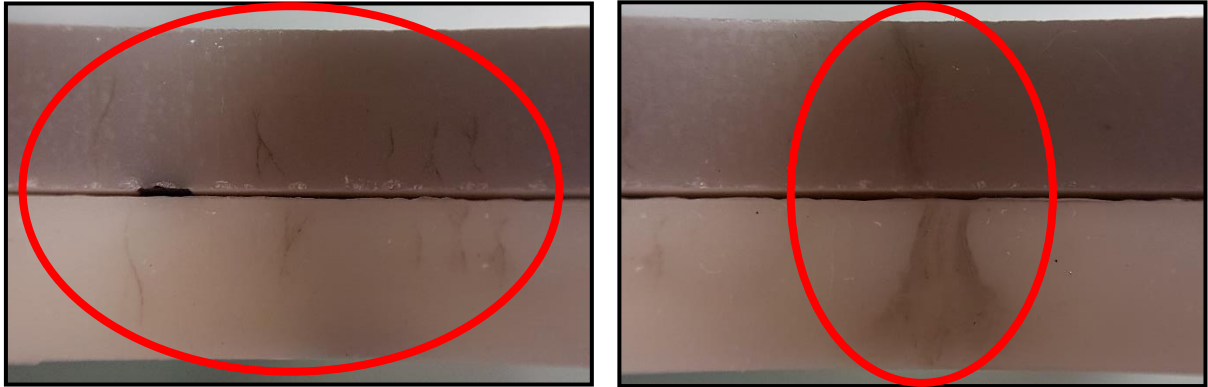
Fig. 5.22: AC breakdown path of heated samples - 1 bar
[lower material- epoxy; upper material- silicon rubber]

Pressure (bar)	AC Breakdown voltage (kV)	Electric field (kV/mm)
1	34	5.67
1	36	6.00
1	34	5.67
1	29	4.83
1	32	5.33

Table 5.11: AC breakdown with heated samples at 1 bar - results

The observations are as follows:

- The breakdown electric field is between **4.8 - 6 kV/mm** compared to 6 kV/mm in *Section 5.2*.

- The breakdown path is **clear** and **distinct**.

- There are **carbonised breakdown tracks**.

- **Multiple** or **branched tracks** are observed.

The interface testing for 2 bar interfacial pressure is tested according to the procedure explained in *Section 5.5.1*. Standard weights of 10 kg (refer *Table 4.1*) are used to create the interfacial pressure.
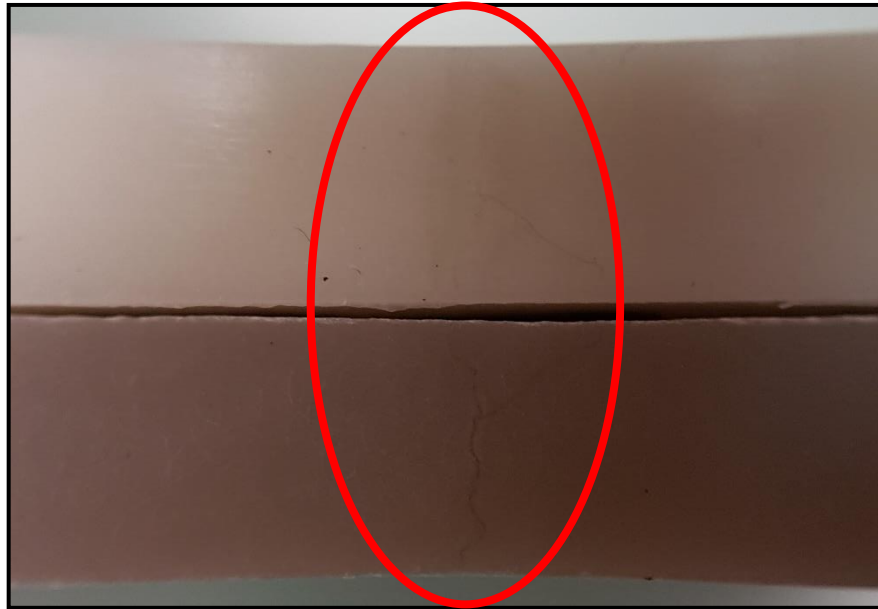
Fig. 5.23: AC breakdown path of heated samples - 2 bar
[lower material- epoxy; upper material- silicon rubber]

Pressure (bar)	AC Breakdown voltage (kV)	Electric field (kV/mm)
2.0	37.00	6.17
2.0	32.77	5.46

Table 5.12: AC breakdown with heated samples at 2 bar - results

The observations are as follows:

- The breakdown electric field is **5.4 – 6.1 kV/mm** compared to 6.7 kV/mm in *Section 5.2*

- The breakdown path is **clear** and **distinct**.

- There are **carbonised breakdown tracks**.

- Multiple or branched tracks are **not** observed in the samples.

5.5.3 Summary

The analysis of heated samples will help to understand the interfacial behaviour during the operating conditions of the cable. The results of these tests show that under heated condition, the interface is **weaker** than the normal case. However, there is some scatter/ spread of data which does not allow to exactly quantify this decrease in performance. The scatter in readings can be attributed to the decrease in temperature of samples.
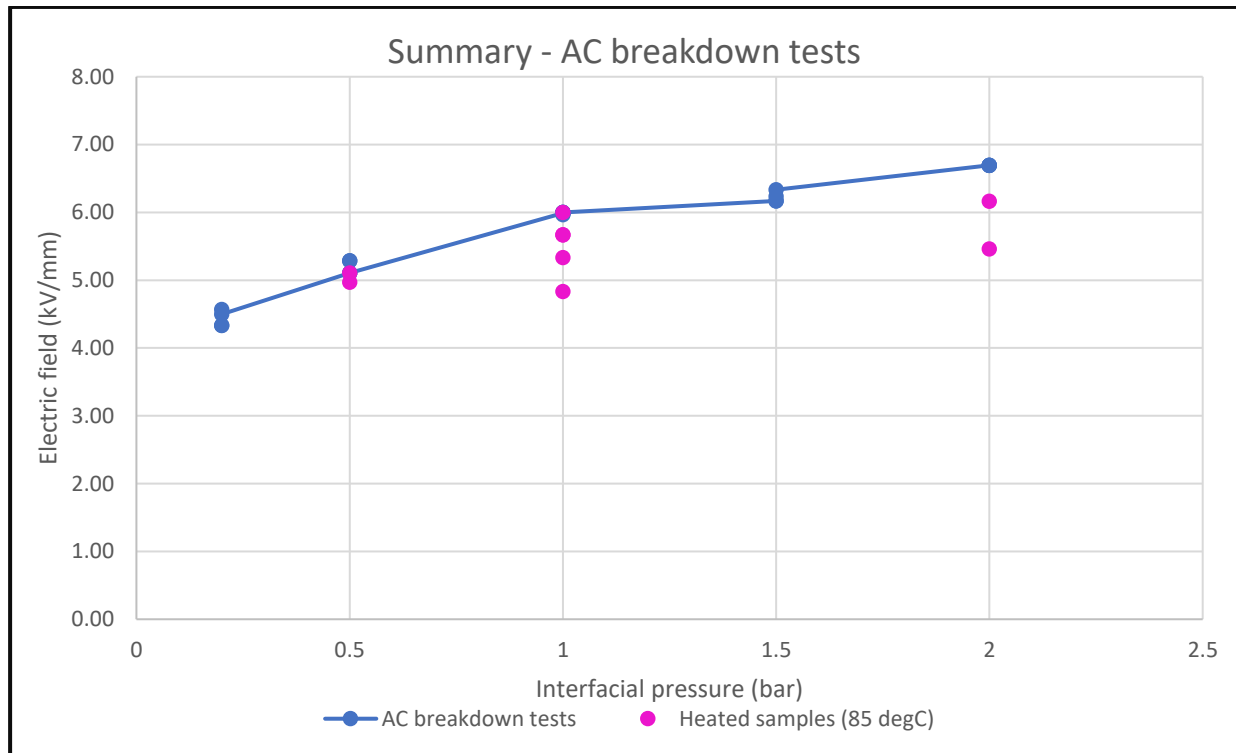
Fig. 5.24: AC breakdown field strength with heated samples – summary

5.6 Lightning Impulse tests

The earlier sections provided an understanding of the performance under AC voltage. However, it is also important to learn about the performance of an interface to LI voltages.

Lightning Impulse tests were carried out at the test cell as described in *section 5.1.2*. As a thumb rule in high voltage engineering, it is considered that the LI breakdown is 2-3 times greater than the normal AC breakdown voltage of any material.

5.6.1 Test procedure

The **test cell** is cleaned, and all unnecessary equipment is disconnected/ moved. Then, the cell is checked for its safety systems.

The **semi-conductive tape** is cut by hand into oval pieces as shown in *Fig. 5.3*. Any sharp corners in the tape are rounded off. The plastic cover on one side of the tape is removed during final assembly.

The **test setup** is assembled by cleaning each of the parts with isopropyl alcohol and drying them. The **electrodes** are also thoroughly cleaned. The parts are then plugged-into the base plate and the entire test setup is assembled. The test setup was placed on a movable cart, to enable the moving of the test setup for cleaning and other practical reasons.

The **epoxy and silicon rubber samples** are first checked for defects/ scratches in the active region (80×6 mm sides). The samples are then cleaned using isopropyl alcohol.

The oval **semi-conductive tape** is stuck to the interface and then the electrode is pressed on the tape to allow good adhesion. The specific **weights** are then kept on the *weight carrying plate*. It is ensured that the weights are kept in the middle to prevent the setup from toppling.

After a few initial tests it was observed that there were flashovers from the inner side of the test setup (through the 6 mm slit). Thus, **silicon grease** was applied to all the corners to prevent flashovers from the inner sides (refer *Fig. 5.12*).

The test cage is closed. Then, a voltage of 40 kV is applied using the impulse analysing and control system. The system gives a plot of the applied voltage. This helps us to know if there was a breakdown. Voltage is increased in **steps of 10kV** until there is a breakdown/ flashover. After breakdown/ flashover, the impulse analysing system plots the front-chopped or tail-chopped waveform. The system is automatically grounded.

The weights are removed and the top sample (silicon rubber) is removed to **investigate** the breakdown area. If the breakdown originates at the triple point (at the edge of the semi-conductive tape), the reading is discarded.

The breakdown paths are photographed. Then, the samples are marked with permanent marker and safely stored in zip lock pouches. The test setup and the electrodes are then cleaned with isopropyl alcohol and the next virgin sample is taken for investigation.

A detailed flowchart of the test procedure is shown in *Fig. 5.25*.
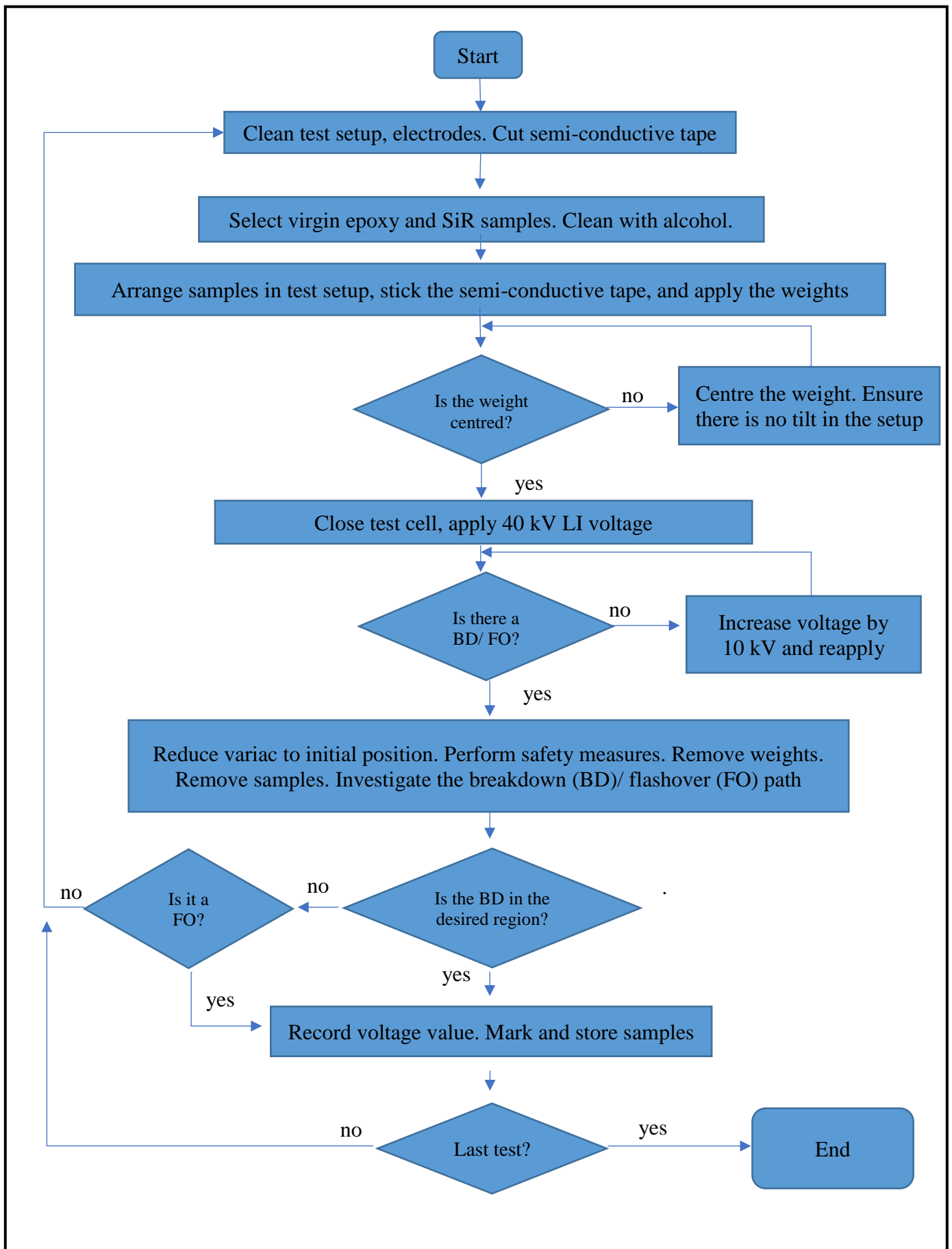
Fig. 5.25: Flowchart- LI breakdown test

5.6.2 Test results

As explained in the earlier sub-section, silicon grease was applied at all the inner-sides/ corners to prevent flashovers. This type of tests was performed at 1 bar interfacial pressure.

5.3.2.1 Interfacial pressure 1 bar

The interface testing for 1 bar interfacial pressure was tested according to the procedure explained in *Section 5.6.1*. Standard weights of 1 kg (refer *Table 4.1*) was used to create the interfacial pressure.

Pressure (bar)	AC Breakdown voltage (kV)	Electric field (kV/mm)
1	> 88.3*	> 14.72
1	> 86.7*	> 14.45
1	> 87*	> 14.50
1	> 88.7*	> 14.78
1	> 89*	> 14.83
1	> 90*	> 15
1	> 90*	> 15

Table 5.13: Lightning Impulse test – 1 bar
[* indicates that there was no breakdown at the interface.
There was a flashover from the outside of the tests setup]

Initially, there are flashovers at around 60 kV from the inner sides of the test setup (through the 6 mm slits in the test holder). Silicon grease is applied (as shown in *Fig. 5.*12) to prevent these flashovers. At around 90 kV, there are flashovers from the outside of the tests setup. There is **no breakdown at the interface** up to 15 kV/mm.

5.6.3 Summary

Due to the conclusion from AC breakdown tests, it was decided to only perform LI tests for one pressure value. The limited availability of samples also prevented testing for multiple pressure values.

After the application of silicon grease, tests were conducted and found that there were flashovers from the outside of the test setup. This indicated the **LI testing limit of the test setup**. Thus, it is concluded that the interface is can withstand **at least 90 kV** (15 kV/mm). Due to exterior flashovers, further tests of this type were not conducted. There was **no breakdown of the interface**.
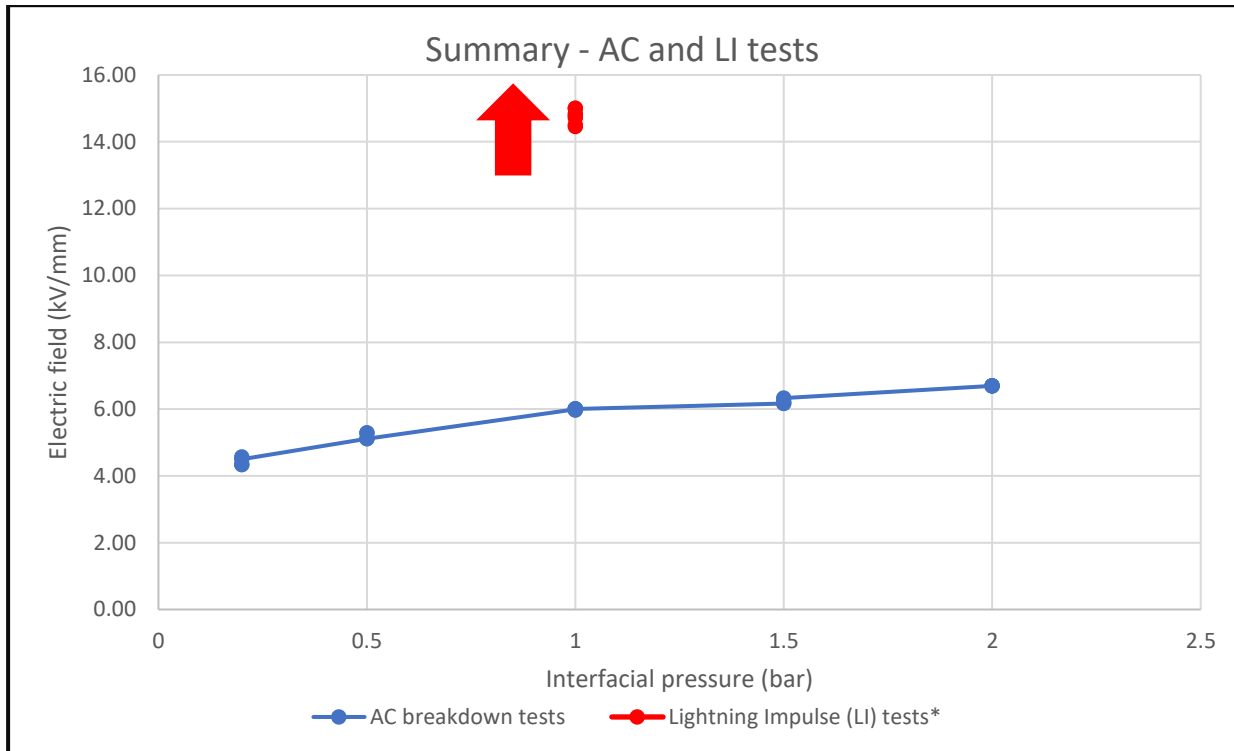
Fig. 5.26: Lightning Impulse breakdown field strength – summary

5.7 *Summary of experimental testing*

The AC breakdown tests (*Section 5.2*) gives an understanding of the variation of electric field strength with respect to interfacial pressure. The **electrical performance of the interface improves with increase in interfacial pressure**. A flat (stable) region is observed **beyond 1 bar** pressure. Thus, **1 bar is taken as a minimum pressure value for the design of the inner-cone termination**.

It must be noted that the value of breakdown voltage is **conservative** in nature. This is because, in this test setup, the electrodes are very close to the interface. This would produce a very strong/ harsh electrical field. However, in a real termination the high voltage and ground parts are far away from the interface. Thus, the effect of the electric field may be milder compared to the test setup. This reason can also be used to reason for the *CIGRE 15-10* recommendation of not having metal electrodes directly at the interface.

The AC tests with oil at the interface (*Section 5.3*), scratch on epoxy (*Section 5.4*), AC test with heated samples (*Section 5.5*) and LI tests (*Section 5.6*) were performed additionally due to the very small deviation in the results of AC breakdown tests (*Section 5.2*). These tests helped to find the limits of the test setup – **50 kV for AC voltage** and **90kV for Lightning Impulse (LI) voltages**. There was a decrease in electrical performance of the interface due to scratch on the surface of epoxy. It was found that a **scratch on the epoxy can reduce the electrical performance of the interface equivalent to a 0.5 bar decrease in interfacial pressure**. Also, a scratch parallel to the interface has a lower breakdown voltage compared to a scratch perpendicular to the interface.

A summary plot of all the tests performed is shown in *Fig. 5.27*.

90

Fig. 5.27: AC and lightning impulse breakdown tests – summary

91

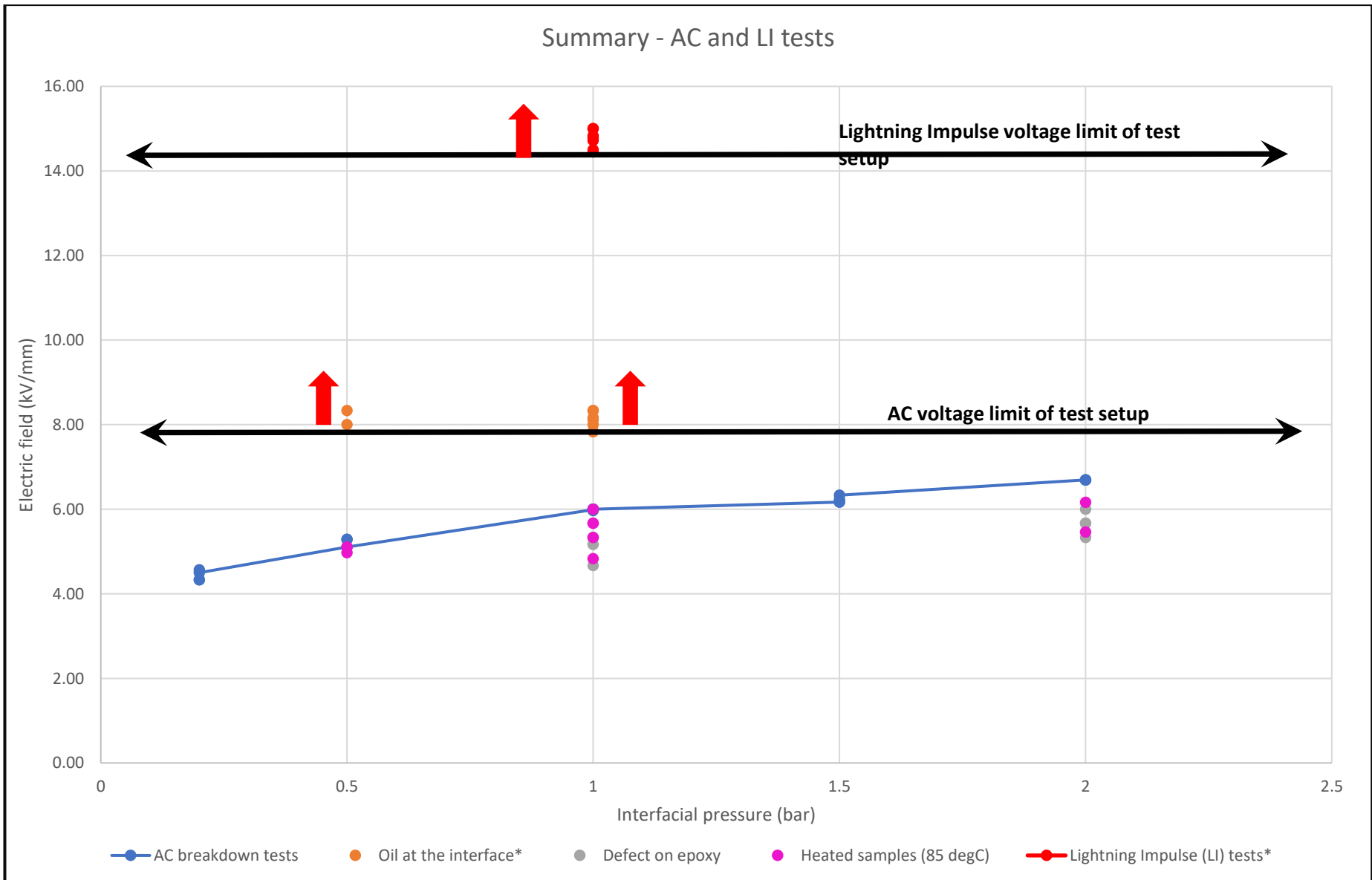# 6. Design of GIS termination

This chapter starts with an overview of the CIGRE JWG design of GIS termination. Next, it introduces the two proposed designs (named 'A' and 'B') of the 145kV inner-cone GIS cable termination. Electrical and Mechanical features of the two designs are also presented.

6.1 CIGRE JWG design

The CIGRE JWG B1 – B3.49 [49] has been setup to propose a standardised design for the 145 kV inner-cone GIS cable termination. This standardised design will be used as a foundation by various cable accessory manufacturers to design their termination. The design recommended by the CIGRE JWG is shown in *Fig. 6.1*.

The new CIGRE design has the following features:

1. The **mechanical connection interface** is the M16 x ■ screw at the top of the integrated electrode in the GIS.

2. The **electrical connection interface** is at the top of the ϕ95 mm upper surface of the integrated electrode. This surface will be silver plated. (marked with red dashed line in *Fig. 6.1*).

3. The **integrated electrode** provides a shielded cavity to have the cable locking mechanism. By providing this cylindrical volume, the standard allows different manufacturers to adapt or modify their respective cable locking mechanisms to fit into this volume.

4. The **epoxy/ silicon rubber interface** (marked in blue dashed line in *Fig. 6.1*) starts from the shielded region with ϕ100 mm up to ϕ185 mm. It can also extend up to the bottom of the design ϕ189 mm.

5. The **current rating** of the termination is $\leq$ 1000 A. **Short circuit rating** of the termination is $\leq$ 40 kA for 1 sec.

6. **Conductor cross sections** are $\leq$ 1000 mm^2 copper or $\leq$ 1600 mm^2 aluminium.

7. The new design meets all the requirements of **IEC 62271 – 209** and **IEC 60840**.

8. The accessory manufacturer is given the freedom to choose the stress cone design and material, the lubricant and the design of the compression device, as long as it is within the limits of the standardised insulator properties.
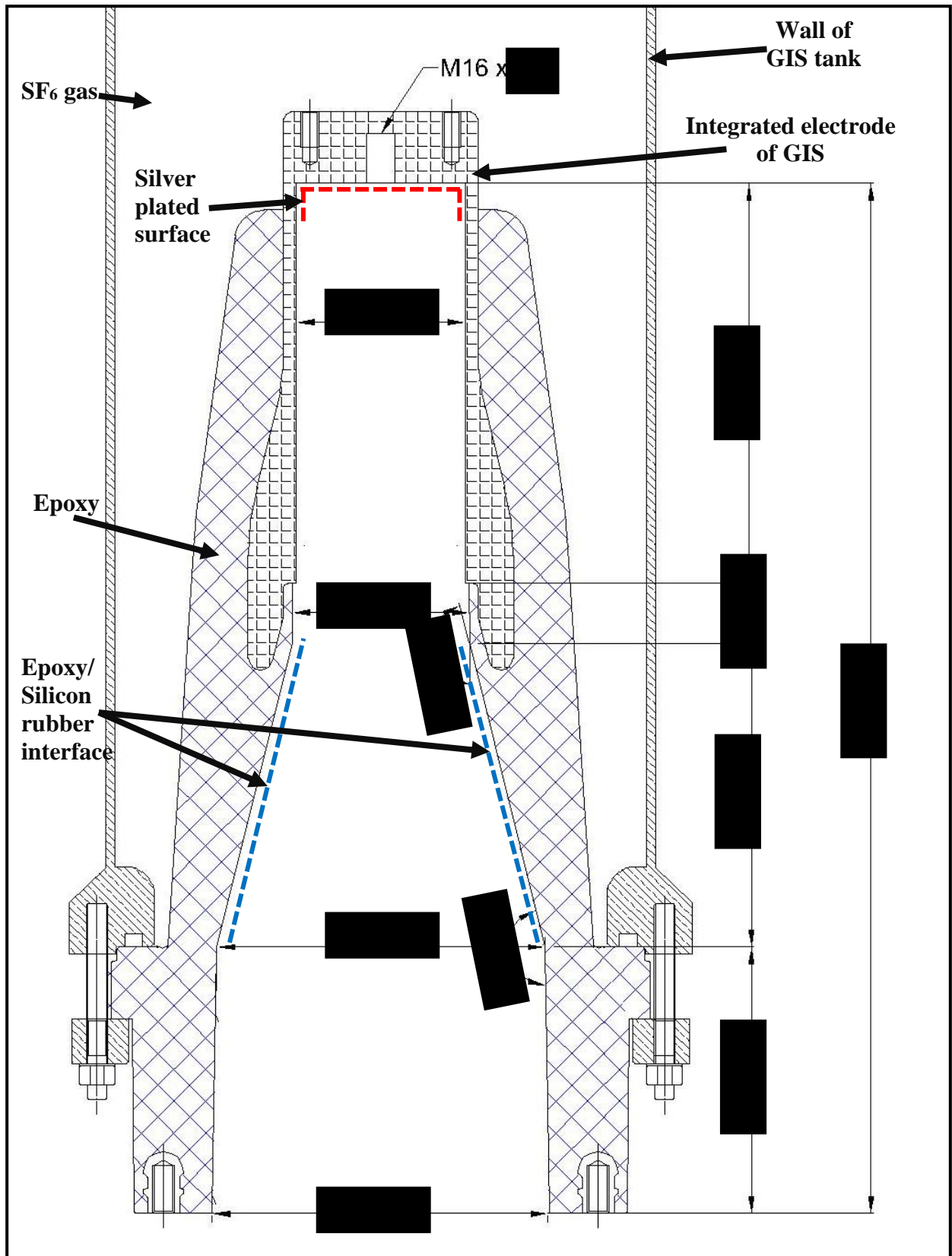
Fig. 6.1: CIGRE JWG B1 – B3.49 standard for 145 kV inner-cone GIS termination [49]

6.2 Design 'A'

Design 'A' is the first design that is proposed in this thesis. It consists of 3 parts- a long aluminium extension rod, the stress cone with embedded metal alloy and the cable. This design incorporates *Prysmian Group's Click-Fit* cable locking mechanism.

The **aluminium extension rod** has a male M16 screw on one end and a Click-Fit style cable end (with pins – refer pink shaded part of *Fig. 6.2*) on the other. This is first screwed into position using a long tool. A depiction of the GIS system with only the aluminium extension rod is shown in *Fig. 6.2*
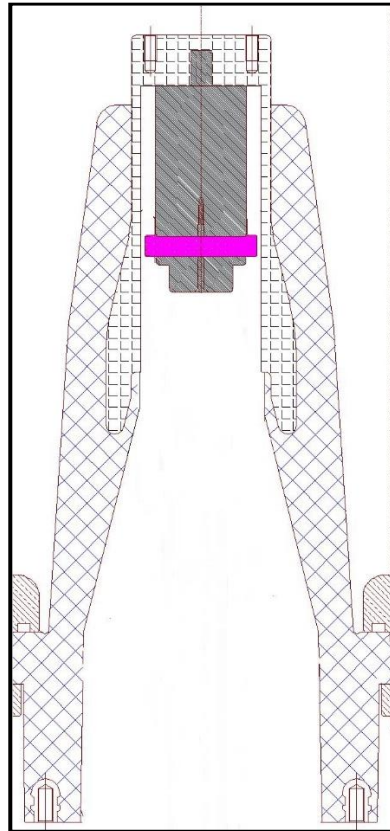
Fig. 6.2: Design 'A' – with aluminium extension rod

Next, the **silicon rubber stress cone** is slid into the GIS inner-cone. The stress cone has an embedded metal alloy for mechanical coupling (refer orange shaded part of *Fig. 6.3*). This alloy clicks and locks into position with the Click-Fit pins of the aluminium extension rod. The alloy also acts an extension of the integrated electrode, thus providing an extended area of HV shielding. *Fig. 6.4* provides an illustration of the design with the aluminium extension rod and the stress cone.

Epoxy

Aluminium extension rod

Integrated electrode

Metal alloy for mechanical coupling

Click-Fit locking pins

Metal ring for electrical coupling

Factory-made cable end

Semi-conductive silicon rubber

Insulating silicon rubber

Semi-conductive silicon rubber

semicon layer

XLPE
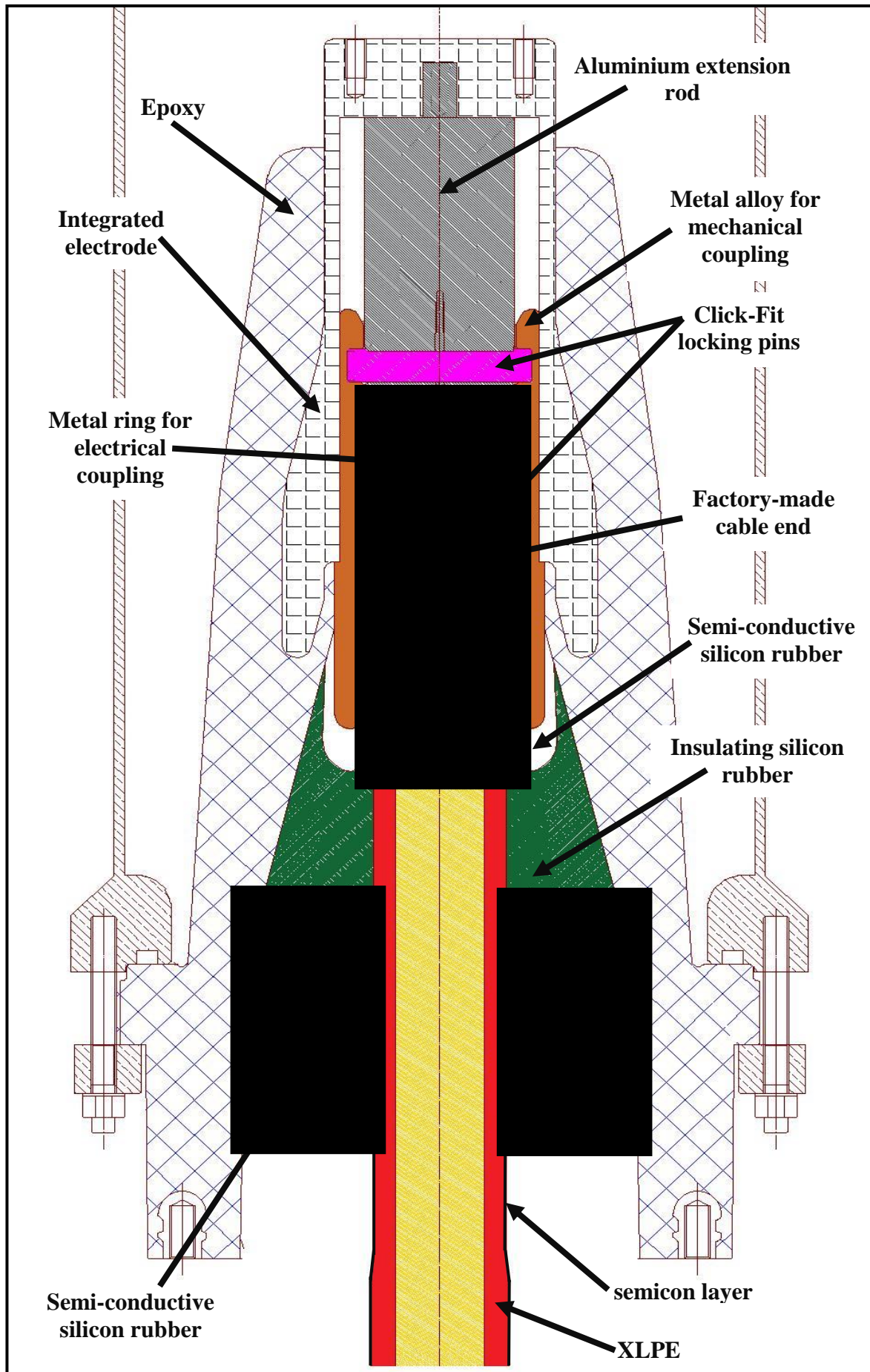
Fig. 6.3: Design 'A' of 145 kV inner-cone termination.

97
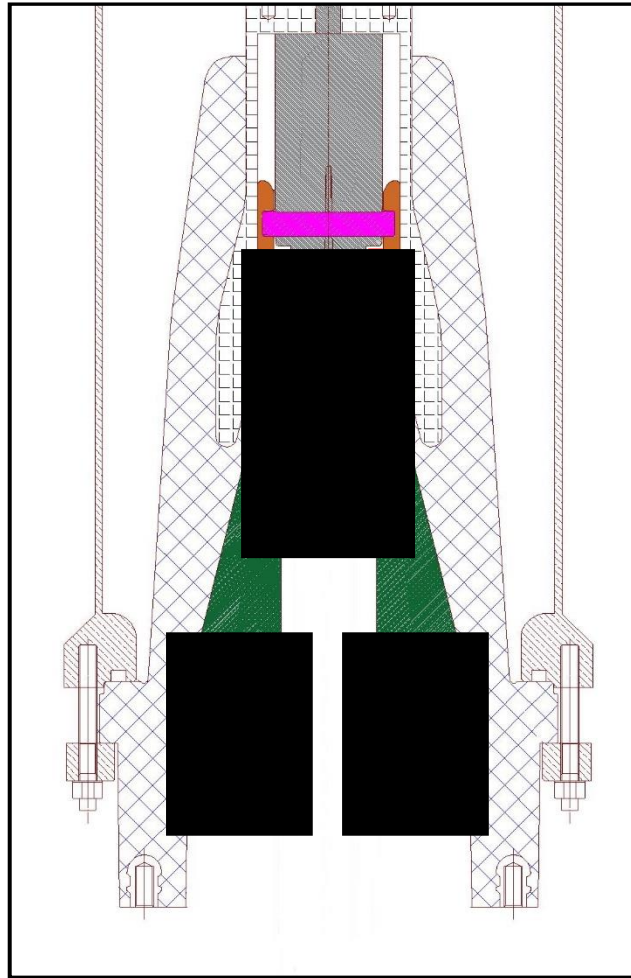
Fig. 6.4: Design 'A' – with aluminium extension rod and stress cone.

The factory-made **cable** end is then plugged into the stress cone (similar to the assembling of pre-moulded joints) until it clicks into the alloy of the stress cone. The necessary grounding of cable outer sheath is then done.

In order to create and to maintain the interfacial pressure, **springs** will be required to provide mechanical pressure. The forces required by the spring is calculated in the following subsections. Finally, the outer flange is bolted into position. The spring and the outer flange is not shown in *Fig. 6.3*, as the focus of this thesis is on the design of the silicon rubber insulator.

A complete illustration of this design is shown in *Fig. 6.3*.

6.3 Design 'B'

Design 'B' is the second design that is proposed in this thesis. It consists of 4 parts- a shorter aluminium extension rod, a cable locking adapter, the stress cone and the cable. This design also incorporates *Prysmian Group's Click-Fit* cable locking mechanism.

The main difference between the two design is the fact that Design 'B' attempts to use the integrated electrode itself for the shielding of the HV connection area. Thus, the aluminium extension rod is significantly smaller. Also, the stress cone is made only of rubber (no metallic inserts). Another important difference is the fact that the silicon rubber stress cone stops at the region where there is a bending of the epoxy. This makes the design simpler as compared to the previous proposal.

The **aluminium extension rod** has a male M16 screw on one end and a Click-Fit style cable end (with pins – refer pink shaded part of *Fig. 6.5*) on the other. This is first screwed into position using a long tool. It must be noted that the rod is significantly shorter than the extension rod proposed in design 'A'. An illustration of the GIS system with only the aluminium extension rod is shown in *Fig. 6.5*
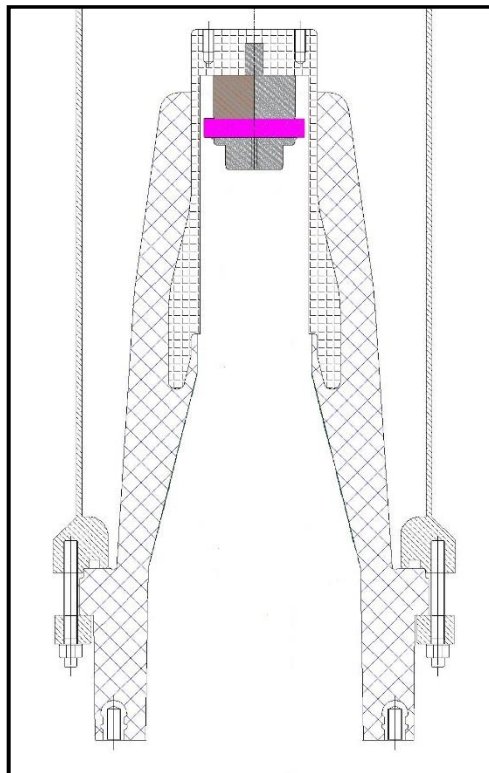
Fig. 6.5: Design 'B' – with aluminium extension rod

Next, the **cable locking adapter** is clicked into the *Click-Fit* pins of the aluminium extension rod. The metal ring for electrical connection (refer red shaded part of *Fig. 6.6*) is also inside this adapter. Thus, it acts as a mechanical and electrical connection between the extension rod and the cable. An illustration of the GIS system with the extension rod and the locking adapter is shown in *Fig. 6.7.*
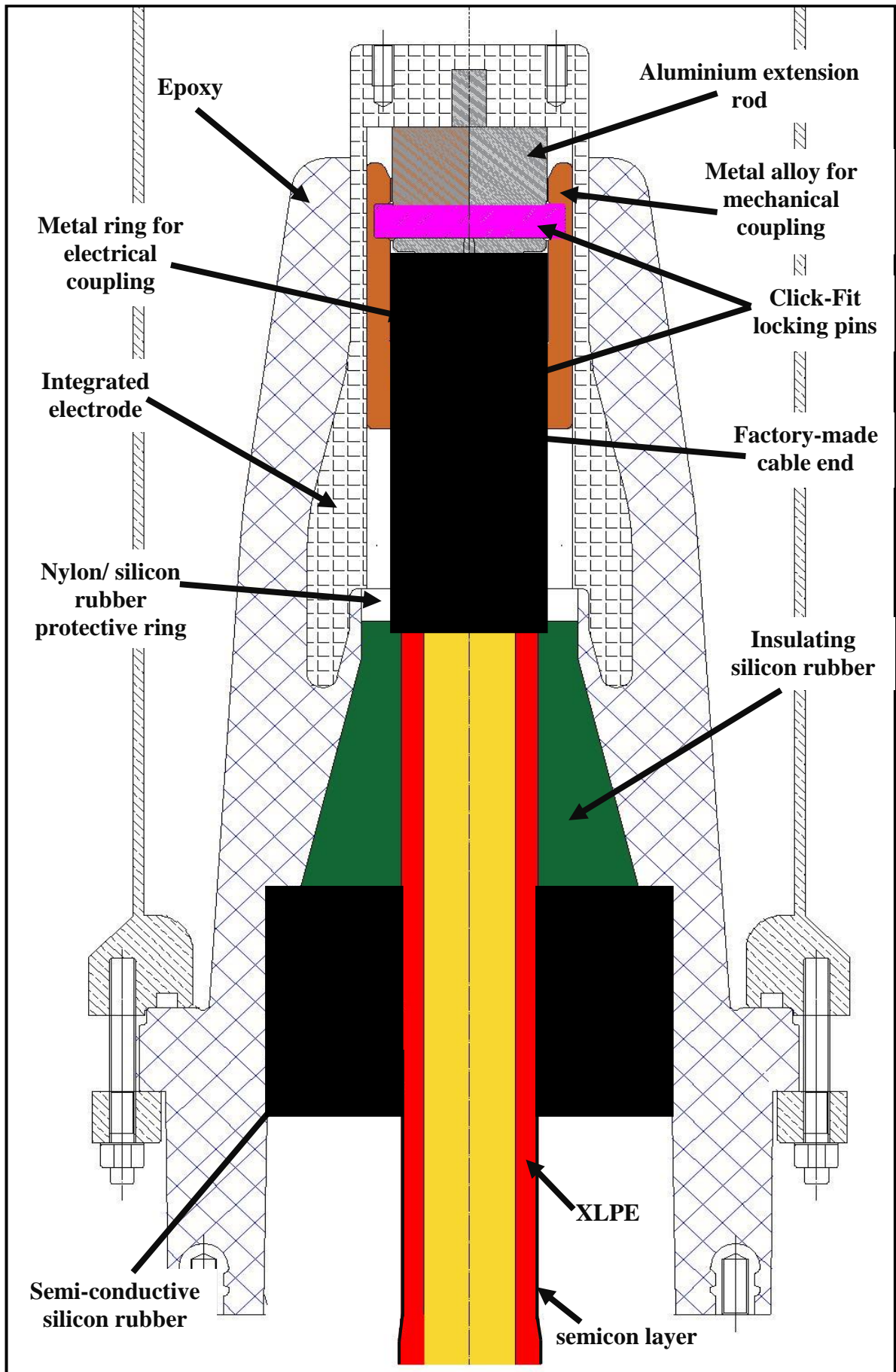
Fig. 6.6: Design 'B' of 145 kV inner-cone termination.

100
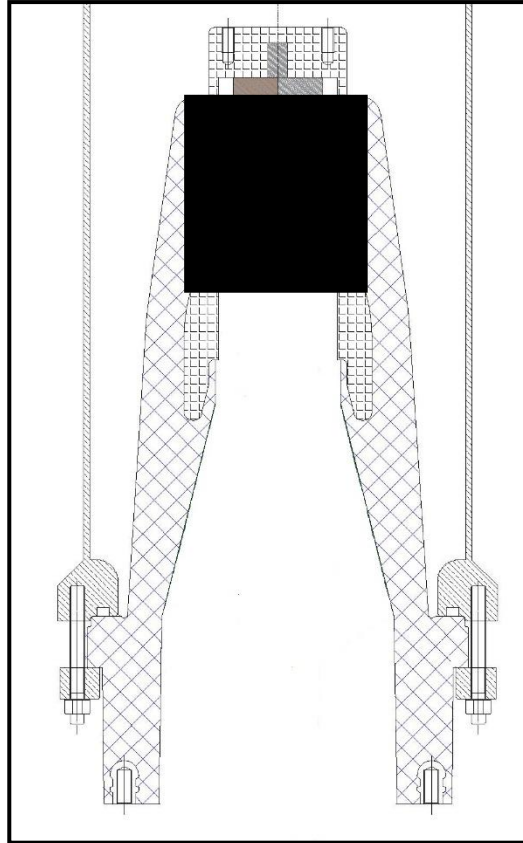
Fig. 6.7: Design 'B' – with aluminium extension rod and cable locking adapter.

Next, the **silicon rubber stress cone** is slid into the factory-made cable-end. These two are then clicked into the locking adapter that was described in the previous paragraph. The necessary grounding of cable outer sheath is then done.

In order to create and to maintain the interfacial pressure, **springs** will be required to provide mechanical pressure. The forces required by the spring is calculated in the following subsections. It must be noted that this design provides more space for the springs as compared to the previous design. Finally, the outer flange is bolted into position. The spring and the outer flange is not shown in *Fig. 6.6*, as the focus of this thesis is on the design of the silicon rubber insulator.

A complete illustration of this design is shown in *Fig. 6.6*.

6.4 Analysis of proposed designs

6.4.1 Electrical performance

The primary consideration of the two designs was to reduce the tangential component of electric field at the interface as low as possible. This was done by **redesigning** the shape of the defectors (semi-conductive rubber) to allow more space between the edge of deflector and the epoxy/ silicon rubber interface. 2D axis-symmetric FEM simulations of the normal electric field of both the designs are shown in *Fig. 6.8* and *Fig. 6.9*. It is observed that the silicon rubber is heavily stressed in design 'A' due to the HV semi-conductive rubber.

A comparative summary of the normal and tangential electric fields (at BIL - 650 kV applied voltage) at different materials/ interfaces of the termination is given in *Table 6.1*. However, it must be noted that the values of designs 'A' and 'B' **must not be quantitatively compared** with the values of existing cable accessories. This is because, the values of existing cable accessories are from outer-cone type of GIS terminations. The values are solely for qualitative comparisons. For ease of identification of these critical points in *Fig. 6.8* and *Fig. 6.9*, black markers (N1, N2 and N3) are used for normal electric field values and red markers (T1, T2 and T3) are used for tangential electric field values.
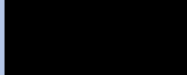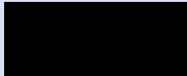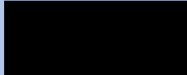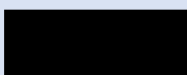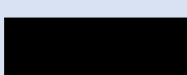
	Design 'A'	Design 'B'	Existing outer-cone accessories [45] (same voltage class)
Max. normal electric field in epoxy (kV/mm) [N1]	11.46	16.69	■
Max. normal electric field in silicon rubber (kV/mm) [N2]	19.49	*	■
Max. normal electric field in SF$_6$ (kV/mm) [N3]	15.45	15.47	■
Max. tangential electric field in XLPE/ SiR interface (kV/mm) [T1]	11.07	11.07	■
Max. tangential electric field in epoxy/ SF6 interface (kV/mm) [T2]	4.48	4.48	■
Max. tangential electric field in epoxy/ SiR interface (kV/mm) [T3]	5.84	5.8	■

Table. 6.1: Comparative summary of electrical performance (in kV/mm for BIL - 650 kV applied voltage) [refer Fig. 6.8 (a) and (b) for locations of the respective critical stresses]

* The maximum normal electric field in silicon rubber for design 'B' is not provided. This is because, the design has no HV semi-conductive rubber. Thus, there is no electrically critical area in N2 region.
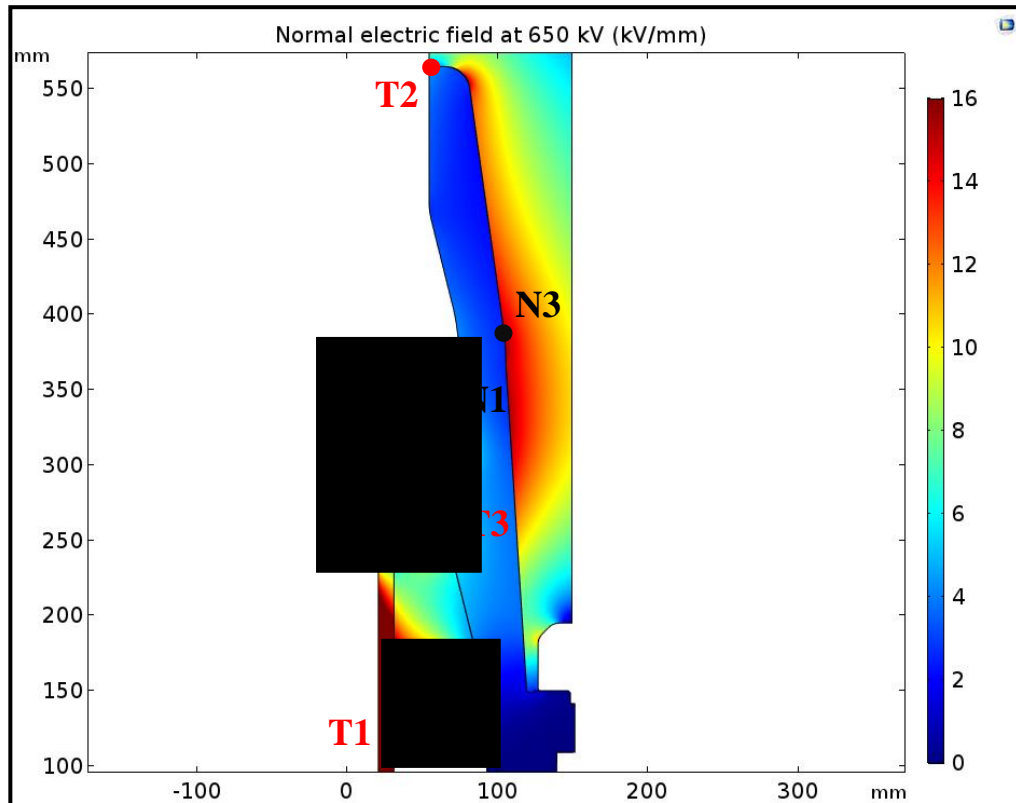
Fig. 6.8 (a): Design 'A' – Normal electric field in kV/mm at 650 kV (BIL).
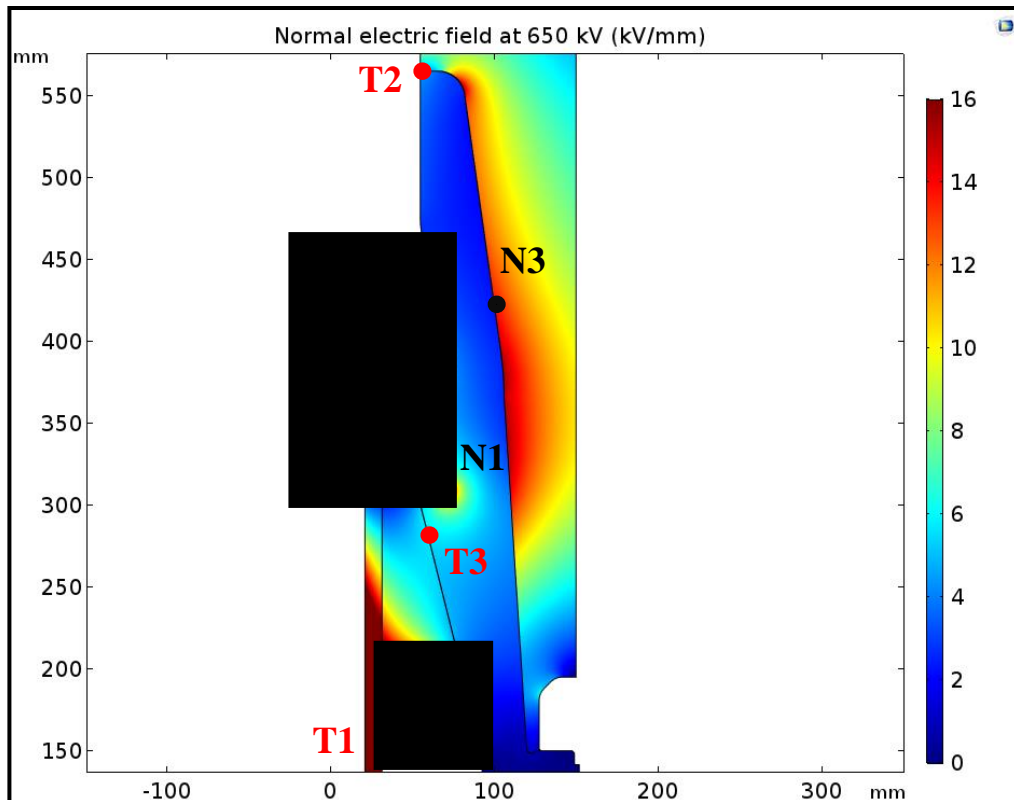
Fig. 6.8 (b): Design 'B' – Normal electric field in kV/mm at 650 kV (BIL).

N1 - *Max. normal electric field in epoxy;*   **T1** - *Max. tangential electric field in XLPE/ SiR interface*
N2 - *Max. normal electric field in silicon rubber;* **T2** - *Max. tangential electric field in epoxy/ SF6 interface*
N3 - *Max. normal electric field in SF6;*   **T3** - *Max. tangential electric field in epoxy/ SiR interface*

Fig. 6.9: Tangential electric field plot of proposed designs
- Epoxy/ silicon rubber interface at BIL - 650 kV (kV/mm)

Fig. 6.10: Tangential electric field plot of existing accessories [45]
- Epoxy/ silicon rubber interface at respective BIL voltages (kV/mm)

Fig. 6.11: Tangential electric field plot of proposed designs
- XLPE/ silicon rubber interface at BIL - 650 kV (kV/mm)

Fig. 6.12: Tangential electric field plot of existing accessories [45]
- XLPE/ silicon rubber interface at respective BIL voltages (kV/mm)
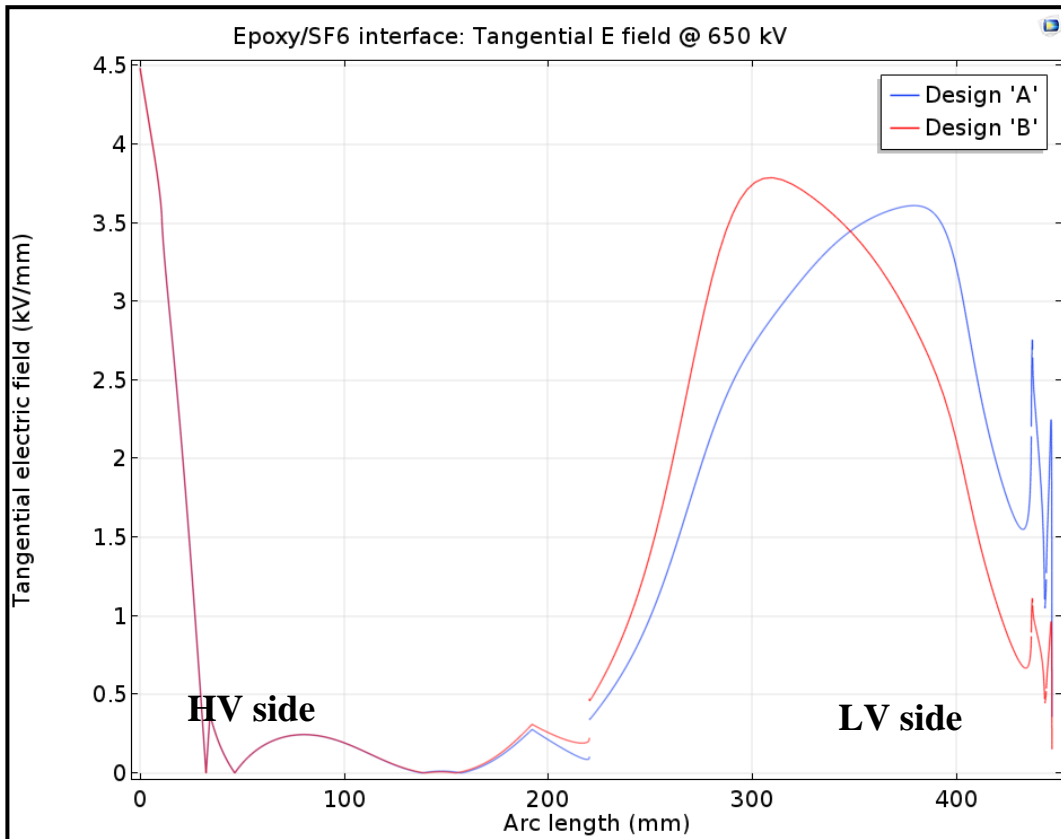
Fig. 6.13: Tangential electric field plot of proposed designs
- epoxy/ SF6 interface at BIL - 650 kV (kV/mm)
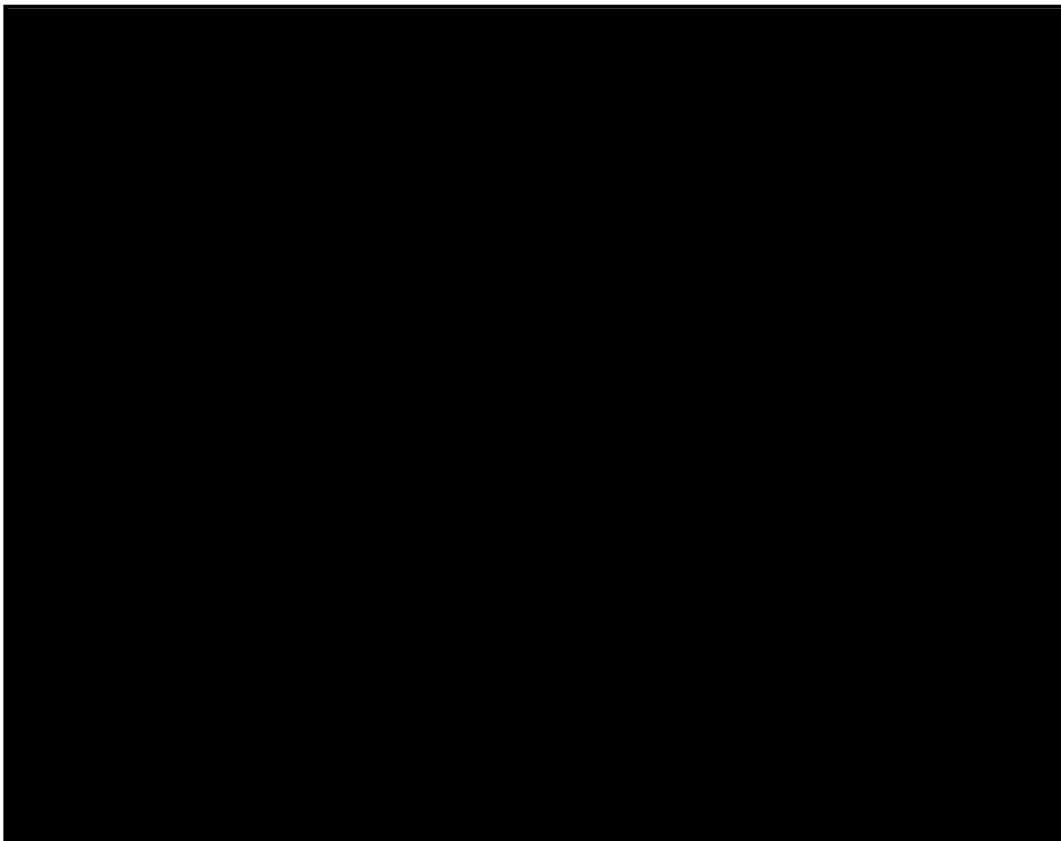
Fig. 6.14: Tangential electric field plot of existing accessories [45]
- epoxy/ SF6 interface at respective BIL voltages (kV/mm)

Epoxy/ silicon rubber interface

A comparison of the tangential electric field strengths of the epoxy/ silicon rubber interface of the proposed designs at basic impulse level voltage is shown in *Fig. 6.9.* Also, a comparative plot of the tangential electric field values of epoxy/ silicon rubber interfaces of existing cable accessories at their respective BIL levels is shown in *Fig. 6.10.* It is clearly observed that both the proposed designs have a lower tangential electric field component as compared to currently used outer-cone designs.

From the experimental results discussed in *Chapter 5,* it was found that for interfacial pressure of 1 bar, the breakdown occurred at 6 kV/mm. It must be noted that this value is conservative due to the harsh nature of the test setup, as explained previously. The tangential electric field values obtained from *Fig. 6.9* are less than 6 kV/mm for BIL voltages. Thus, **both the proposed designs will have good/ satisfactory electrical performance of the epoxy/ silicon rubber interface for interfacial pressures greater than 1 bar**.
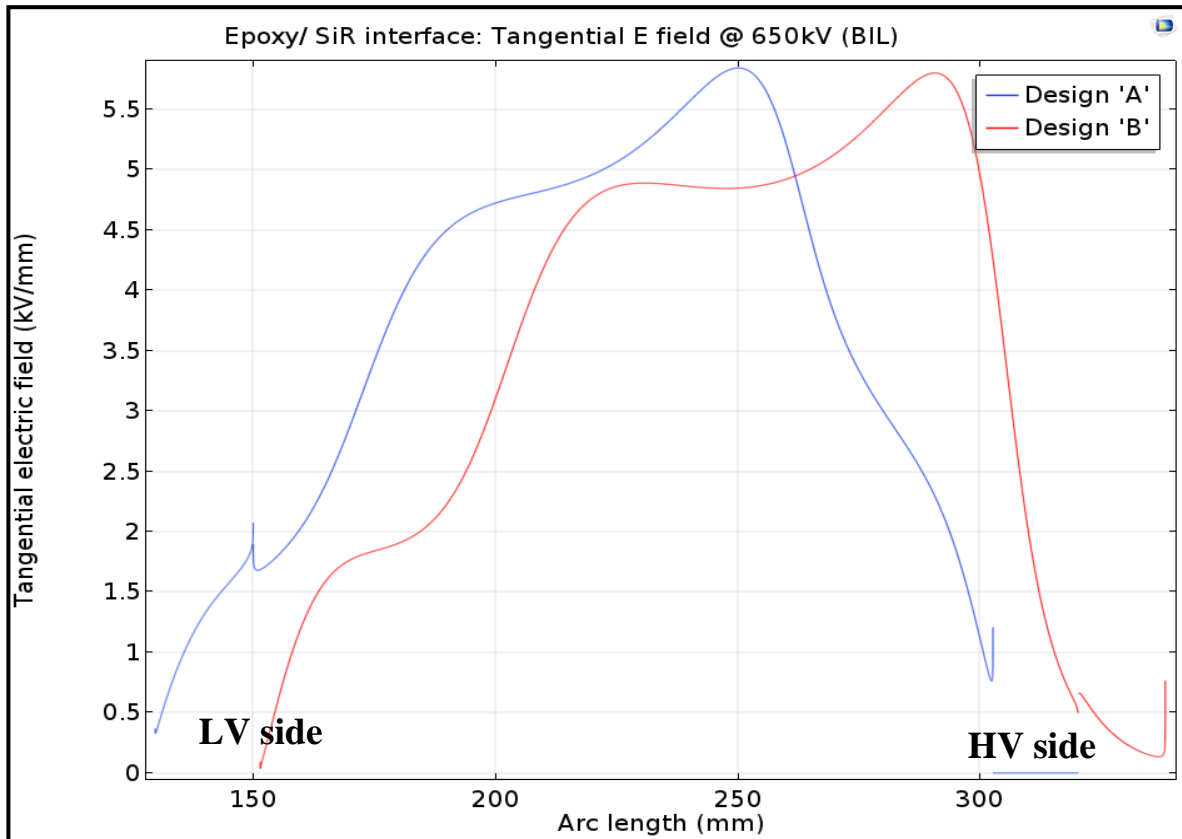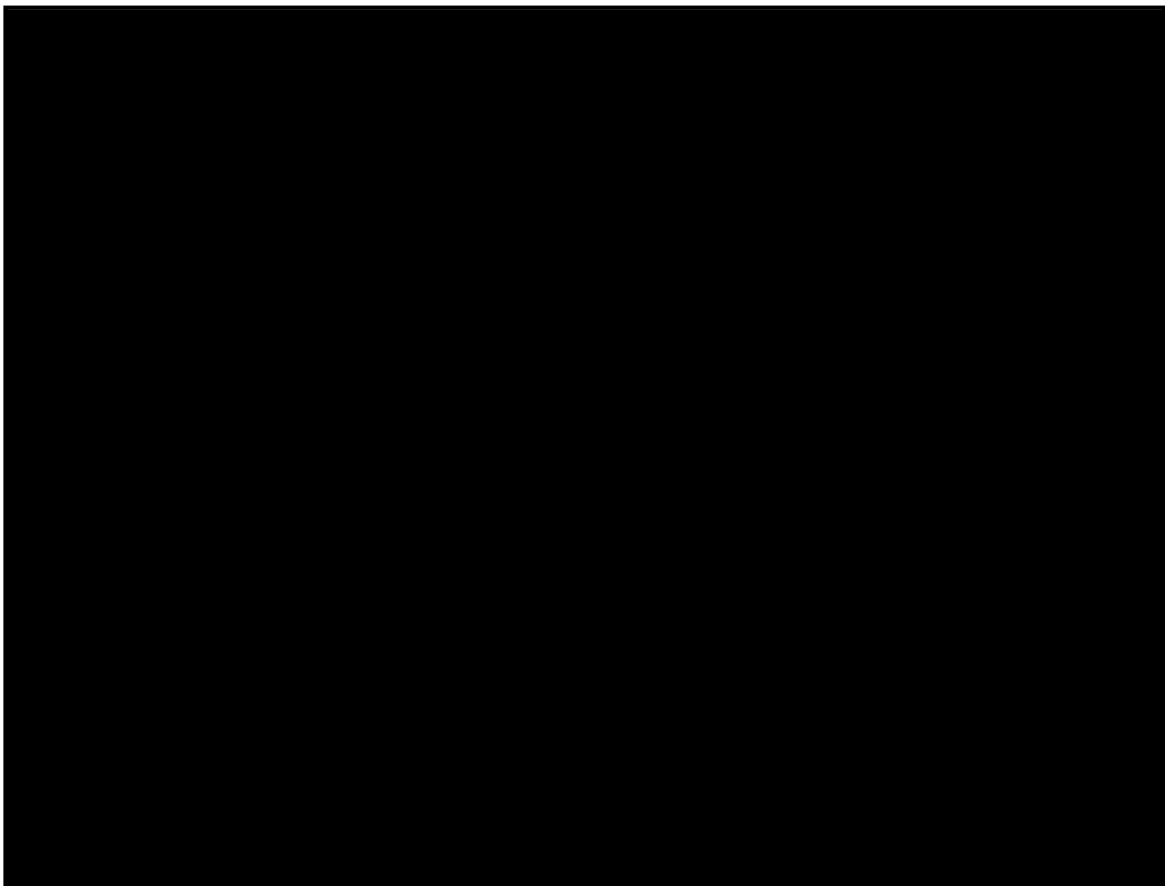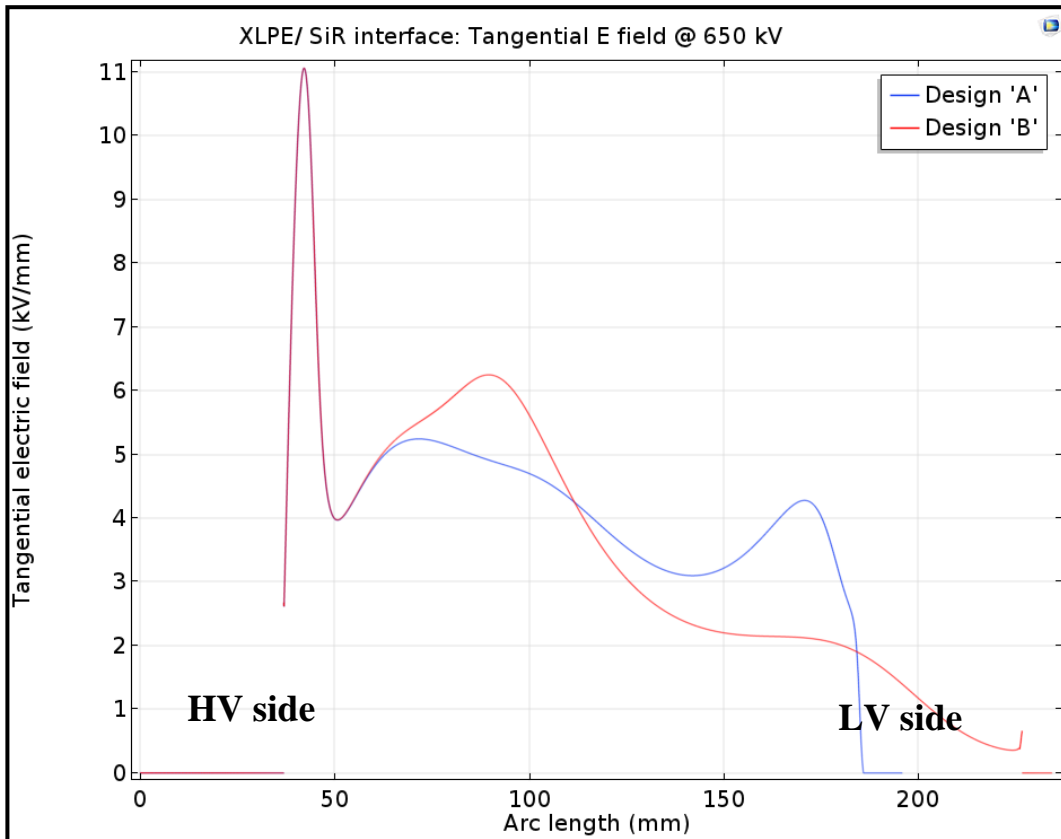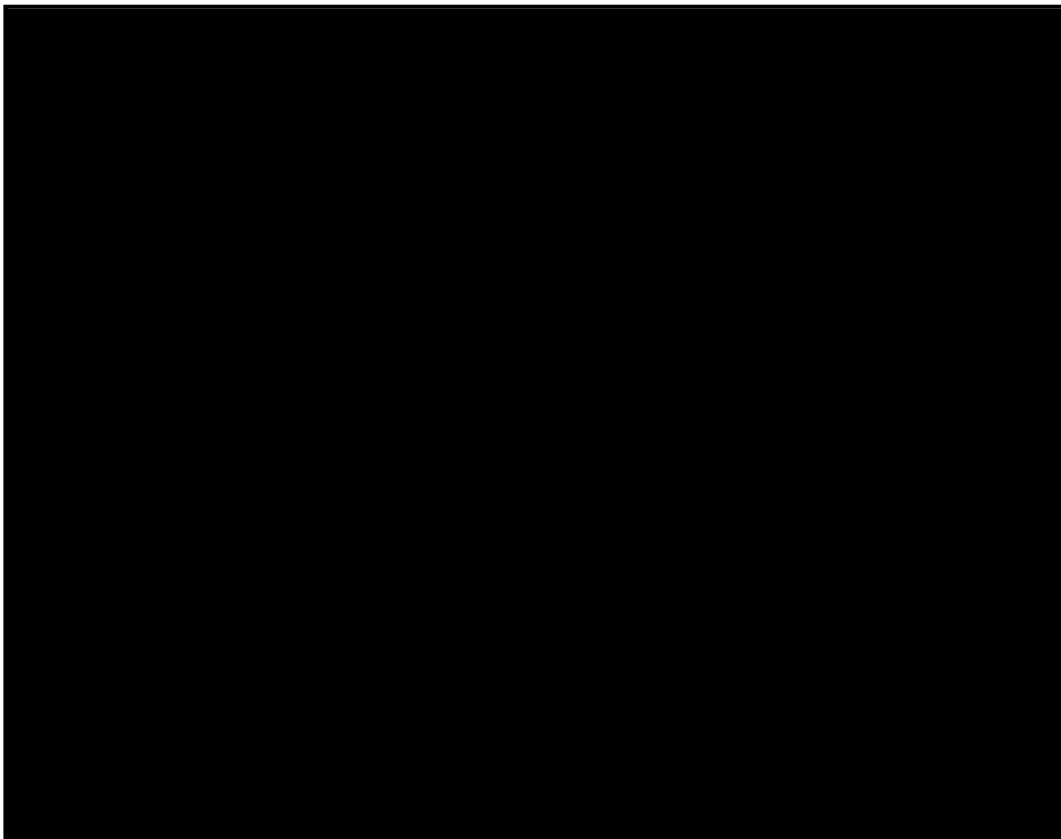
XLPE/ silicon rubber interface

A comparison of the tangential electric field strengths of the XLPE/ silicon rubber interface of the two proposed designs [maximum value 11.07 kV/mm] at basic impulse level voltage is shown in *Fig. 6.11.* Also, a comparative plot of the tangential electric field values of XLPE/ silicon rubber interfaces of existing cable accessories [maximum value ■ kV/mm] at their respective BIL levels is shown in *Fig. 6.12.* It is clearly observed that **both the proposed designs have a lower tangential electric field component as compared to currently used outer-cone designs.**

Epoxy/ SF6 interface

A comparison of the tangential electric field strengths of the epoxy/ SF6 interface of the two proposed designs [maximum value 4.48 kV/mm] at basic impulse level voltage is shown in *Fig. 6.13.* Also, a comparative plot of the tangential electric field values of epoxy/ SF6 interfaces of existing cable accessories [maximum value ■ kV/mm] at their respective BIL levels is shown in *Fig. 6.14.* It is clearly observed that **both the proposed designs have a lower tangential electric field component as compared to currently used outer-cone designs.**

Based on calculations and the experimental findings, it is evident that both the proposed designs have better electrical performance than the currently used outer-cone GIS cable terminations.

6.4.2 Mechanical performance

The expansion/ contraction of silicon rubber due to heating/ cooling cycles in operation may vary the pressure at the critical epoxy/ silicon rubber interface, Thus, as discussed during the earlier sections, a spring may be required to ensure that the interfacial pressure at the epoxy/ silicon rubber interface is maintained above 1 bar (as concluded from the experimental study). This section analyses both the proposed designs for their behaviour to spring pressure.

Hyperelastic material modelling is used to simulate the two designs to determine the external pressure that must be applied (by springs) to maintain an interfacial pressure greater than 1 bar. Mooney-Rivlin 5 parameter model was used as discussed in *Chapter 3*.
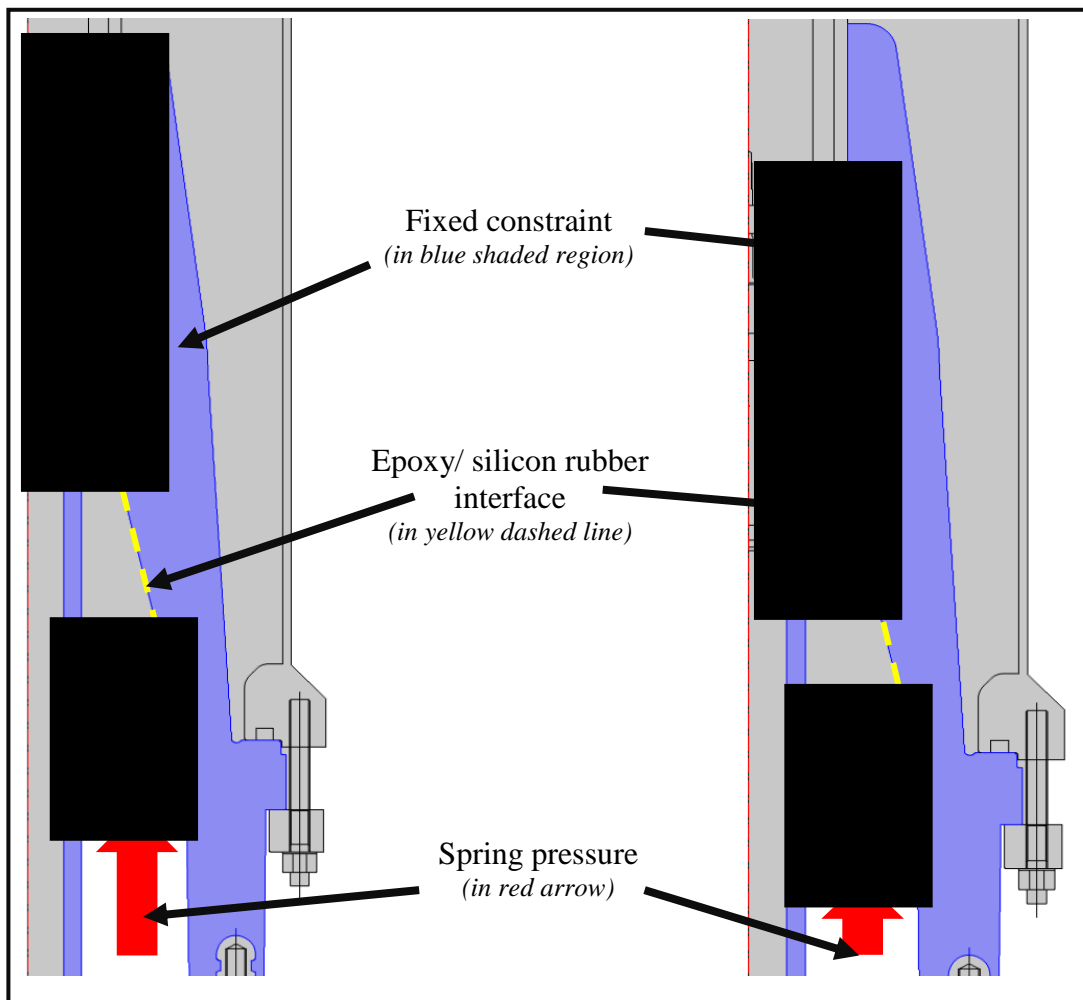
Fig. 6.15: Boundary conditions for mechanical FEM simulations

The boundary conditions for the mechanical simulations is shown in *Fig. 6.15*, the region in blue is taken as a fixed (immovable) constraint. The direction of the spring force is shown by the red arrow. It must be noted that due to practical limitations in FEM computation, the outward horizontal force exerted by the cable on the silicon rubber is ignored.
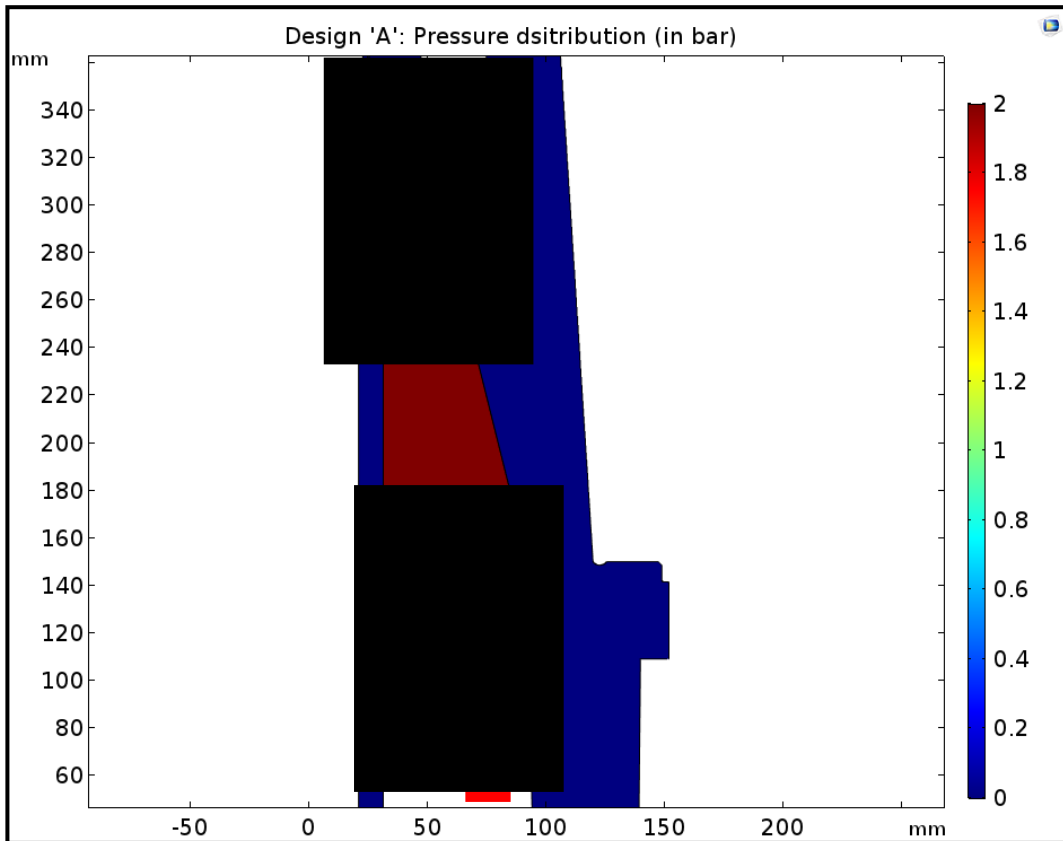
*Fig. 6.16: Design 'A'- plot of pressure distribution (in bar) for a spring force
(shown by red arrow) of 5 bar*
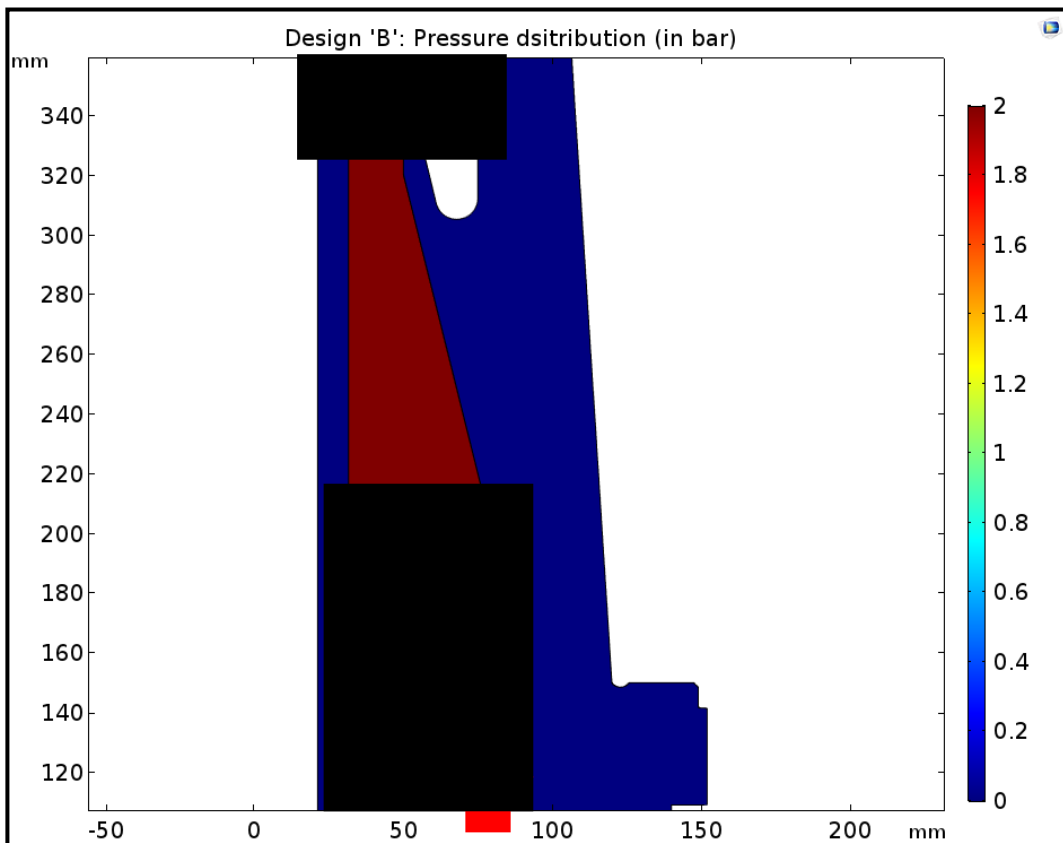
*Fig. 6.17: Design 'B'- plot of pressure distribution (in bar) for a spring force
(shown by red arrow) of 5 bar*

From the experimental study, it was concluded that a minimum interfacial pressure of 1 bar is necessary to ensure satisfactory performance of the interface. Thus, different values of spring pressure (shown by the red arrows in *Fig. 6.16* and *Fig. 6.17*) were applied to see its effect on the interfacial pressure.
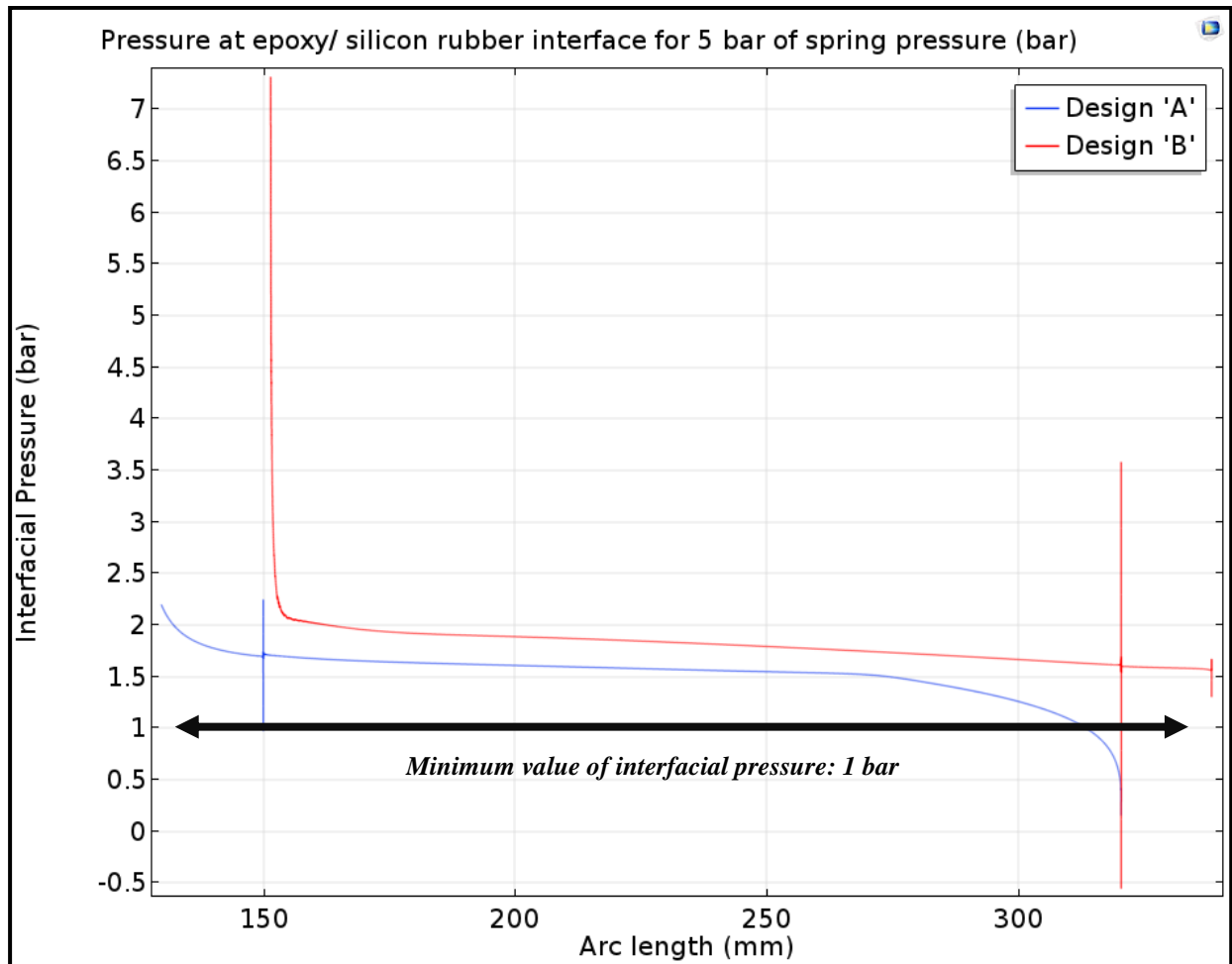
Fig. 6.18: Comparative plot of pressure distribution (in bar) at the epoxy/ silicon rubber interface for a spring force of 5 bar

The plot of interfacial pressure for 5 bar of spring pressure is shown in *Fig. 6.18*. The vertical lines in the plot are due to the changes in slopes of the rubber cone. The arc length in the plot refers to the y-axis of *Fig. 6.16* and *Fig. 6.17*.

It is found that at a **spring pressure of 5 bar**, the interface pressure is safely above the limit determined in *Chapter 5*. However, it must be noted that in practice, the silicon rubber stress cone is stretched up to 40% of its original size to ensure tight fit with the cable. This stretching of the stress cone will positively influence the interfacial pressure of the epoxy/ silicon rubber interface. Thus, a lower value of spring pressure may be used in practice.

6.5 *Summary*

It is observed that both the proposed designs would need a **spring** in the bottom (shown by the red arrow in *Fig. 6.15*). The spring would ensure that the interfacial pressure at the critical epoxy/ silicon rubber interface is maintained above 1 bar, during its operational cycles.

Design 'B' is more suitable from a product perspective. This is because of its simpler design (no embedded metal), which would result in ease of manufacture and lower production costs.

The **modularity** offered by this standardisation in combination with the ease and lower installation cost/ time would be an USP for this type of products.

This product is of significance due to the upcoming **refurbishment** of the 145 kV grids by TSOs in the EU. Owing to this commercial aspect, these types of terminations are expected to be commercially available soon. These standardised designs have the following unique advantages:

1. They are a new standardisation, which means that all accessories manufacturers will soon showcase their standardised designs. This would promote healthy competition and possible further development of this technology for other voltage classes.

2. The flexibility (modularity) given to the GIS manufacturer by the standardised interface would enable them to test the entire GIS switchgear with the epoxy at once.

3. The insulator is independent of the cable manufacturer. This standardisation would allow the utilities to plan GIS projects without considering the cable manufacturer, as the cable part can be dealt with, in the later stages of the project.

7. Conclusions and future scope

This chapter summarises the conclusions from the various experiments and FEM calculations performed during the course of this thesis work. It also gives answers to the research goals of this work. Recommendations for future research are also stated.

7.1 *Conclusions*

The final objective of this M.Sc. thesis is to propose the design for a new 145 kV inner-cone GIS termination in accordance to *CIGRE JWG B1-B3.49* recommendations. This new (design) technology required a detailed study of the epoxy/ silicon rubber interface. Which in turn required the design of a new test setup for interfacial testing. All these objectives have been successfully achieved. A summary of the conclusions from different sections of this work are presented below:

Modelling of silicon rubber:

1. It was found that a new type of material modelling technique (**hyperelastic material modelling**) must be used to accurately model the behaviour of the silicon rubber.

2. Various mechanical tests were performed on the silicon rubber to characterise and deduce its characteristic modelling technique.

3. It is found that at standard room temperature (23°C) and at elevated temperature (80°C), the **Mooney-Rivlin 5 parameter model** provides the best representation of the mechanical behaviour of the silicon rubber.

Test setup:

4. A new test setup for interfacial testing was **designed**, **built** and **successfully tested**.

5. It is observed that the setup shows very good **reproducibility** of breakdown values.

6. Due to the design of this test setup, immersion of test setup in oil was **not** necessary.

7. The AC breakdown voltage and LI voltage limits are determined for the experimental test setup at standard room temperature. The AC breakdown limit is found to be **50 kV**, while the LI limit is found to be **90 kV**.

8. The test setup satisfies **all the requirements of the CIGRE 15-10 WG** (refer *Section 2.1.1*) for interfacial testing of insulation materials.

Experimental testing of epoxy/ silicon rubber interface:

9. It is validated that the **electrical performance of the interface improves with increase in interfacial pressure**.

10. The increase in electrical performance of the interface saturates after 1 bar of interfacial pressure. Thus, this range (**1 bar – 2 bar**) of interfacial pressure is recommended to be the interfacial pressure of the epoxy/ silicon rubber interface.

11. It is found that for interfacial pressure of 1 bar, the interface has a breakdown strength of 6 kV/mm at standard room temperature. This is a conservative value.

12. It is found that the presence of silicon grease, increases the electrical strength of the interface by at least 40 %.

13. A scratch on the epoxy surface can **reduce** the electrical performance of the interface by **up to 11 %.** This is equivalent to a **0.5 bar decrease** in interfacial pressure.

14. It is found that heated samples (testing at elevated temperature of 85 - 90°C) **reduces** the electrical performance of the interface as compared to the results obtained from the AC breakdown tests.

15. It is concluded that the interface can withstand **at least 90 kV of LI voltage** for 1 bar of interfacial pressure (at standard room temperature).

Design of 145 kV inner-cone GIS cable termination:

16. Two designs are proposed adhering to the design limitations as laid down by the CIGRE JWG B1 – B3.49 JWG.

17. Both the designs use an aluminium extension rod (of different lengths) to connect with the M16 bolt of the GIS.

18. The Click-Fit locking concept is retained in both the designs. This aligns the new inner-cone termination with all existing Click-Fit cable accessories of Prysmian Group.

19. Design 'A' has a silicon rubber stress cone with an embedded metal alloy for mechanical connection. This stress cone contains the mechanical and electrical connection regions.

20. Design 'B' has a silicon rubber stress cone purely for field control of the cable end. The electrical and mechanical connection with the GIS is made through a separate connector and the aluminium extension rod. This design is simpler because it has no embedded metal alloy.

21. A spring is necessary to ensure sufficient interfacial pressure of the epoxy/ silicon rubber interface. About 5 bar of spring force is required.

7.2 Answers to research goals/ questions

In order to fulfil the academic requirements of a Master of Science thesis, certain scientific research goals need to be achieved. All the research goals planned at the start of this thesis have been successfully achieved.

Goal 1: *To **design a test setup** to obtain the relation between electric field strength with respect to interfacial pressure*

> A new modular test setup has been successfully designed, built and tested. The test setup satisfies all the requirements of the CIGRE 15-10 WG.

Goal 2: *To experimentally obtain **the relation between interfacial pressure and electric performance** of epoxy/ silicon rubber interface.*

> AC breakdown tests were carried out for a wide range (0.2 bar – 2 bar) of interfacial pressures. The values of interfacial pressures showed very low scatter/ dispersion. Thus, the remaining samples were used for additional tests to further characterise the interface behaviour.

Additional tests:
> AC breakdown test with silicon grease at the interface
> AC breakdown test with scratch on epoxy surface
> AC breakdown test at elevated temperature
> Lightning Impulse (LI) test

> The additional tests helped to provide a better and more complete understanding of the interfacial electrical behaviour.

Goal 3: *To **propose a design for an inner-cone GIS cable termination** and elucidate its electrical and mechanical features.*

> **Two new designs** of the new 145 kV inner-cone GIS cable termination have been proposed. Comparison of the electrical and mechanical characteristics of both the designs has been performed. A comparison of critical electrical parameters with those of existing cable accessories has been also performed.

Apart from these goals, the following additional finding has also been made during this thesis:

> A new material modelling technique for insulating silicon rubber has been studied in detail. Extensive mechanical tests were performed to characterise and validate the material model of silicon rubber. This will help to understand the behaviour of silicon rubber in existing/ future designs of cable accessories.

The performance of the test setup has been extremely stable and shows very low standard deviation. Thus, the design of this test setup will be shared with the larger scientific community through an IEEE publication.

7.3 Recommendations for future work

The following recommendations are made for further study in this domain:

1. Due to lack of standardised method for testing interfaces, it is not possible to compare and collaborate the works of different authors/ institutes. Thus, relevant bodies must device standardised procedures and test setups for interfacial testing.

2. The proposed test setup in this thesis may be modified/ adapted to perform tan δ, leakage current and partial discharge measurements

3. A study for mathematical/ theoretical breakdown performance of interfaces (using interface models) and validation by experimental results could be performed.

4. In accordance with the trend of the cable industry, the behaviour of interfaces under DC and low frequency AC voltage should also be explored.

5. For the hyperelastic modelling of silicon rubber, further tests like biaxial, shear and volumetric could be performed. These tests will give a better accuracy and understanding of the hyperelastic material model of the rubber.

Bibliography

[1.] A. Rodrigo Mor. ET8020. Class Lecture, Topic: "Diagnostics of High Voltage and Asset Management". Faculty of Electrical Engineering, Mathematics and Computer Science, TU Delft, The Netherlands, June 2017.

[2.] A.N..Gent. Engineering with Rubber - How to Design Rubber Components. ISBN 978-3446427648.

[3.] ANSYS Inc. Ansys theory reference 5.6. URL http://research.me.udel.edu/~lwang/teaching/MEx81/ansys56manual.pdf.

[4.] Standard Test Method for Dielectric Breakdown Voltage and Dielectric Strength of Solid Electrical Insulating Materials at Commercial Power Frequencies, ASTM D149-09, (2013).

[5.] B. Du and L. Gu. "Effects of interfacial pressure on tracking failure between XLPE and silicon rubber". IEEE Transactions on Dielectrics and Electrical Insulation, vol. 17, no. 6, pp. 1922-1930, 2010.

[6.] B. Parmigiani. Accessories for underground and submarine cable systems. Italy: Prysmian S.P.A.,, 2013.

[7.] C. Forssen and A. Christerson. "Test cell for interfacial electric strength testing". IEEE International Conference on Solid Dielectrics (ICSD), 2013.

[8.] C. Forssen, A. Christerson and D. Borg. "Test cell for electric strength of rubber-epoxy interfaces". 2015 IEEE Conference on Electrical Insulation and Dielectric Phenomena (CEIDP), 2015.

[9.] C. Zhang, J. Kucera and R. Kaluzny. "The Electrical Behaviours of the Interface in Solid-Insulated Distribution Equipment". 2008 Annual Report Conference on Electrical Insulation and Dielectric Phenomena, 2008.

[10.] COMSOL AB. "Introduction to COMSOL Multiphysics". Internet: http://www-cs-faculty.stanford.edu/~uno/abcde.html [November 8, 2017].

[11.] D. Bortoli, E. Wrubleski, R.J. Marczak and J.G. Junior . "Hyperfit - curve fitting software for incompressible hyperelastic material models". Brazilian Congress of Mechanical Engineering, 2011.

[12.] D. Fournier and L. Lamarre. "Effect of Pressure and Length on Interfacial Breakdown Between Two Dielectric Surfaces". IEEE International Symposium on Electrical Insulation, Baltimore, MD USA, pp. 270-272, 1992.

[13.] D. Fournier and L. Lamarre. "Effect of pressure and temperature on interfacial breakdown between two dielectric surfaces". Proc. 1992 Annual Report: Conference on Electrical Insulation and Dielectric Phenomena, Victoria, B.C., pp. 229-235, 1992.

[14.] D. Panagiotopoulos. "AC Electrical Breakdown Strength of Solid Solid Interfaces: A study about the effect of elasticity, pressure and interface conditions.", M.Sc. thesis. Norwegian University of Science and Technology, Norway, 2015.

[15.] D. Roylance. "Stress Strain Curves". Internet: http://web.mit.edu/course/3/3.11/www/modules/ss.pdf , August 23, 2001 [January 26, 2018].

[16.] E. Kantar, D. Panagiotopoulos and E. Ildstad. "Factors influencing the tangential AC breakdown strength of solid-solid interfaces". IEEE Electrical Insulation Magazine, vol. 23, no. 3, pp. 1778-1788, 2016.

[17.] E. Kantar and E. Ildstad. "Modelling Longitudinal Breakdown Strength of Solid – Solid Interfaces using Contact Theory". 2016 IEEE International Conference on Dielectrics, vol. 1, pp. 398 – 401, July 2016.

[18.] E. Kantar, F. Mauseth and E. Ildstad. "Effect of Pressure and Elastic Modulus on Tangential Breakdown Strength of Solid – Solid Interfaces". IEEE Electrical Insulation Conference, Montreal, Canada, pp. 431 – 435, June 2016.

[19.] F. H. Kreuger. Industrial High Voltage Vol. I. Delft University Press, 1991. ISBN 978-9062755615.

[20.] F. H. Kreuger. Industrial High Voltage Vol. II. Delft University Press, 1992. ISBN 978-9062755622.

[21.] Feasibility of a common dry type plug-in interface for GIS and power cables above 52kV, CIGRE JWG B1-B3.33.

[22.] H. Lobo and B. Croop. "Testing, modelling and validation for rubber simulation in ANSYS". Internet: http://engr.bd.psu.edu/ansysug/2016-10-1/2DPLworkshopOct2016_HyperWorking.pdf. [December 22, 2017]

[23.] High-voltage switchgear and control gear - Part 209: Cable connections for gas insulated metal-enclosed switchgear for rated voltages above 52kV - Fluid-filled and extruded insulation cables - Fluid-filled and dry-type cable-terminations, IEC 62271-209:2007-08.

[24.] High-voltage test techniques – Part 1: general definitions and test requirements, IEC 60060-1:2010.

[25.] IEC/IEEE Guide for the Statistical Analysis of Electrical Insulation Breakdown Data (Adoption of IEEE Std. 930-2004), IEEE Standard 62539, 2007.

[26.] Insulation coordination – Part 1: Definitions, principles and rules, IEC 60071-1:2006.

[27.] Interfaces in accessories for extruded HV and EHV cables, CIGRE Joint Task Force 21/15(210), August 2002.

[28.] J. Andersson, S. Gubanski and H.Hillborg. "Properties of interfaces between silicone rubber and epoxy". IEEE Electrical Insulation Magazine, vol. 15, no. 5, pp. 1360-1367, 2008.

[29.] J. Svahn. L. Hedman and S.M. Gubanski. "Development of Cell for Testing of the Interfacial Electric Strength". CIGRE WG15-10, 1998.

[30.] J. T. Bauman. Fatigue, Stress and Strain of Rubber Components - Guide for Design Engineers. ISBN 978-3446416819.

[31.] M. Sasso, G. Palmieri, G. Chiappini and D. Amodio. "Characterization of hyperelastic rubber-like materials by biaxial and uniaxial stretching tests based on optical methods". Elsevier - Polymer Testing, vol. 27, pp. 994-1004, 2008.

[32.] M.Z. Siddiqui M. Shahzad, A. Kamran and M. Farhan. Mechanical characterization and finite element modelling of a hyperelastic material. 18, 2015.

[33.] NPTEL. "Mechanical properties of materials". Internet: http://nptel.ac.in/courses/107103012/module1/lec4.pdf [February 14, 2018]

[34.] Oil immersed cable connection assemblies for transformers and reactors having highest voltage for equipment U_m from 72.5kV to 550kV - Part 2: Dry-type cable terminations, NEN-EN 50299-2.

[35.] Pfisterer Kontaktsysteme GmbH. "High Voltage Cable Plug". US Patent 2016/ 0352036, Dec 1, 2016.

[36.] P.T.M. Vaessen. ET4103. Class Lecture, Topic: "High Voltage Constructions". Faculty of Electrical Engineering, Mathematics and Computer Science, TU Delft, The Netherlands, February 2017.

[37.] Power Cables with extruded insulation and their accessories for rated voltages above 30 kV (Um = 36 kV) up to 150 kV (Um= 170 kV) – Test methods and requirements, IEC 60840:2011.

[38.] Prysmian Group. "Click-Fit". URL: http://www.click-fit.org/ [April 12, 2018].

[39.] R. Jakel. "Analysis of hyperelastic materials with mechanica - theory and application examples". Internet: http://qucosa.de/fileadmin/data/qucosa/documents/5995/data/Analysis_of_Hyperelastic_Materials_with_MECHANICA.pdf. [February 2, 2018].

[40.] R. Ross. "Dealing with interface problems in polymer cable terminations". IEEE Electrical Insulation Magazine, vol. 15, no. 4, pp. 5-9, 1999.

[41.] R.W. Ogden, G. Saccomandi and I. Sgura. "Fitting hyperelastic models to experimental data". Springer – Computational Mechanics, 2004.

[42.] Rubber, vulcanised or thermoplastic -Determination of tensile stress-strain properties, NEN-ISO 37: 2017.

[43.] Rubber vulcanized or thermoplastic - Determination of compression set - Part 1: At ambient or elevated temperatures, NEN-ISO 815-1:2008.

[44.] S. Ganeshan, J. Murugesan, A. Cavallini, F. Negri, B. Valecillos and U. Piovan. "Identification of partial discharges in power transformers: An approach driven by practical experience". IEEE Electrical Insulation Magazine, vol. 33, no. 5, pp. 23-31, 2017.

[45.] S. Ganeshan, "Electrical analysis of power cable accessories" Internship report, TU Delft, The Netherlands, 2017.

[46.] S. Hasheminezhad, E. Ildstad and A. Nysveen. "Breakdown strength of solid - solid interface". IEEE International Conference on Solid Dielectrics, 2010.

[47.] S. Hasheminezhad. "Breakdown strength of solid | solid interfaces". IEEE Trondheim PowerTech, 2011.

[48.] S. Rowland. "Position Paper on Interfaces in Solid Dielectric Insulation Systems". URL: http://www.hubnet.org.uk/filebyid/634/Solid_Dielectrics.pdf [November 9, 2017].

[49.] Standard design of a common, dry type plug-in interface for GIS and power cables up to 145kV, CIGRE WG B1-B3.49. [March 20, 2018]

[50.] Standard Test Methods for Rubber Properties in Compression, ASTM D575 - 91(2012).

[51.] T. Sussman and K.J. Bathe. "A model of incompressible isotropic hyperelastic material behaviour using spline interpolations of tension-compression data". Wiley InterScience - Communications in Numerical Methods in Engineering, vol. 25, pp. 53-63, 2008.

[52.] T. Takahashi, T. Okamoto, Y. Ohki and K. Shibata. "Breakdown strength at the interface between epoxy resin and silicone rubber - A basic study for the development of all solid insulation". IEEE Electrical Insulation Magazine, vol. 12, no. 4, pp. 719-724, 2005.

[53.] T. Tanaka. "Polymer Interfaces Associated with Electric Insulation Systems". CIGRE SC 15 colloquium, Bedford, Mass., USA, 1997.

[54.] University of Colorado- Boulder. "Ch. 5 Stress- strain material laws". [On-line]. Available: https://www.colorado.edu/engineering/CAS/courses.d/Structures.d/IAST.Lect05.d/IAST.Lect05.pdf [February 2, 2018]